INSTITUTE OF GEOPHYSICS
POLISH ACADEMY OF SCIENCES

PUBLICATIONS OF THE INSTITUTE OF GEOPHYSICS POLISH ACADEMY OF SCIENCES

MONOGRAPHIC VOLUME

E-9 (405)

MANAGEMENT OF THE STORAGE RESERVOIR INFLUENCING THE PROTECTED NATURAL ENVIRONMENT – UPPER NAREW RIVER SYSTEM CASE STUDY

WARSZAWA 2008

PUBLS. INST. GEOPHYS. POL. ACAD. SC., E-9 (405), 2008

Management of the Storage Reservoir Influencing the Protected Natural Environment – Upper Narew River System Case Study

Preface

Jarosław J. NAPIÓRKOWSKI and Renata J. ROMANOWICZ
(Editors of the Issue)

Institute of Geophysics, Polish Academy of Sciences
Ks. Janusza 64, 01-452 Warszawa, Poland
e-mail: inn@igf.edu.pl

One of the aims of the recently introduced Framework Water Directive (Directive 2000/60/WE) is the protection of the natural environment from further degradation. In the case of catchment systems, in which water retention reservoirs play an important role, maintenance of the desirable status of the natural environment under protection requires not only securing higher flows during periods of vegetation growth, but also introducing or keeping the flood impulse.

River floods are commonly considered as natural phenomena with threats to life and health and loss of property. However, in some situations they are a positive occurrence, helping to preserve the natural features of a particular region. This is true for the Narew valley, in particular the area within the borders of the Narew National Park (NNP), where spring floods not only cause no material damage, but also bring positive effects for preserving the natural qualities of the region.

The Narew National Park was formed in order to maintain the hydrographic system of the anastomosing river and water-peat ecosystem, which is unique at the European scale. Unfortunately, at present, the natural vegetation of the park is endangered by the on-going delapidation of the valley and postponement of the agricultural use of the meadows. Settlement changes in the lower reach of the River Narew follow the regulation of its channel and are also due to natural causes. A new river channel was built during drainage works. It is wider, deeper, and straighter than the former channel, causing the lowering of water levels in the river and decreasing and shortening surface flooding, as well as increasing groundwater levels in the valley. Drying of the whole valley is also enhanced by the weather conditions. Mild winters, small snowfall and, in part, the decrease in rainfall, influence the decrease of river flooding and groundwater resources.

To maintain the required status of riverine wetlands with fluvial-glacial feed, it is necessary to retain, during the river's vegetation growth period, higher than minimum flows according to a hydro-biological criterion and also to keep or introduce a flood impulse. The concept of flood impulse was introduced by Junk *et al*. (1989) for tropical rivers and was further developed by Tockner *et al*. (2000) for rivers situated in intermediate climate zones. Nowadays ecologists claim that it is a key paradigm for the ecology of running waters. According to this concept, the flood impulse should help sustain high-level biodiversity in the flooded river terraces as an integral part of the feed for fluvial-glacial wetlands (Okruszko *et al*. 1996).

In many cases people cause the deterioration of their habitat through ignorance, organizational inefficiency and lack of information. Hence, it seems desirable to begin actions leading to the intensification of research on the improvement of the whole system of environmental protection, and in particular, on the management of the river systems containing water storage reservoirs that influence the natural environment. Therefore, an intensification of the study of various aspects of the above mentioned problems is a must and is challenging not only for the scientific community but also for decision makers at both local and state levels.

This monograph reflects the results of the project supported by the Polish Committee for Scientific Research "Management of the Storage Reservoir Influencing the Protected Natural Environment – Upper Narew River System Case Study", registered as Grant No.6 PO4D 032 19 and coordinated by the Institute of Geophysics, PAS.

The goal of the project was the development of control techniques that would help in re-establishing the appropriate water conditions in the Narew National Park by the management of the flood impulse in the section between the Siemianówka storage reservoir and the Narew National Park.

In this monograph, the first details of the GPS measurement programme in the Narew National Park are presented. However, the project team performed over fifty measurements of selected cross-sections of the riverbed and the valley, undertook hydrometric measurements, and assessed the decline of water level in the section from the Siemianówka reservoir to Rzędziany. Measurements covered most of commonly used topographic and hydraulic characteristics. The resulting cross-sections were used to build a numerical model of the area and for hydraulic calculations.

We further present two approaches to specifying an appropriate hydrological regime within a wetland, necessary for maintaining goods and services. This regime is related to the source of water, which varies with the type of wetland.

The next problem addressed in this monograph is the selection of a proper rainfall-flow/flow-routing model of the upper River Narew catchment and the river reach between Bondary and Suraż. Solution of the flood management problem in the reservoir system requires the repeated solving of unsteady flow equations for successively generated operation scenarios. Thus the solution algorithms applied in such cases should be maximally efficient, not only with respect to the computer capability requirements, but – particularly important in this case – time of computation required to obtain the solution. Within the project, simulation research was undertaken that resulted in an

estimation of the effectiveness and applicability of numerical solutions of the inverse problem of flow equations.

Finally, a computer-based analysis and control mechanisms for the control of a flood impulse in the system are presented. An uncertainty analysis of the predictions obtained is performed, and an influence of the uncertainty of model structure and observations on the reservoir control performance is analysed. The study is based on the Global Sensitivity Analysis (GSA) and Generalised Likelihood Uncertainty Estimation (GLUE) techniques. Additionally, these techniques were applied to study transport processes in the NNP reach of the River Narew.

The predictions of flood extent will undoubtedly play an important role in water management best practice, following the principles of sustainable development in the Narew National Park and an adequate control of the Siemianówka storage reservoir.

References

Junk, W.J., P.B. Bayley, and R.E. Sparks (1989), *The flood pulse concept in river-floodplain systems*, Can. Spec. Publ. Fish. Aquat. Sci. **106**, 110-127.

Okruszko, T., D. Pusłowska, S. Tyszewski, W. Dembek, and J. Oświt (1996), *The Water Management Rules in the Upper Narew River Basin*, Proceedings of International Conference on "Aspects of Conflicts in Reservoir Development and Management", City University, London.

Tockner, K., F. Malard, and J.V. Ward (2000), *An extension of the flood pulse concept*, Hydrol. Process. **14**, 2861-2883.

PUBLS. INST. GEOPHYS. POL. ACAD. SC., E-9 (405), 2008

Derivation of a Numerical Model of River Narew Valley Cross-Sections Using Remote Sensing and Ground Survey

Mariusz FIGURSKI, Marcin GAŁUSZKIEWICZ and Maciej WRONA

Faculty of Civil Engineering and Geodesy
Military University of Technology
e-mail: mfigurski@wat.edu.pl

Abstract

This study introduces GPS measurements into the Narew National Park. The main task of the campaign was to develop three-dimensional information as a help in creating Numerical Model of the area. The whole methodology and technology of satellite measurements, including field work and postprocessing, is described. Double difference receivers in differential mode were used. The authors show the ability of GPS measurements in this kind of works and also the usefulness and effectiveness of the methodology described.

1. Introduction

Satellite measurements based on Global Positioning Systems have recently been widely applied in all sorts of geodetic work and navigation. This is mainly due to advantages of satellite technologies over traditional ground-based ones, namely their higher accuracy, instantaneous location readout capability, almost full automation of measurements and processing, as well as lower cost. Usage of satellite systems enables interdisciplinary approach to scientific and technological problems. This approach was applied by scientists from the Institute of Geophysics of the Polish Academy of Sciences, and the Faculty of Civil Engineering and Geodesy of the Military University of Technology, who jointly made measurements and data analysis to prepare a dynamic modeling of the River Narew. The project discussed here combines traditional technologies of river bed study with satellite technologies for precise measurement of River Narew Valley cross-sections. Inaccessibility for direct measurements and high costs of photogrammetric technologies were the arguments for using satellite technologies to acquire the field data.

2. Measurement method

The field measurements made on profiles in the Narew National Park were conducted by means of combination of three measuring methods: static, fast static, and kinematic

with OTF. The kinematic methods are based on processing of phase observations on two frequencies, which can be written in the form of the following equations:

$$L_1 = \lambda_1\varphi_1 = \rho + c\ \ \Delta t_r - \Delta t_s\ \ + T - I/f_1^2 + \lambda_1 N_1 + \varepsilon_{\varphi_1}, \tag{1}$$

$$L_2 = \lambda_2\varphi_2 = \rho + c\ \ \Delta t_r - \Delta t_s\ \ + T - I/f_2^2 + \lambda_2 N_2 + \varepsilon_{\varphi_2}, \tag{2}$$

where φ is the carrier phase, ρ is the geometrical distance between the satellite and the receiver, Δt_s and Δt_r are errors of the satellite and the receiver clocks, respectively, $I = 40.3\,\mathrm{TEC}$ is the component of the signal delay in the ionosphere, TEC is the total content of free electrons in the ionosphere, N_1 and N_2 are uncertainties of phase, T is the signal delay in the troposphere, λ is the wavelength and ε is the measurement error. The above equations include a few essential systematic errors which impair the quality of the observations. In case of observations made simultaneously in two points it is possible to differentiate the observations (1) and (2), which leads to elimination or suppression of the systematic errors. The method of double or triple differentiating used in the study enables to eliminate the clock errors of the receiver and the satellite and determine the phase discontinuity. Having two frequencies recorded, a linear combination of Eqs. (1) and (2) (the so-called "iono-free" L_3 combination) was used to eliminate the dispersion component of the first order. It comprises about 95% of the total effect of the ionospheric refraction. Figure 1 shows the scheme of positioning by means of the differential method.

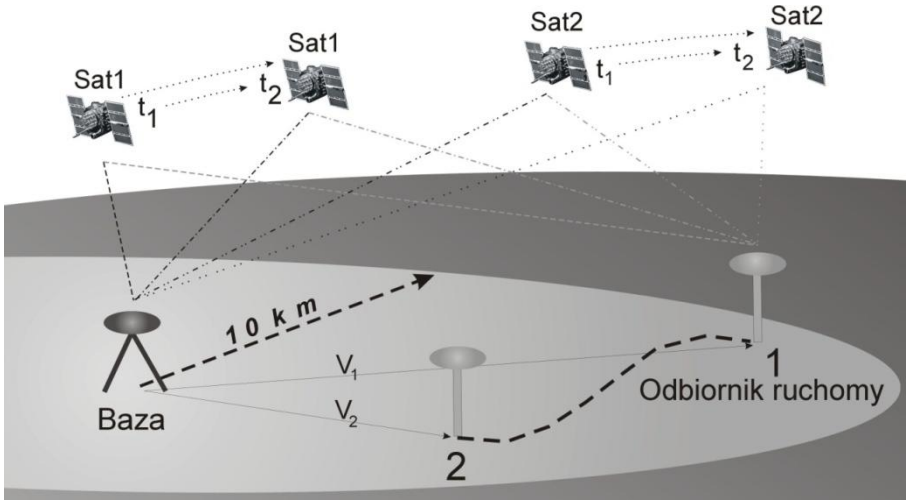

Fig. 1. Scheme of positioning by means of the differential GPS (Baza = Base, Odbiornik ruchomy = Mobile receiver).

Processing of observations was made in two phases. Phase one included precise determination of local reference station coordinates which were related to the permanent GNSS stations: in Lamkówek (LAMA), Józefosław (JOZE), Military University of Technology in Warsaw (WAT1) and Vilnius (VLNS), while phase two included processing of kinematic measurements using local reference station coordinates de-

termined in advance. This approach has been used by our team for a few years. Reference stations coordinates are monitored continuously and they are uniformly determined in the ETRS system. This eliminates, on one hand, the potential risk of using erroneous observations, and, on the other, it provides a reference system precisely realized by the coordinates.

In the majority of cases, a local reference station is active all the time when the measurements are made in the field, which means that the observations are collected even for a few hours. Such a long period is quite sufficient for transferring the coordinates even a few hundred kilometers with an accuracy of about 1 cm. The only problem in this approach is the quality of the satellite ephemerid. The orbit elements transmitted in the navigational message may be used for measuring a distance between the receivers only within a few dozen kilometers; for longer distances it is required to use precise ephemerid: ultra-rapid, rapid or final. The error of the measurement of distance between the receivers may be assessed using the following formula (Beser and Parkinson 1982):

$$db = \frac{b}{20000} dr,$$

where *db* is the distance measurement error [m], *b* the distance between stations [km], and *dr* the orbit error [m]. For example, if the distance between the stations is 100 km, and the onboard orbit error is 2.5 m, then the error of the distance measurement may be estimated at the level of 1.25 cm. This simply means that the onboard ephemerid must not be used for transferring precise coordinates on long distances.

In the proposed method, the location of the mobile receiver is determined with relation to a local base – the "terrain reference station" – whose coordinates are known (determined earlier or retrieved from the catalogue). Determination of the coordinates is described above. The catalogue data may contain errors that are not simply verifiable. This problem may be eliminated and verified only when the ASG-EUPOS network becomes available in Poland and a calibration campaign for the first class basic grid has been done. Atmospheric refraction and ephemerid accuracy impact was reduced by introducing the maximum distance between the receivers – the mobile and the basic ones – limited to 10 km. This assumption enabled to use the onboard ephemerid transmitted in the GPS message without loosing the accuracy of determined coordinates.

3. Field measurements

Three sets of Trimble receivers for real time work using the RTK method and post processing were used for the field measurements:

1. Trimble 5700 basic receiver with Zephyr Geodetic antenna;
2. Trimble 4700 basic receiver with Microcentered + GP antenna;
3. Trimble 5700 mobile receiver with TSC1 controller and Zephyr antenna.

Terrain conditions were analyzed before the measurements, which enabled us to select the optimal measurement method. First of all, the RTK method was considered.

Fast measurement and a few centimeters accuracy are its unquestionable advantages, while the range from the base is limited usually to a few kilometers. The accuracy of the RTK method decreases with increasing distance from the basic station. The terrain in which the profiles measurements were planned was very complicated. The River Narew neighborhood is mainly swamps with lush vegetation and wilderness in the area. Making profiles measurements using the RTK method in such a terrain is not only burdensome due to breaks in transmission of differential corrections, but first of all dangerous. Having all those problems in mind, we gave up the RTK method and chose the STOP&GO method based on phase measurements with a distinguished basic station and mobile receiver processed in the post processing. From the point of view of data processing, it differs from the RTK method only in the fact that the coordinates are not obtained in real time. Its disadvantage is the inability to fully control the observations which may sporadically lead to a necessity of repeating some measurements. We partially solved the problem by using two synchronically working basic stations for measurements on some profiles (Fig. 5 later in the text).

The basic (reference) receiver recorded code and phase data with a frequency of 1 Hz for the minimum elevation of tracked satellites of 10° above the horizon and maximum PDOP (Percent Dilution of Precision) coefficient of 5. It worked continuously during each measurement session. Correlated phase observations from the reference station and the mobile receiver enabled to reduce the systematic errors down to values that had no impact on location determination with an accuracy of a few centimeters. The local reference station may be located almost anywhere; however, it must be in an open area without electromagnetic interference at the frequencies of the GPS system. This is especially important in urban areas where numerous devices working in various wavelengths are present. Location of the basic receiver during the measurements in the Narew National Park is presented in Fig. 2.

Fig. 2. The reference point base.

Fig. 3. The mobile set (rover).

The mobile (kinematic) receiver recorded data with a frequency of 1 Hz for the minimum elevation of tracked satellites of 10° above the horizon and maximum PDOP

coefficient of 5. The measurement process was realized using the STOP&GO method with the minimum number of tracked GPS satellites of 5. This selection was a compromise between the profile node measurement time and the coordinates accuracy. The set of receivers used for the profiles measurements enabled to obtain the coordinates for a single point in about 8 seconds (with an initiated receiver – FIX) which is a competitive solution for the RTK method. The New Point method was applied to initiate the measurements. The observer controlling the mobile set (antenna, receiver, controller) made measurements in characteristic points of the terrain (Fig. 3). In points of poor visibility of the horizon or during breaks in the process of tracking the satellites, it was necessary to initiate the receiver again (renewed determination of the phase uncertainty) which resulted in extension of the measurement time at a single point even up to 2 minutes. This happened sporadically during the measurement campaign. The applied method proved to be good both during the profiles measurements and during measurements of the characteristic points of the orography. Three profiles of about 2 km, i.e., about 200 points, were measured within one day.

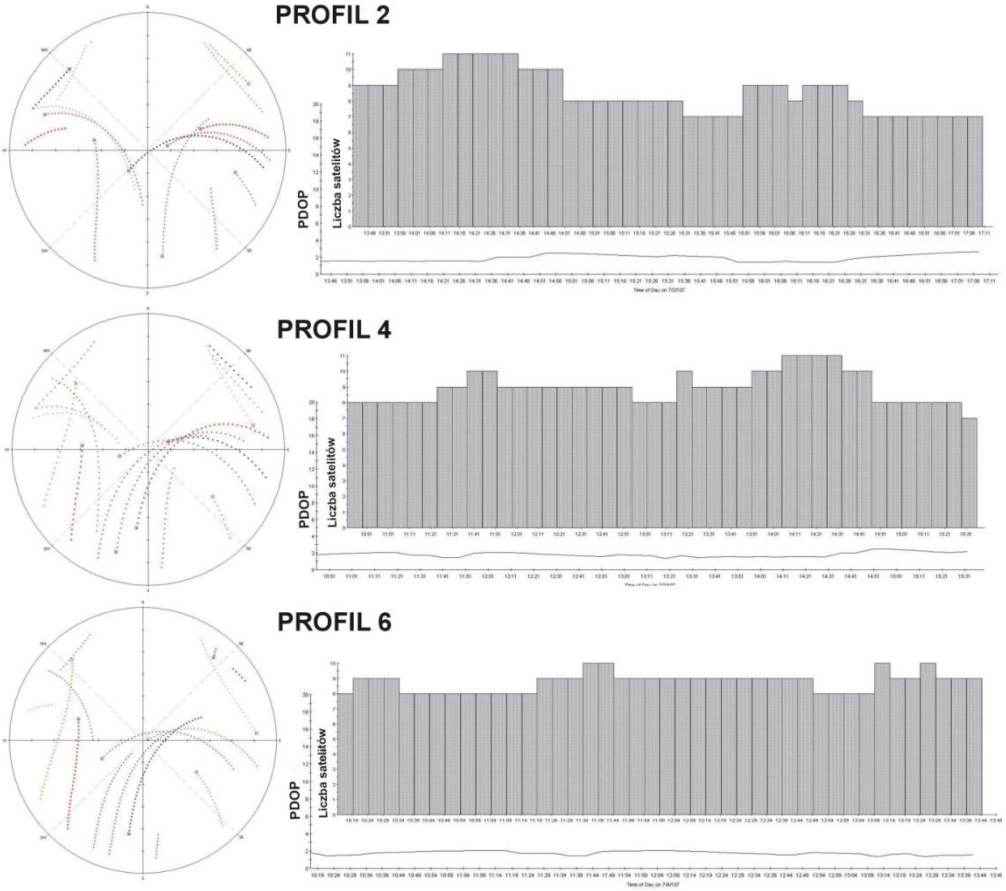

Fig. 4. On the left hand side are the trajectories of the satellites in the sky. On the right – the numbers of visible satellites and PDOP coefficient values during the measurements (profiles 2, 4, 6).

A key parameter in kinematic observations is the PDOP coefficient informing the operator about the current geometrical configuration of the tracked satellites. The smaller the coefficient's value, the more favorable the constellation for correct results. Figure 4 presents the number of visible satellites and distribution of the PDOP coefficient during measurements of the example profiles 2, 4 and 6. The figure also presents the trajectories of the satellites as observed in the sky from the measurement site. Due to specific constellation of the satellite orbits of the GPS system, the northern direction over the territory of Poland is called "a dead area" which means that satellites are not observed there.

4. Processing results

Data from the base and the mobile receiver were processed by means of the Trimble Geomatic Office. The software automatically constructs vectors between the base and the mobile receiver using data collected in the terrain (Fig. 5). The maximum accuracy of determining the distance between the reference and the mobile receivers depends directly on the characteristics of the differential phase measurements and equals about 2 mm (10^{-2} of the phase cycle of the carrier). The continuity of phase observations is crucial for the correct determination of coordinates.

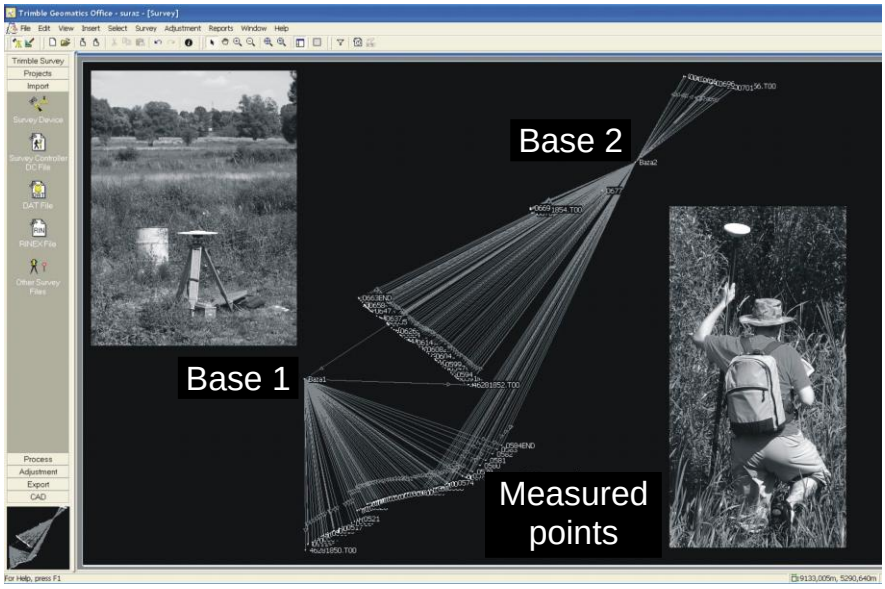

Fig. 5. TGO window – coordinates along profiles 5, 6 and 7 determined using differential measurements related to base 1 and 2.

To improve the quality of results, accurate GPS satellites ephemerid including corrected parameters of orbits and satellite clocks were used in the computational process. Similarly, coordinates of piezometers were determined in a separate measurement campaign (Fig. 6). Unlike during the profiles measurements, to reach a higher accuracy, classical static GPS measurement was applied. Thirty-minute measure-

ment enabled us to increase the accuracy and reliability of water level determination. The necessity of applying a longer period of data acquisition results directly from the satellite measurements characteristics in which the error of height (H) determination is significantly larger than the horizontal coordinates (NE) error.

Fig. 6. Static measurement on piezometers.

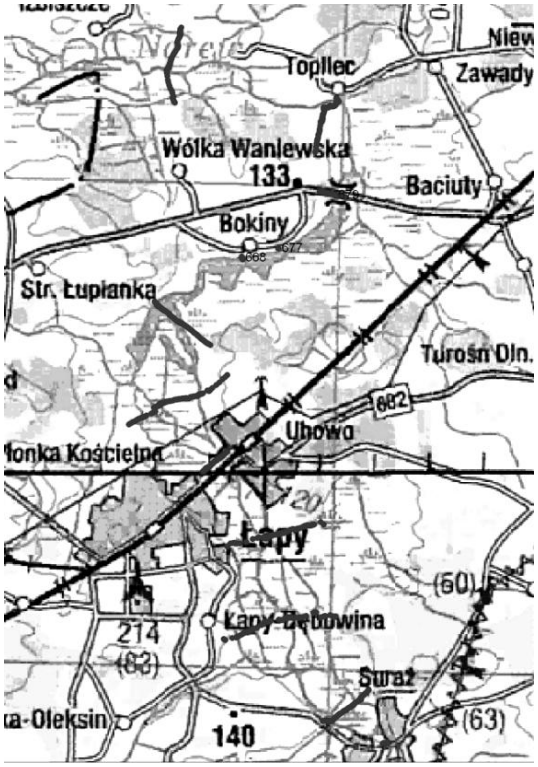

Fig. 7. Representation of measurement profiles on a 1:250 000 scale map.

5. Results and conclusions

The ETRF reference system, common in Europe, was used to process the satellite data. All reference stations in Poland and neighboring countries have accurate coordinates in the system. It is a geocentric system that has transformation formulae to "1992" and "2000" systems. The determined coordinates of the profiles and points of piezometers were converted to the "1992" system. Figure 7 shows profiles represented on a 1:250 000 scale map. Points 668 and 677 indicate points of static measurements on piezometers.

The diagrams in Fig. 8 present course of changes of heights of the selected profiles 2, 4 and 6. The diagrams include also mean errors of the profile points. The values of measurement errors in specific directions are correlated. The changing values of the mean errors depend directly on tropospheric refraction and secondary waves interference. Non-compensated errors of orbits and second order errors of satellite and GPS

receiver clocks are included in indirect errors. Changes of coordinate errors along the measured profiles are within 1 cm, and only in a few points they reach 2 cm. Figure 9 presents changes of coordinates of the analyzed profile points in the "1992" system.

Fig. 8. Measured altitudes (ellipsoidal heights) on profiles 2, 4 and 6, and diagrams of errors of location components (NEH) determination in subsequent points.

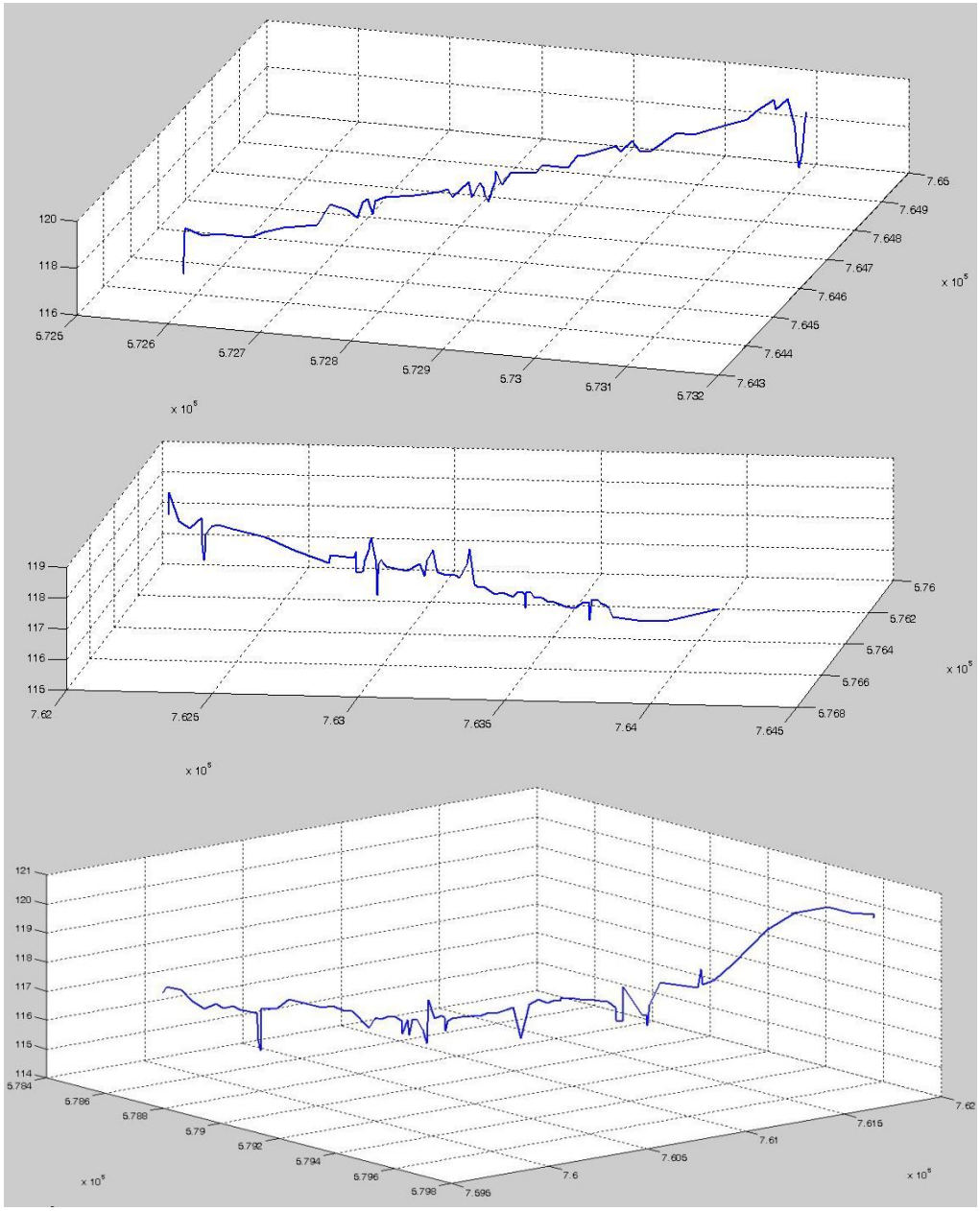

Fig. 9. 3D diagram presenting coordinates of profiles 2, 4 and 6 in the "1992" system.

6. Conclusions

Application of satellite technologies to the acquisition of profiles and consequently to building a numerical model of terrain seems to be justified. Firstly, the economical aspect: the required information concerning fairly large research area was obtained at a relatively low cost. Secondly, the accuracy and reliability of the results is compara-

ble with III-class grid, which is in this case a very good achievement. Mean errors in the profiles do not exceed 1.5 cm for the horizontal components and 3 cm for the vertical component. Determination of the coordinates of local bases using accurate ephemerid had errors of the horizontal components of less than 5 mm and of the vertical component of less than 1 cm. The use of kinematic technology "Stop&Go" proved to be the most effective method of data acquisition for the Narew National Park area.

References

Beser, J., and B.W. Parkinson (1982), *The application of NAVSTAR differential GPS in the civilian community*, Navigation **29**, 2, 107-136.

Bosy, J., and M. Figurski (2003), *Problematyka opracowania obserwacji satelitarnych GPS w precyzyjnych sieciach lokalnych*, Wydawnictwo Akademii Rolniczej, Wrocław.

GUGiK (2005), Zarządzenie Głównego Geodety Kraju nr 20 z dnia 18.11.2005r.

Figurski, M., M. Gałuszkiewicz, and P. Kamiński (2006), *Monitorowanie polskiej sieci stacji referencyjnych GPS*. VIII Sympozjum "Współczesne problemy podstawowych sieci geodezyjnych" 18-19 wrzesień 2006, Kraków.

Lamparski, J. (2001), *Navstar GPS od teorii do praktyki*, Wydawnictwo Uniwersytetu Warmińsko-Mazurskiego.

Specht, C. (2007), *System GPS*, Pelplin.

Wawrzyn, J., and M. Antosiewicz (2003), *Aktywna Sieć Geodezyjna ASG-PL. Podstawowe cele, struktura, zastosowanie, kierunki rozwoju*. Seminarium "Otwarcie Centrum Zarządzania Aktywną Siecią Geodezyjną ASG-PL", Katowice, 25 luty.

PUBLS. INST. GEOPHYS. POL. ACAD. SC., E-9 (405), 2008

Modelling Hydrological Changes of Fluviogenous Wetland: a Landscape-Scale GIS Approach

Andrzej KAMOCKI and Piotr BANASZUK

Institute of Environmental Engineering and Environmental Protection
Białystok Technical University, Wiejska 45a, 15-351 Białystok
e-mail: banaszuk@pb.bialystok.pl

Abstract

Protected wetland of the Narew River valley is experiencing a significant change in water resources, which results in changes in soil and vegetation and affects all groups of wildlife that are dependent on peatland and wet grassland. To counteract this loss of diversity, there is an urgent need to re-establish the appropriate water conditions in order to suppress N and P mineralization and support the development of *Carex gracilis* and *C. elata*. In order to prevent further soil transformations and satisfy the demand of target plant species it is necessary to increase the valley's water storage by ca. $1.1 \cdot 10^6$ m^3. The improvement of hydrological conditions of wetland may be partly achieved by managed flood releases from the Siemianówka Reservoir as well as by reduction of evapotranspiration by vegetation manipulation in the form of mowing or grazing of *Phragmites* stands.

Key words: GIS, DEM, upper Narew River, groundwater, water management.

1. Introduction

Hydrology plays a key role in wetland ecosystem processes, and in determining wetland's structure and functions. An important factor is the water budget of a wetland, which combines inputs from flooding, groundwater and precipitation with outputs from drainage, and evapotranspiration. Amplitude and frequency of water level fluctuations control biota and such characteristics of wetland as organic matter accumulation rates and decomposition (Keddy 2000). Water conditions change over many time scales and are related to a range of external factors, such as fluctuations in water source, climate, and land use within a catchment or within a wetland itself (Mitsch and Gosselink 1993). Climate change has been projected to have major impacts on regional and temporal water distribution and availability. Based on the global model of climate change, it has been concluded that the most vulnerable areas are those characterized with temperate climate conditions where most of precipitation currently occurs mainly in the form of winter snowfall and the stream-flow is largely generated by

spring and summer snowmelt. In these areas, a temperature increase may lead to an increased winter runoff and a reduced spring flood pulse (Bergkamp and Orlando 1999).

The upper part of the Narew River valley upstream of Rzędziany (NE Poland) is one of the last extensive undrained, non-reclaimed valley wetlands in Central Europe. However, for many years, negative changes in habitats and vegetation of the Narew floodplain are observed (Banaszuk H. 1996). The extensive multidisciplinary researches, carried out in the years 2000-2002, pointed to a reduction in the depth and duration of the river flooding, as well as to the drop in groundwater levels, both of which result in changes in soil and vegetation and affect all groups of wildlife, which are dependent on peatland and wet grassland.

The main objective of this study is to model water resources of Narew wetlands within protected area of the Narew National Park (NNP) and calculate water shortages that need to be replenished in order to satisfy the demand of key plant communities.

2. Study area

The Narew River originates in the Dikoe Bołoto wetland area in western Belarus at a height of 159 m a.s.l. With a length of 484 km (36 km in Belarus and 448 in Poland) it is the fifth longest Polish river (Fig. 1). The valley ecosystem was characterized by a mosaic of diverse wetland biotopes: fluviogenous peatlands, alluvial marshes, active and abandoned channels of anastomosing river, as well as small mineral islands that stretched along the whole river from its source to the junction with the Biebrza River. From 1969 to 1980, the course of the Narew River between the junction with the Biebrza River and Rzędziany village (ca. 50 km) was comprehensively regulated. The regulation lowered the average river level (Mioduszewski and Gajewska 2000), resulting in a decrease in flooding frequency and depth, which had a rapid and negative effect on the hydrology, soil, vegetation and wildlife of adjacent marshes. In locations neighbouring the river bed that was channelled, mineralization and compression of drained peat led to surface subsidence of up to 3-4 cm/yr. Reclamation of the floodplain also caused near-complete disappearance of the network of interconnected channels and old river beds that make up the anastomosing Narew River (Banaszuk H. 1996). The anastomosing river system and its characteristic multiple riverbeds and extensive fluviogenous peatlands have survived only in the valley between Rzędziany and Suraż. Since 1996, this part of the valley has been legally protected as the Narew National Park (NNP).

Mean river discharge at Suraż amounts to about 15 $m^3 s^{-1}$, ranging from 120 to 5 $m^3 s^{-1}$. In periods of extremely high flood, water discharges can reach up to 250 $m^3 s^{-1}$ (recorded in 1979). The Narew's flow regime reflects the influence of snowmelt; hence the highest flows occur in late winter and early spring. Annual flooding usually occurs in the period from the beginning of March until May, occasionally until June. During this period, considerable parts of the valley are inundated (Banaszuk H. 1996).

The vegetation of NNP still consists of natural peat-forming plant communities – sedge *Caricetum elatae* and *C. gracilis* community and reedy rushes *Phragmitetum*

communis. Small clusters of *Salicetum pentandro-cinereae* and single arborescent willows occur locally. Alder carrs (*Ribo nigri-alnetum*) are found sporadically at the valley margins (Dembek *et al*. 2002). Due to its exceptional importance for birds, NNP has been designated a Wetland of International Importance under the terms of the RAMSAR Convention.

On the upper course of the Narew River, near the Poland-Belarus border, the artificial dam reservoir of "Lake Siemianówka" was constructed (Fig. 1). The reservoir was placed about 80 km above the southern boundary of the NNP and has an area of 3000 ha and a mean water capacity of ca. $80 \cdot 10^6$ m^3. It is the only important artificial factor which may potentially alter natural flood pulse dynamics of the river.

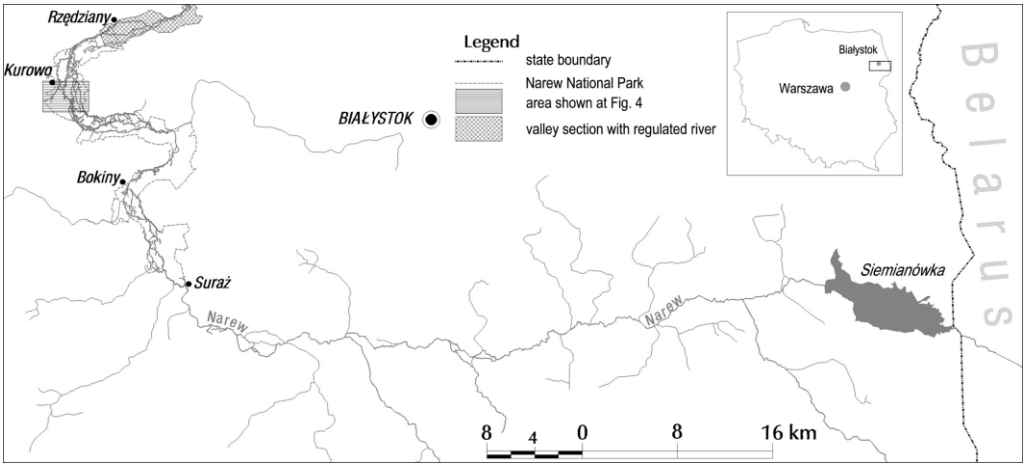

Fig. 1. Location of study site within the upper Narew River system.

NE Poland is located in a temperate climatic zone with distinctly marked continental and a lesser boreal influence. Mean air temperature is 6.9°C. Monthly average temperatures range from –4.5°C in the coldest month of the year (January) to 17.3°C in the warmest (July).The mean annual precipitation in the region is 584 mm (1956-2006), of which 60-70% falls between April and September. Permanent snow cover occurs on average on 70-80 days every year, between late December and early March. In winter, the depth of ground frost penetration varies from 30-50 cm depending on atmospheric conditions. On average, storms occur on 20-25 days a year (Górniak 2000).

3. Materials and methods

The environmental characteristics thought to affect or to be related to hydrological conditions of Narew River wetland habitats were compiled in digital form using a Geographical Information System (GIS) and included Digital Elevation Models (DEM), thickness and types of surficial deposits and soils, measurements of the groundwater table (Banaszuk P. 2004) and water properties of organic deposits (Jaros 2004). Modelling was conducted by use of Bentley's GeoEngineering GIS software.

4. Digital Elevation Models (DEM)

Digital Terrain Model (DTM)

Geodetic and photogrametric positions have been used to define the geometry of both the River Narew valley and the adjacent area. The method has made it possible to increase DTM optical resolution in the valley area where land surveying was scattered. DTM has been developed with the use of triangle irregular network (TIN) and GRID vector data models.

DEM of subpeat elevation

Digital Elevation Model (DEM) of subpeat features has been developed on the basis of point records of organic deposits thickness obtained from auger boring (> 300 points) and soil maps. As a result of volume analysis which involved subtracting the DEM of the peat bottom from the DTM containing information on the wetland surface elevation a three-dimensional model of the depth of organic deposits has been developed.

DEM of groundwater level during summer droughts

In order to determine the current water shortage, DEM illustrating the elevation of water table registered in the summers of 2000 and 2001 (> 300 measurements) has been developed. The main problem connected with an accuracy of the DEM was its resolution and quality – relatively small number of measurements performed at various times. The DEM did not cover the whole mire area protected within the borders of NNP (6 810 ha) and was carried out only for part of mire (4 587 ha, 67% of the area of NNP) where reliable data were available.

DEM of required groundwater level

The DEM was obtained basing on the assumption that the depth of groundwater, favourable for growth of target Carex communities, should lay not deeper than –20 cm below the ground's surface during summer and autumn months. The 20 cm layer was subtracted from the elevation of mire surface within the reference boundaries.

5. Water retention

The main data source for the calculation of water retention was a set of types of surficial deposits elaborated in the digital form as a part of the dataset included in the "Narew National Park Protection Plan". We divided soil types into homogeneous units characterized by different water retaining capabilities: paludified peat soils, muck-peat soils, muck soils and mud soils. Each three-dimensional soil unit was sliced into a series of layers, 10 cm deep, and to each layer (according to degree of humification and botanical composition of the peat) the averaged value of water storage capacity was attributed. For those purposes we collected all available data from field and laboratory experiments on different organic sediments under various land uses and water management conditions in the Narew mire.

Basing on readings of water table depth made during a vegetation period of the years 2000-2001 (> 300 measurements) the following characteristics were calculated for each of the delineated units:

- the maximum water storage capacity in saturated part of soil profiles using volumetric water content,
- the water storage capacity in saturated part of soil profiles during the drought period when the lowest stage of water table was observed,
- the required water storage capacity in saturated part of soil profiles with respect to demand of target plant communities based on the assumption that the groundwater for summer and autumn should lay not deeper than 20 cm below the ground's surface.

6. Results and discussion

In recent decades, earlier snowmelt and runoff led to a reduction in surface-water inflows to the valley floodplain, diminished the duration and degree (area and depth) of flooding and resulted in diminished availability of water during periods of high demand. The water shortages have been exacerbated by a decrease in summer rainfall; therefore, from the mid 1980s, a steep decline in the groundwater table and a decrease in the volume of water stored in organic sediments of the valley were observed (Banaszuk and Kamocki 2008).

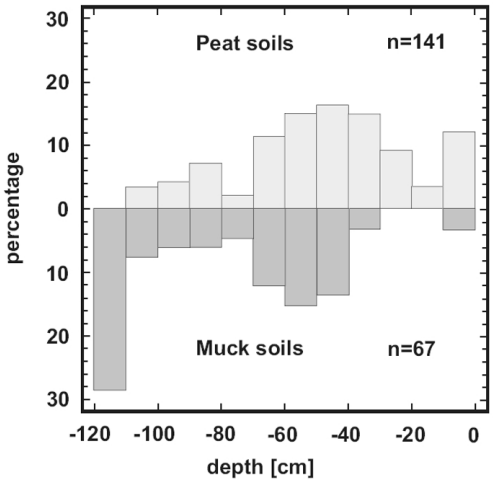

Fig. 2. Frequency histogram of groundwater table measured in peat soils (upper panel) and muck soils (lower panel) during summer months (June-August) of the years 2000-2002 (after Banaszuk and Kamocki, 2008).

In the wet 1970s, throughout the summer months, groundwater level occurred with the highest frequency between +10 and +20 cm and for one half of the period the mire was inundated (Banaszuk and Kamocki 2008). Progressing dewatering of the mire resulted in groundwater table drawdown. The frequency histogram of the groundwater

levels measured in peat soils in the summer (June-August) of 2000-2001, with its mode 40-50 cm below ground surface, reflected the lowered water supply by overbank flooding and atmospheric precipitation (Fig. 2). Significantly worse water conditions characterized muck-peat and muck soils where, in summer, groundwater level occurred with a highest frequency at 50-60 cm below ground surface. In driest places, the water table dropped well below –100 cm.

The observed changes in occurrence of the water table affected the water resources stored in the organic sediments. In the summer months of the extremely dry years 2000-2001 volume of water stored in the saturated part of the soil profiles reached $39.7 \cdot 10^6$ m^3, while maximum calculated water storage amounted up to $42.8 \cdot 10^6$ m^3 (Table 1).

Table 1

Water retention of hydrogenic soils

Type of soil	Maximum retention	Dry-period retention	Desirable retention
	[10^6 m^3]	[10^6 m^3]	[10^6 m^3]
Paludified peat soil	15.16	14.73	14.82
Muck soil	8.15	7.39	7.66
Muck-peat soil	15.70	14.40	15.12
Mud soil	3.29	3.21	3.23
Total	42.30	39.73	40.83

We calculated the water shortages with respect to groundwater level favorable to development of *Carex gracilis* and *C. elata*, which have been appointed as key target plant species in the Narew mire (Dembek *et al*., 2002). At present, *Carex* experiences a water stress, with the groundwater table falling below its ideal range, which has been estimated (Koska, 2001) to lay between –30 and +30 and more, with the median depth occurring no deeper than 20 cm below the ground's surface. In dry years 2000-2001 the preferred water level was not reached on 73% of the studied area (note histogram at Fig. 3). The worst water conditions for *Carex* development were found in the longitudinal stretch of the valley northern of Łapy and between Kolonia Topilec and Izbiszcze, where water table lays deeper than 40 cm below optimal range (Fig. 3). Low water level was also typical for the interchannel areas far away from the watercourses where groundwater levels fell to 50-70 cm below ground (Fig. 4). Favorable waterlogged conditions were found only locally, in a narrow belt along river branches or in places where prominent groundwater discharge from hillslope aquifers occurred and impermeable near-stream sediments impeded seepage toward the river, leading to inundation of topographical depressions behind the natural fluvial levee. Such hydrological conditions were typical for the valley stretch between Bokiny and Topilec. Waterlogged areas were also found sporadically in small depressions located between river branches in northern part of NNP (Fig. 3).

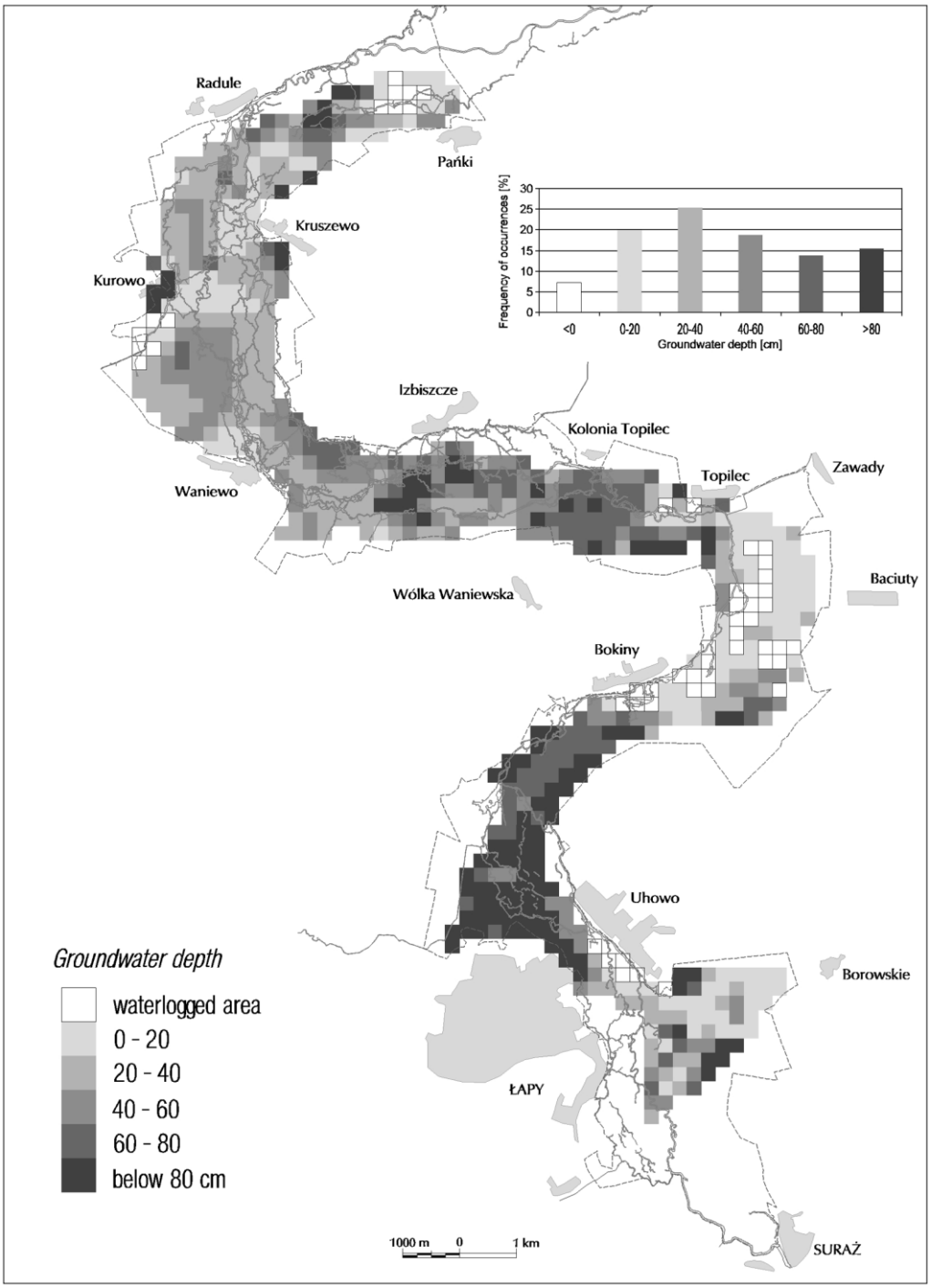

Fig. 3. Groundwater shortages, showed as differences between measured and desirable (20 cm below surface) depth to the water table, with respect to demand of *Carex elata* and *C. gracilis* along the Narew River wetland – the grid model with discretization of 250 m.

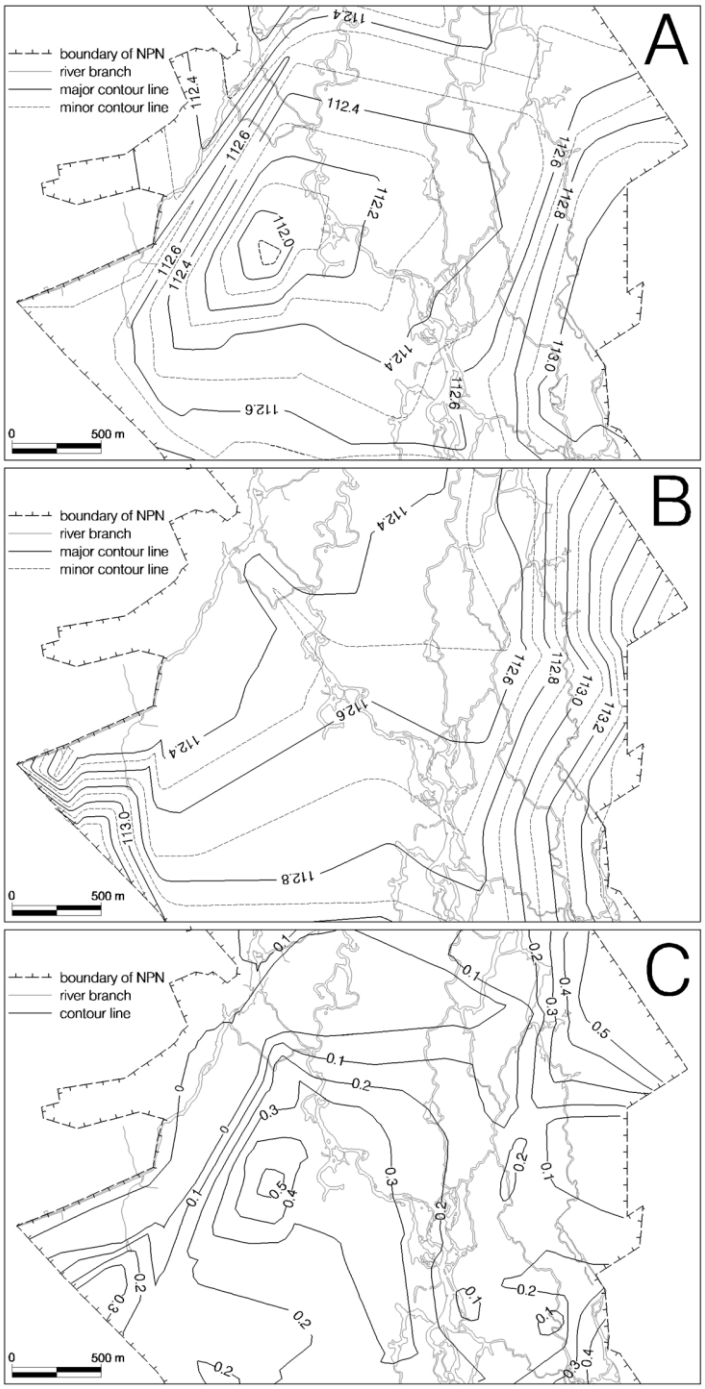

Fig. 4. The water conditions of Narew wetlands in the vicinity of Kurowo village. Panel A – contour model of groundwater elevation during summer droughts (July-August) 2000-2002; panel B – preferred water level; panel C – water deficiency with respect to demands of *Carex elata* and *C. gracilis*.

Lowered water level has ultimately negative effects on Narew wetlands, resulting in enhanced soil organic matter decomposition, release of biogens, and consequently in eutrophication of habitats. Increased productivity is of special concern, as it was found to support the spread of *Phragmites* at the expense of other plant species, which are unsuccessful in competing for light (Wassen *et al*. 2005). In the long run, a progressive internal eutrophication of mire may lead to complete elimination of the low-productive floodplain zone, which is usually responsible for most conservation values of riparian fens (Wassen *et al*. 2005). A spread of tall halophytes (*Phragmites*) also affected bird species richness (Sterzyńska 2004).

To counteract this negative alteration of wetland ecosystem, there is an urgent need to re-establish the appropriate water conditions in order to suppress N and P mineralization and support the development of *Carex gracilis* and *C. elata*. Our calculations showed that in order to prevent further soil transformations and satisfy the demand of target plant species it is necessary to increase the valley's water storage by ca. $1.1 \cdot 10^6$ m^3.

Our previous study suggested that the countering of climate-related threats to hydrology and biodiversity of the Narew mire by use of common restoration techniques (blocking of ditches or damming of watercourses) might be difficult if at all possible (Banaszuk and Kamocki 2008). It deems that the hydrological conditions of wetlands may be greatly improved by managed flood releases from Siemianówka Reservoir. However, at present, nature protection needs are not taken into account by the dam operators. Moreover, responsibilities for planning and regulation of Siemianówka operation regime are spread across several institutions, which would complicate management co-ordination and the identification of responsibility for realization of recommended environmental measures.

The improvement of hydrological conditions of wetland may be partly achieved by large vegetation manipulation in the form of mowing or grazing. This could reduce evapotranspiration (ET) by 170 mm·m^{-2}·year^{-1} and might lead to minimizing both the extent and the duration of groundwater drawdowns (Banaszuk and Kamocki 2008).

7. Conclusions

The protected wetland of the Narew River valley is experiencing a significant change in water resources, which results in changes in soil and vegetation and affects all groups of wildlife that are dependent on peatland and wet grassland. To counteract this loss of diversity, there is an urgent need to re-establish the appropriate water conditions in order to suppress N and P mineralization and support the development of *Carex gracilis* and *C. elata*. In order to prevent further soil transformations and satisfy the demand of target plant species it is necessary to increase the valley's water storage by ca. $1.1 \cdot 10^6$ m^3. The improvement of hydrological conditions of wetland may be partly achieved by managed flood releases from Siemianówka Reservoir as well as by reduction of ET by vegetation manipulation in the form of mowing or grazing of *Phragmites* stands.

Acknowledgements. This research was funded by Ministry of Higher Education and Science (grant 2 P04D 009 29) and Technical University of Białystok (grant S/WBiIIŚ/21/08).

References

Banaszuk, H. (ed.) (2004), *Przyroda Podlasia. Narwiański Park Narodowy*, Wyd. Ekonomia i Środowisko, 432 pp.

Banaszuk, H. (1996), *Paleogeografia, naturalne i antropogeniczne przekształcenia doliny Górnej Narwi*, Wyd. Ekonomia i Środowisko, Białystok, 213 pp.

Banaszuk, P. (2004), *Gleby i siedliska glebotwórcze Narwiańskiego Parku Narodowego*. **In:** H. Banaszuk (ed.), "Przyroda Podlasia. Narwiański Park Narodowy", Wyd. Ekonomia i Środowisko, 141-158.

Banaszuk, P., and A. Kamocki (2008), *Effects of climatic fluctuations and land-use changes on the hydrology of temperate fluviogenous mire*, Ecol. Eng. **32**, 2, 133-146.

Bergkamp, G., and B. Orlando (1999), *Wetlands and climate change: exploring collaboration between the convention on wetlands (Ramsar, Iran, 1971) and UN framework convention on climate change*, IUCN, Gland, Switzerland.

Dembek, W., M. Szewczyk, and Z. Oświęcimska (2002), *Ochrona Ekosystemów lądowych. Plan Ochrony Narwiańskiego Parku Narodowego*, manuscript.

Górniak, A. (2000), *Klimat województwa podlaskiego*, IMiGW, Białystok.

Jaros, H. (2004), *Właściwości retencyjne gleb Narwiańskiego Parku Narodowego*. **In:** H. Banaszuk (ed.), "Przyroda Podlasia. Narwiański Park Narodowy". Wyd. Ekonomia i Środo-wisko, 172-184.

Keddy, P.A. (2000), *Wetland ecology, principles and conservation. Cambridge Studies in ecology*, Cambridge University Press, UK.

Mioduszewski, W., and B. Gajewska (1999), *The effect of the Narew River regulation on water levels in the lower part of the Biebrza River*. **In:** W. Mioduszewski, and M.J. Wassen (eds.), "Assessment of the effect of changes in water management within the Central Biebrza Basin", Falenty, Poland.

Mitsch, W.J., and J.G. Gosselink (1993), *Wetlands*, 2nd Edition. New York: Van Nostrand Reinhold.

Sterzyńska, M. (2004), *Fauna lądowa*. **In:** H. Banaszuk (ed.), "Przyroda Podlasia", Narwiański Park Narodowy, Wyd. Ekonomia i Środowisko, 281-304.

Wassen, M.J., H.O. Venterink, E.D. Lapshina, and F. Tanneberg (2005), *Endangered plants persist under phosphorus limitation*, Nature **437**, 547-550.

PUBLS. INST. GEOPHYS. POL. ACAD. SC., E-9 (405), 2008

Assessment of Water Requirements of Swamp Communities: the River Narew Case Study

Tomasz OKRUSZKO[1] and Adam KICZKO[2]

[1)] Division of Hydrology and Water Resources,
Warsaw University of Life Sciences
ul. Narutowicza 11/12, 80-952 Gdańsk, Poland
e-mail: t.okruszko@levis.sggw.pl

[2)] Institute of Geophysics, Polish Academy of Sciences
ul. Księcia Janusza 64, 01-452 Warszawa, Poland
e-mail: akiczko@igf.edu.pl

Abstract

An appropriate hydrological regime within a wetland area is essential for the survival of its ecosystems. This regime is related to the water inputs which vary with the type of wetland. Swamps are characterized by a long lasting inundation formed by the flooding condition in the river, which is a main source of water for this kind of wetland. In the valley of River Narew, swamps are under protection within the Narew National Park. This paper presents an estimate of the water requirements of the Narew swamps using a hydrodynamic model and historical data prior to recent major changes in the hydrological regime of the system. Three swamp plant communities were analysed, namely: reeds, sedges and alder forest with willow bushes. The analyses were performed for seven representative valley transects. The frequency of flooding in each community for every transect was identified using 15-year historical data. The analysis resulted in the estimation of the average frequency of flooding required for the protected wetland ecosystems. Those estimates can be used as an environmental flow that should be maintained in the water system of the Upper Narew river basin.

1. Introduction

"Hydrology is probably the single most important determinant of the establishment and maintenance of specific types of wetlands and wetland processes" (Mitsch and Gosselink 2000). An appropriate hydrological regime within a wetland is essential to maintaining goods and services, such as habitat provision for plant and animal species that may be important for socio-economic reasons or for their biodiversity. The regime may vary in different parts of any wetland, creating a mosaic of different conditions.

Significant changes to the hydrological regime of wetlands from its natural state may lead to a decline in ecological status. Thus, knowledge of the hydrological characteristics of wetland communities forms a basis for their protection or restoration (Ackerman *et al.* 2005). For the protection of riparian wetlands, environmental flows should be recognised as those which can meet the water requirements of wetland plant communities.

2. Wetland's classifications and water needs

There is no strict answer to the question: "What is a wetland?" Depending on who is asking and for what purpose, there are many wetland definitions and the terms used are often confusing and even contradictory. Amongst all the most commonly used definitions of wetlands (Ramsar Convention definition, US Fish and Wildlife Service definition, Committee on Characterization of Wetlands definition) three main features may be distinguished: (1) areas classified as wetlands can be recognized by the presence of water, either at the surface or within the root zone; (2) they often have unique conditions that differ from adjacent uplands (accumulated organic plant material that decomposes slowly) and (3) they support a variety of plants (*hydrophytes*) and animals adapted to the saturated conditions. Unfortunately, the terminology for describing wetlands varies among both human societies scientific communities (Gore 1983, Keddy 2000).

In order to avoid the use of a confusing number of terms and names, wetlands in this work were divided into four different classes based on peat accumulation and major hydrological characteristics. Where peat is being accumulated wetlands are called mires. Depending on the main source of water, mires can be divided into bogs and fens. Wetlands where peat does not occur are called marshes. Swamps are wetlands where there is no requirement that peat is formed. They are characterized by a very long inundation period during each year. (Sometimes the word "swamp" is also used as a synonym of wetland forest with almost permanent water presence above the soil surface, but this is not the case here).

Mire is a kind of wetland where peat formation is present. Peatland is an area of peat accumulation that is being drained for farming, peat extraction or any other purposes.

Fen usually emerges in land depressions or river valleys. It is fed mainly by groundwater, with some additional input of surface water and rain. Considerable water movement through a shallow peat layer provides nutrients and minerals, which ensures rich vegetation. Due to alkaline reaction, fen is characterized by grasses (mostly dominated by sedges), reeds and tree communities, such as willows (*Salix sp*.), birches (*Betula L*.) and alders (*Alnus sp*.).

Bogs are formed in two cases, either in a watershed location where rainfall has no drainage network and locally inundates the earth surface for a long period or in the case where the peat layer builds up and separates the fen from its groundwater supply for a certain time period. In the latter case the fen receives fewer nutrients and may transform into an acidic bog fed only by a direct rainfall. It can then grow, above the

level of the fen, receiving moisture from the precipitation. Rain not only washes the hydroxide ions out of the peat but also adds carbonic acid from carbon dioxide dissolved in the rainy water, changing the ground pH to more acidic. Nutrients are provided entirely by precipitation, which accounts for their low plant nutrient status. Vegetation adapted to acidic conditions is characteristic of bogs: *Sphagnum* moss and small sedges, pines and dwarf birches rooted in deep peat.

Fens and bogs are typical of the northern hemisphere and are generally associated with low temperatures and short growing seasons, where ample precipitation and high humidity cause excessive moisture to accumulate. Examples of fen-type wetlands include the extensive peat accumulating areas in northern Canada and Russia, as well as smaller seepage areas (fens) or watershed zones (bogs) throughout the temperate zone.

As already mentioned, there is no commonly accepted definition of swamps. According to the U.S. definition, swamp is a wetland with prevalent area covered by trees or shrubs. In Europe, forested fens (alder forest) or wetlands dominated by reed grass are also called swamps.

In this work it is assumed that swamp is a wetland dominated by reed grass (*Phragmites)*, woody vegetation (mostly *Alnus sp*) or papyrus (African wetlands). This type of wetland is permanently inundated by shallow water bodies with substantial numbers of hummocks or dry land protrusions. Unlike fens and bogs, swamps are not always peat-accumulating wetlands. In a number of cases, the major soil type developed here is mud. Due to environmental conditions, swamp vegetation is adapted to growing in standing or slowly flowing water. Similarly to the previously mentioned wetland types, water in swamps is rich in tannins from decaying vegetation, which gives it a characteristic brownish colour. Swamps are usually associated with adjacent rivers or lakes.

Marsh is a frequently or continually inundated wetland, which is shallower and has less open water surface than a swamp. The flooding phenomena are much more dynamic, leading to the development of alluvial soils. Also in contrast to a swamp, marsh has no woody vegetation. Marsh receives most of its water supply from surface water, sometimes being also fed by groundwater. Nutrients are plentiful and the pH is usually neutral leading to an abundance of plant and animal life. The flora colonizing marshes is typically herbaceous, dominated by grasses, rushes, reeds, typhas and sedges. Plants are rooted in mineral soil substrate and they are perfectly adapted to temporally saturated soil conditions.

3. Swamps and marshes of the River Narew

The need for identification of the water requirements of wetland communities arises from the main water management problem of the valley of Upper Narew (NE Poland), where there is a question of conflicting mitigation between flood control and wetland protection in the area downstream of the medium-sized (70 mln m^3) Siemianówka Reservoir. The area of the catchment of the Upper Narew covers approximately 7300 km^2 and the river's hydrological regime is typical of those for the lowland rivers. It is characterized by a single spring flood caused by snow melting, and quite a balanced

summer runoff. Raised water stages in summer occur occasionally. Given the morphological conditions (Banaszuk H. 1996, Banaszuk P. 1996), three reaches of the Upper River Narew valley can be distinguished (Fig. 1).

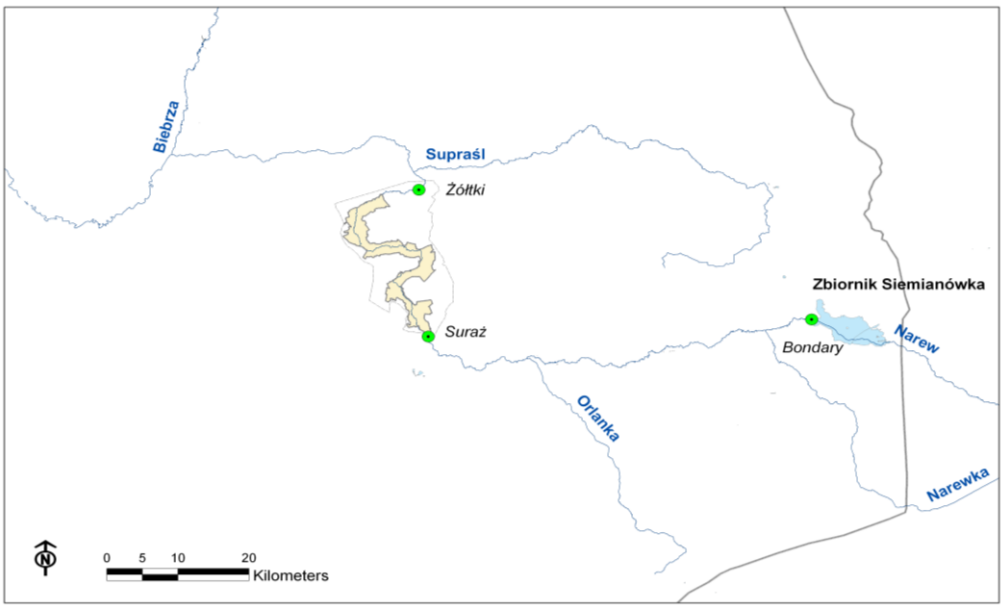

Fig. 1. The hydrographic system of the Upper River Narew.

The first reach extends from the Siemianówka Reservoir to the narrowing of the valley in the vicinity of the Suraż settlement. It is a relatively narrow valley, flooded for a short time every year. It is typical of marsh wet meadows becoming dry-ground forests. In the lower part, increasing inundation has formed some swamps covered by reeds.

The second valley reach includes the wetlands between Suraż and the Żółtki gauge. In 1994 the Narew National Park (NNP) was established to preserve the unique nature of this part of the valley. The Park is an area of outstanding natural value, including unique ecosystems of plant communities, favoring the existence of a variety of bird species. It seems, however, that local conservations measures may be insufficient to maintain wetland processes because the level of surface waters in the Park depends to a greater extent on the water resources in the upper part of the catchment than on its own resources. The basic objective of water management for this area is the maintenance of flow rates in the river which ensure the appropriate soil moisture in the surrounding swamps.

The third reach extends downstream of the NNP boundary. River training works on the bed of the River Narew and reclamation measures took place in the 1970s. Those activities dramatically changed the features of the valley, which used to be a swamp area similar to those located in the upstream part, although with longer periods of inundation. At present the numerous drainage and irrigation (subsurface) systems allow for intensive grassland and pastures cultivation.

Marsh and swamp communities present in the valley of the River Narew depend on habitats inundated by surface water during the flooding period (spring). In order to protect the unique value of the wetland ecosystems (especially the ecosystems located within the NNP area) environmental flow conditions should be identified which will be a part of the water management scheme for the Siemianówka storage reservoir. Thus, the hydrological characteristics important for wetland ecosystems should be recognised.

4. Identification of water requirements using historical flows

4.1 Hydrological characteristics important for wetland ecosystems

In general, there are two main tools used for establishing water management plans on the catchment scale, namely, surface water balance models and/or regional groundwater models. A water management scenario is chosen on the basis of different decision criteria, describing the consequences of water deficit.

In order to perform the necessary calculations for catchments where wetlands are present, the water demand of different type of wetlands and their water supply system should be identified. In this paper, an approach which uses hydrological characteristics of particular wetland ecosystems has been employed (Okruszko 2005). The type of hydrological feeding describes the main sources of water, from the rain, ground water or surface water. Then the hydrological parameters for the different habitats (e.g., flooding frequency, maximum depth of groundwater, average water logging period, etc.) can be used as decision criteria.

Swamps and marshes belong to the habitats with the so-called fluviogenic type of hydrological input, which means that the river plays a major role in creating the water logging conditions. The role of the river is not only in flooding but also in draining the habitat – faster, in the case of marshes and slower, allowing for long inundation in the case of swamps. This means that the frequency of flooding specifying how many days during the year water is above the soil surface is the best single hydrological characteristic describing the water requirement of the wetland. For the riparian wetlands (i.e., wetlands neighbouring the river and being supplied with water from the river), environmental flow should be identified using this characteristic.

4.2 Value of information given by historical flows

Wetlands form dynamic systems which can be relatively easily disturbed by changing water conditions. Depending on the severity of hydrological changes, different processes take place leading to a secondary succession and new vegetation (Kotowski 2002). Such processes are often non-reversible (Bootsma M. 2000). Such a change can be created either by *in situ* activity such as drainage or dykes construction, or by activities located downstream from, or upstream of, the wetland.

In the case of the River Narew wetlands, the second option took place. In the late 1970s the River Narew was partly transformed by river training downstream from the Żółtki gauging station. This activity was buffered by construction of a weir at Rzędziany (downstream of the NNP border) and by building the so-called buffer zone

which allowed for a gradual decrease in water level from the park area to the neighbouring actively drained grasslands. More significant impact was detected after construction of the Siemianówka reservoir in the upstream part of the Narew River (see Fig. 1) in 1992. This multipurpose water reservoir can be relatively efficient in flood protection in the first reach of the system and in some cases also in the second, which was proved by the hydrological modelling by Kubrak *et al*. (2005).

In order to estimate the water requirements of the swamp communities of the Narew National Park, historical flow records prior to the reservoir construction have been chosen for the analysis. This approach, suggesting research in relatively undisturbed conditions, was used in some eco-hydrological studies by Wassen *et al*. (2002) or Van Asmuth *et al*. (2002). Moreover, Dembek *et al*. (2004) suggested that swamps and marshes of the Narew are undergoing ecological changes since the early 1990s. This information leads to a main assumption of the current work that the identification of historical records of inundation frequency in protected habitat should serve as a water requirement of swamp vegetation in the area of NNP.

4.3 Matching historical flows and wetland plant communities

The hydrological characteristics might be derived using hydraulic models of the particular habitats. For the riparian wetlands, the most important are the characteristics of the inundation of certain parts of the floodplain by the river. Steady-state models of surface water might be used to identify the extent of the flood or average depth of flooding; unsteady state models can be used for calculating flooding frequency or duration of inundation. Okruszko *et al*. (2006) proved that there is a good match between the modelled extension of flooding, the identified source of water and the presence of major wetland plant communities.

In the case of the swamps located in the valley of the Upper River Narew, a hydrodynamic model has been chosen as an appropriate tool for inundation frequency identification. The model simulated water stages in the river and the river valley during floods in the historical data. As there is no good quality Digital Elevation Model (DEM) for the park area, a method of representative transects has been chosen in order to match the extension of historical flows and wetland plant communities, which cover the hydrogenic part of the river valley. The habitats of interest were identified on transects and their extension through the valley was estimated. It was assumed that in order to overcome model and transects identification errors, a certain number of river sections will be chosen and the results will be averaged for each swamp community.

5. Identification of environmental flows for wetland protection in the valley of the Upper Narew River

5.1 Swamp communities in the River Narew Valley

The wetlands of the River Narew Valley within the borders of NNP have a fluviogenic type of hydrological feeding. Inundated peat soils and mud cover more than 80% of the park area (Banaszuk P. 2002). It means that the river and especially river flooding play the most important roles in habitat formation. Groundwater and precipitation are

much less significant. As peat soils are formed in anaerobic plant decomposition, the duration of flooding should be long enough to exclude the aeration of the soil profile. Thus, we can classify wetlands located in NNP as swamps, using the simplified hydrological and soil classification of wetlands presented in the first section of this paper.

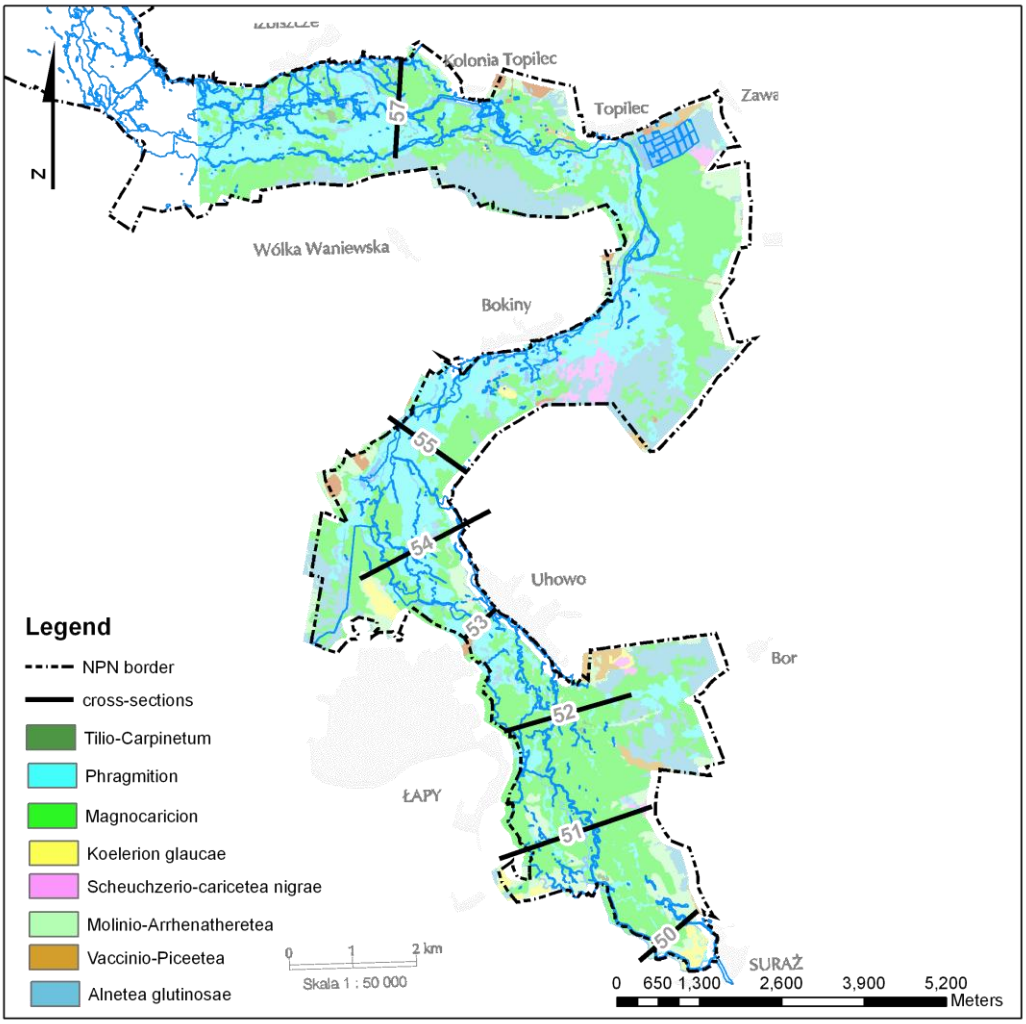

Fig. 2. Major types of vegetation in the Narew National Park (Dembek *et al*. 2004).

According to the map presented in Fig 2, there are five major wetland plant communities in the valley. Two of them are reeds (*Phragmition)* and big sedges (*Magnocaricion*) typical of the swamp valley flooded by the river. Alder and willow *(Alnetea glutinosae)* communities are located closer to the valley edge; in the lower part they are supported by the river but sometimes in the drier period also by the ground water. Two other communities, namely small sedge community *(Scheuchzerio-caricetea nigrae)* and *Molinio-Arrhenatheretea* meadows, are located close to the valley edge

and are supplied by groundwater (forming the so-called soligenic type of feeding). For the further analysis, the three first wetland communities were chosen.

5.2 Hydrodynamic model of the flooding phenomena in the Narew valley

The Upper River Narew system was modelled using the UNET model (Barkau 1993) designed to perform one-dimensional hydraulic calculations for a full network of natural and constructed channels. Model calibration was performed by adjusting the Manning coefficients separately for the main channel and left and right floodplains, as described in (Kiczko *et al*. 2008). It was assumed that it is possible to distinguish subreaches of the river where roughness coefficients do not change. In this application, the river was divided into 4 such sub-reaches between the river gauges for which observations were available. Water surface slope was used as a downstream boundary condition.

Because of the lack of data on lateral inflows, with the exception of the Narewka and Orlanka tributaries, the model mass balance was a problematic issue. It was assumed that unmeasured lateral inflows are linearly correlated with the two known tributaries and can be estimated using linear regression.

The roughness of channel and floodplains varies seasonally due to the variation of vegetation throughout a year. However, in order to reduce the size of parameter space, roughness parameters were set constant during a year. Therefore, the calibration was performed for mixed conditions to include different vegetations periods, for 12 roughness coefficients and 2 linear correlation coefficients for unobserved inflows (see Kiczko *et al*. 2008).

5.3 Simulation of historical flows

The UNET model simulations were performed using 15 years of historical flow data. The period of simulations prior to the construction of the Siemianówka reservoir was chosen. The flow data were taken from the gauging stations upstream of the Narew National Park and two controlled lateral inflows of the rivers Narewka and Orlanka.

Water stages were calculated for all cross-sections but only seven valley cross-sections were chosen for further analysis. Three major types of swamp vegetation, reeds, big sedges and alder wood with willows bushes, are present in these cross-sections (Fig. 3).

The results of the simulations have the form of hygrograms of water stages in the cross-sections of interest. An example is presented in Fig. 4.

5.4 Identification of frequency of flooding of selected marsh communities

The frequency of flooding was calculated by comparing the length of section covered by the targeted vegetation type with the length of that section inundated by water for each day. The numbers of days when inundation took place within 50%, 75% and 100% of each cross-section were calculated and divided by the number of days of simulation. The results of the calculations are presented in Table 1. There is a very

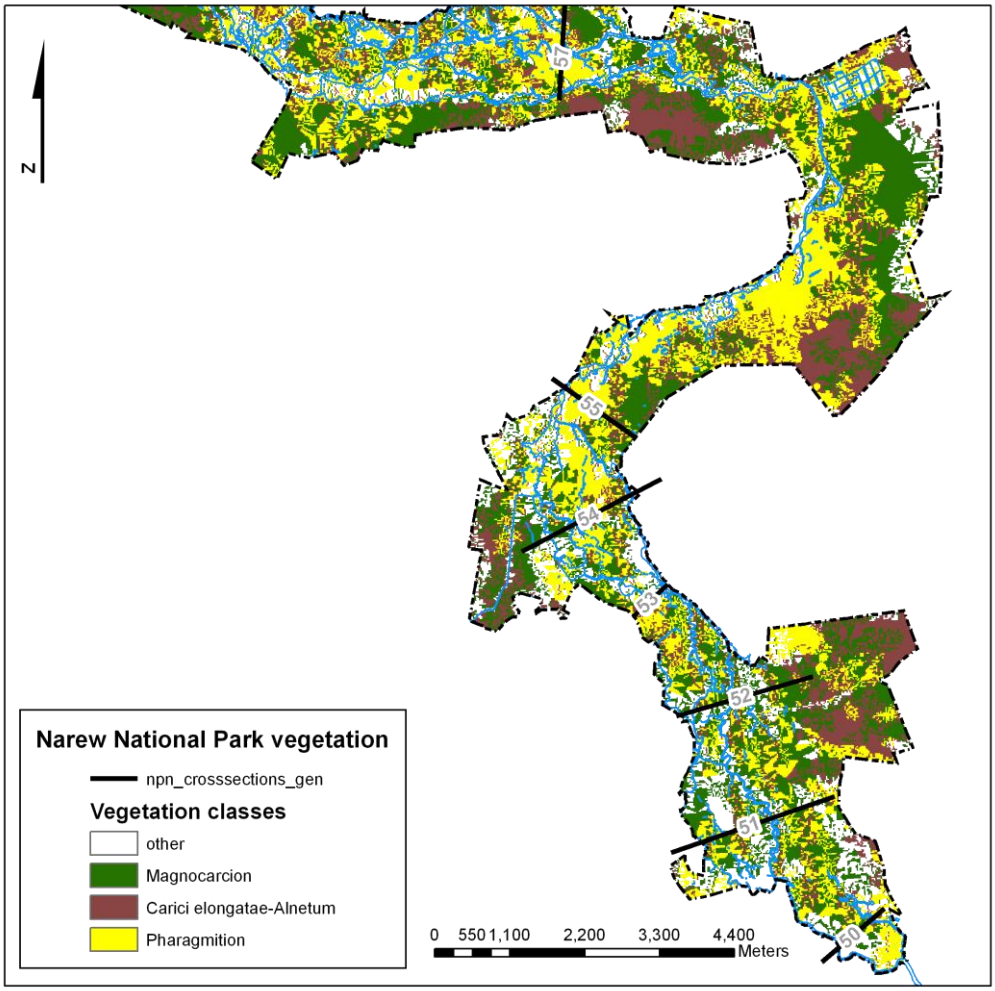

Fig. 3. Map of three main types of vegetation in NNP.

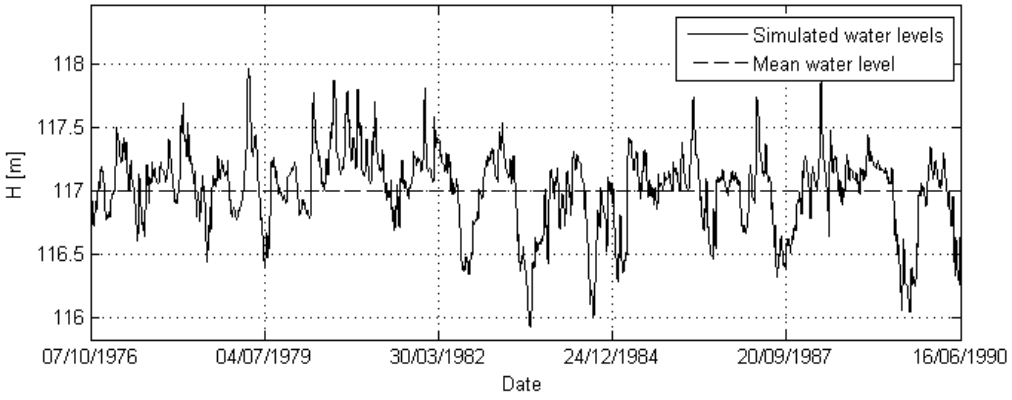

Fig. 4. Simulation of water stage for cross-section 53.

Table 1

Historical flooding frequency for major types of marsh and swamp plant communities

Wetland community	Section number	Length of section [m]	Frequency of flooding		
			min 50% of section	min 75% of section	100% of section
Magnocaricion	51	392	0. 99	0.99	0.86
	52	1773	0.71	0.42	0.006
	53	1804	0.87	0.82	0,00
	54	231	0.85	0.85	0.85
	55	725	1.00	0.65	0.03
	56	314	0.13	0.09	0.00
	57	519	1.00	1.00	0.01
Alder forest	51	4	0.99	0.99	0.92
	52	182	0.91	0.90	0.03
	53	135	0.61	0.61	0.01
	54	16	0.85	0.85	0.85
	55	109	1.00	1.00	0.03
	56	102	0.69	0.13	0.00
	57	180	1.00	1.00	0.005
Reed communities	51	4	0.99	0.99	0.93
	52	159	0.91	0.90	0.07
	53	229	0.61	0.61	0.03
	54	279	0.85	0.85	0.29
	55	619	1.00	1.00	0.04
	56	819	0.97	0.70	0.11
	57	762	0.92	0.92	0.02

good match between the data for 50% and 75% section cover and quite a big discrepancy when compared with the 100% section cover. This discrepancy, and minor differences between the section for the same wetland community, result from model errors, cross-sections geometry errors and the accuracy of delimitation of the plant communities on the vegetation map.

In the next step of the analysis, the results of 100% of section cover were neglected assuming that the accuracy of vegetation delimitation was too low to show the exact length of each section with the uniform plant cover. Moreover, the largest mix of vegetation is present in the buffer zone where one vegetation type is being exchanged by the other. The vertical difference between the beginning and the end of each section, termed the height of the section, was also analysed (Table 2) and compared with the average model error (14 cm). All results for sections with a height lower than 10 cm were neglected in the further analysis. As there is a good match between 50%

and 75% results, the latter values were chosen as an average for each vegetation type. Results of the calculations are presented in Table 3.

The results presented in Table 3 were compared with the other works performed for the same region and earlier short-term piezometric measurements done by the Institute of Land Reclamation and Grassland Farming (IMUiZ) in the Narew valley in the 1970s. Matowicka (1996) presented an assessment of water levels for the alder forests and Oświt (1991) showed the water conditions for the reed and Magnocaricion communities in neighbouring Biebrza valley. The results of Matowicka and Oświt were obtained for the vegetation period only. Moreover, the results of Matowicka were derived from the period after the changes in the valley occurred. Therefore, the inundation frequency obtained in the present study is slightly higher than that reported by Matowicka. On the other hand, the piezometric records of IMUiZ are slightly lower than the modelling results presented here, but there is no information what plant communities were measured by IMUiZ. The results of Oświt are in the range of results obtained in the present study. In conclusion, long-period simulations of hydrological conditions in the whole valley confirmed our hypothesis that inundation should be above the soil level for more than a half of the year in order to maintain peat forming processes that were present in this valley in the past, and to maintain swamp communities.

Table 2

The height of particular sections covered by swamp communities

The height of the section covered by swamp communities [m]			
Section number	Magnocaricion	Alder forest	Reed communities
51	0.04	0.01	2.45
52	0.54	0.06	0.01
53	0.50	1.93	1.11
54	1.58	1.49	1.44
55	0.01	0.01	1.66
56	1.34	3.75	3.84
57	1.16	1.17	1.18

Table 3

Average flood frequency for marsh and swamp communities of the Narew National Park

Swamp communities	Average flood frequency
Magnocaricion	0.64
Alder forest	0.70
Reeds	0.84

6. Conclusions

The results of the simulation of historical hydrological conditions for three swamp communities of the Narew National Park allow us to draw the following conclusions:

1. A 1-D hydrodynamic model has been an appropriate tool for the reconstruction of flood dynamics in the protected part of the River Narew Valley.

2. The results of simulation showed that the most important communities in the Narew National Park, i.e., magnocarcion, reed community and alder forests, belong to the swamp type of wetlands habitats, characterized by a very long and frequent inundation period amounting to ¾ of the average year. The estimated frequency of flooding is comparable to the results of the research (short term piezometric measurements) conducted in the lower basin of the River Biebrza.

3. The water management goal and, in particular, the water release policy of the Siemianówka reservoir should focus on achieving a similar flooding frequency in the protected habitat of NNP as that estimated during the present study.

4. The hydraulic model was successful in the terms of the simulation of water levels along the modelled reach, but it requires improvement of the identification of subcatchment lateral inflow as well as a verification of the spatial extent of flooding using the RS data for the historical floods. A high-accuracy DEM would also improve the results of this study by allowing for an areal comparison of the flooding history and plant cover.

Acknowledgments. This work was supported in part by grant 2 P04D 009 29 from Ministry of Science and Higher Education. We thank Marzena Osuch for her valuable comments.

References

Ackerman, M. (ed.) (2005), EUROWET: Integration of European Wetland research in sustainable management of the water cycle; Hydrology Task Force review paper, manuscript, 45 pages.

Banaszuk, H. (1996), *Paleogeography, natural and anthropogenic changes in Upper Narew Valley*, (in Polish), Wyd. Ekonomia i Środowisko, Białystok.

Banaszuk, P. (1996), *Soil forming habitats and soils in the Upper Narew Valley at Suraż-Biebrza river reach*, (in Polish), Zesz. Probl. Post. Nauk. Roln. **428**.

Banaszuk, P. (2002), *Narew National Park environmental impact statement*, (in Polish), Białystok.

Barkau, R.L. (1993), *UNET, one-dimensional flow through a full network of open channels, user's manual version 2.1*. Publication CPD-66, U.S. Army Corps of Engineers, Davis, CA, Hydrologic Engineering Center.

Bootsma, M. (2000), *Stress and recovery in wetland ecosystems*, PhD Thesis, Utrecht University: 193.

Dembek, W., M. Szewczyk, and A. Kamocki (2004), *Response of riparian vegetation to the decrease of flooding: the Narew National Park, Poland*, (in Polish), Woda-Środowisko-Obszary-Wiejskie 4, 2b (12) pp. 225-237.

Gore, A.J.P. (1983), *Ecosystems of the Word 4A. Mires: swamp, bog, fen and moor*, General Studies, Amsterdam, Oxford, New York 1983.

Keddy, P.A. (2000), *Wetland Ecology, Principles and Conservation*, Cambridge University Press.

Kiczko, A., R.J. Romanowicz, J.J. Napiórkowski and A. Piotrowski (2008), *Integration of reservoir management and flow routing model – Upper Narew case study*, Publ. Inst. Geophys. Pol. Acad. Sc. **E-9** (405), (this issue).

Kotowski, W. (2002), *Fen communities. Ecological Mechanisms and Conservation Strategies*, Van Denderen BV, Groningen: 184 pp.

Kubrak, J., T. Okruszko, D.M. Świątek, and I. Kardel (2005), *Recognition of hydraulic conditions in the Upper Narew River System and their influence on the wetland habitats in the river valley*, Publ. Inst. Geophys. Pol. Acad. Sc. **E-5** (387), 209-237.

Matowicka, B. (1996), *Ground water level changes in alder forests localized along meliorated river system*, (in Polish), Zesz. Nauk. P. Biał. 105, Inż. Środ. 8: 89-111.

Mitsch, W.J., and J.G. Gosselink (2000), *Wetlands*, Third edition, Wiley.

Okruszko, T. (2005), *Hydrologic criteria in the protection of wetlands*, (in Polish), Wydawnictwo SGGW, Seria: Rozprawy Naukowe i Monografie, 151 p.

Okruszko, T., J. Chormanski, and D. Swiatek (2006), *Interaction between surface and groundwater in the flooding of riparian wetlands: Biebrza wetlands case study*. **In:** S. Demuth, A. Gustard, E. Planos, F. Scatena, and E. Servat (eds.), FRIEND Conference in Havana, Cuba "Climate Variability and Change – Hydrological Impacts, IAHS Publ., No 306, str. 573-578.

Oświt, J. (1991), *River wetland vegetation and habitats in relation to water conditions*, (in Polish), Roczniki Nauk Rolniczych, seria D, monografie, t. 221, Wydawnictwo Naukowe PWN, Warszawa, str. 229.

Van Asmuth J.R., A.P. Grootjans, E.J. Lammerts, and A.J.M. Jansen (2002), *Eco-hydrological modelling using response characteristics of hydrological systems*. Third International Conference on Water Resources and Environment Research, 22-25 July 2002, Dresden University of Technology.

Wassen, M.J., W.H.M. Peeters, and H. Olde Venterink (2002), *Patterns in vegetation, hydrology and nutrient availability in an undisturbed river floodplain in Poland*, Plant Ecol. **165**, 27-43.

PUBLS. INST. GEOPHYS. POL. ACAD. SC., E-9 (405), 2008

Integration of Reservoir Management and Flow Routing Model – Upper Narew Case Study

Adam KICZKO, Renata J. ROMANOWICZ, Jarosław J. NAPIÓRKOWSKI, and Adam PIOTROWSKI

Institute of Geophysics, Polish Academy of Sciences
Ks. Janusza 64, 01-452 Warszawa, Poland
e-mail: akiczko@igf.edu.pl

Abstract

This paper analyses the possibilities of reaching required flow conditions in the reaches of an ecologically valuable river, using reservoir management techniques. The study utilizes a one-dimensional flow routing model and a global optimisation procedure, with a special focus on ecological criteria. The methodology is applied to the valley of the Upper Narew, in north-east Poland. The work is focused on improving water conditions in the Narew National Park, which encloses one of the most valuable swamp ecosystems in Europe. The study area includes a 100 km long reach that begins at the outflow of the Siemianówka Water Reservoir and ends at the National Park. The reach of the River Narew studied has a rather complex anastomosic structure. An analysis is carried out on several historical scenarios. In each case the outflow from the reservoir is optimised to provide ecologically required flow conditions. The results point to the need for a reconsideration of the management of the Siemianówka reservoir.

1. Introduction

The aim of this paper is to analyse the possibility of reaching required water conditions at ecologically valuable wetland sites through reservoir management. After a presentation of the study area, control objectives conditioned on ecological and economical issues are formulated and subsequently the applied methods are presented. Then an investigation of optimal management scenarios against the observed river states is made, followed by a discussion of the effectiveness of a reservoir situated upstream in the mitigation of undesired changes in the river regime. Finally, a sensitivity analysis of the objective function evaluating the obtained management scenarios to the violation of some of the assumptions applied during the analysis is described.

In natural rivers, water conditions vary spatially along the floodplain and therefore a distributed approach to flow modelling is required where both ecological and economic issues are addressed. In this study, river flow is described using a One-

Dimensional Unsteady Flow Through a Full Network of Open Channels model (UNET) (Barkau 1993). Optimization of river roughness coefficients required by UNET and reservoir management is performed using the Differential Evolution Algorithm technique (Storn and Price 1995). In addition, a sensitivity analysis of reservoir management reaction time on desirable objectives is performed following Global Sensitivity Analysis (GSA) (Archer *et al.* 1997).

2. Case study

The Narew National Park (NNP) (Fig. 1) is situated in north-east Poland and encloses valuable water-peat ecosystems of the anastomosing upper River Narew, making this region unique in Europe. The NNP's flora consists of more than 600 species of vascular plants, including many protected varieties. Park wetland areas provide habitats for about 200 bird species, being one of the most important stop-over points for migrating birds. Due to its unique features, the NPN is an important site in the European Network of Natura 2000 (Dembek and Danielewska 1996, IWOR 2002).

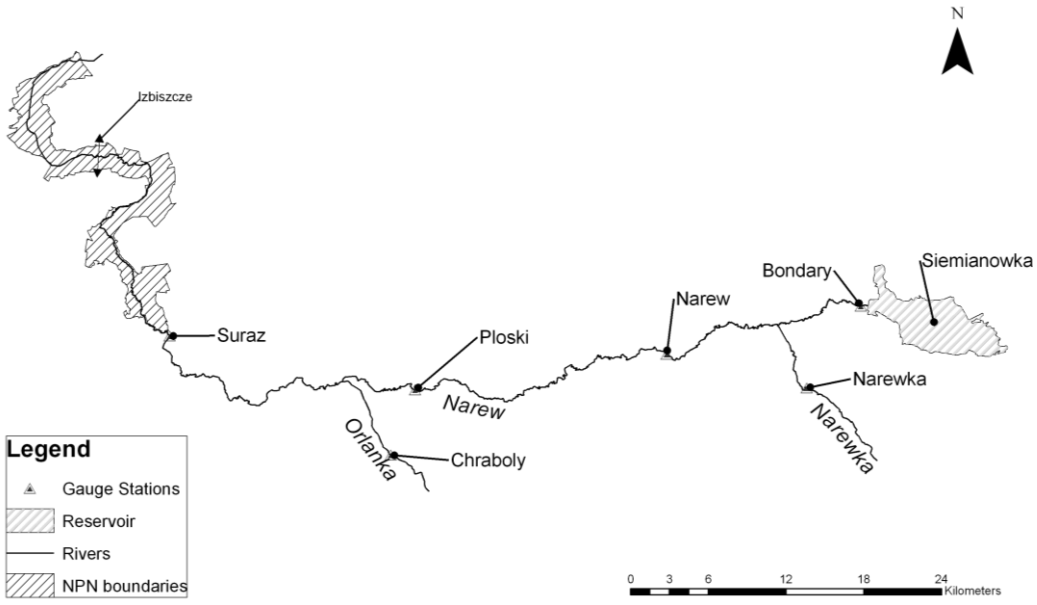

Fig. 1. Schematic map of study area.

The river reach under consideration is a primary, semi-natural form of a lowland river system, with relatively small water slope values, at the level of 0.2‰. The annual river discharge at Suraż is 15.5 m^3/s. The river reach is represented by 57 cross-sections at 2 km intervals obtained from a terrain survey.

Alarming changes have been observed in the Upper River Narew hydrologic regime in recent years, manifested in a reduction of mean flows and shorter flooding periods. This results in a serious threat to the rich wetland ecosystems. On one hand it is caused by local climate changes. Mild winters combined with a reduction in annual

rain levels have resulted in a reduction of the valley's groundwater resources. However, recent human activities also have had a significant influence on the deterioration of wetlands water conditions. River regulation work performed in the lower river reach has lowered water levels. Additionally, a water storage reservoir constructed upstream of the NNP has had an important impact on water conditions, causing a reduction in flood wave peaks.

3. Methodology

3.1 Statement of reservoir management problem

Wetland ecosystems depend largely on river flow conditions, especially on flooding (Junk *et al*. 1989). Therefore, actions aimed at preserving the Park's quasi-natural character rely generally on an improvement of the river's water levels and flooding characteristics, such as flooding area, average depth and flood frequency in the wetland area (Kubrak *et al*. 2005, Okruszko *et al*. 1996).

A statement of straightforward criteria for the river flow conditions required by the wetland ecosystem is a difficult task. For the NNP region only qualitative information on ecologically demanded water levels is available. Providing a maximal extent of spring flooding is most important from the ecological point of view. During the rest of the year, a minimum admissible water level should also be maintained. On the basis of available information (IWOR 2002), it was possible to estimate the minimum desirable water levels for the Upper Narew during a hydrological year with a flood period included.

However, in order to meet socio-economical criteria, maximum admissible water levels also have to be specified to protect farmland and urban areas from flooding. The Narew valley is used for extensive agricultural production and the water demand for crops varies in time, depending on the stage of the growing season.

Because of spatial heterogeneity in water demand along the river, water level criteria have to be spatially distributed. In this paper water levels were controlled at discrete representative cross-sections. Optimal water level ranges during the whole hydrologic year were determined for each of the chosen cross-sections. This type of approach should provide a proper representation of water conditions in the wetland area at the NNP.

In this application, Siemianówka reservoir discharges are used as control variables. Although the reservoir is located nearly 100 km upstream from the NNP, it has a significant impact on water levels in this area (Kiczko *et al*. 2007). For reservoir management, additional objectives concerning the physical characteristics of the reservoir, such as maximum and minimum storage and discharge and hydro-power plant effectiveness, have to be considered.

Control performance of the reservoir system depends on river water levels H and reservoir storage V and is evaluated using "fuzzy-like" measures (Romanowicz and Beven 2003) assuming a knowledge of desirable conditions for both variables. The first measure $M(H, \mathbf{g}_H)$ is shown in Fig. 2. Vector $\mathbf{g}_H = [g_{H1}, g_{H2}, g_{H3}, g_{H4}]$ of the desirable water levels depends on time and location of the cross-section along the

river. Note that the measure function is 0 if H meets the evaluation criteria on $H \in [g_{H2}, g_{H3}]$ and increases to 1 following a parabolic function when the water levels are outside the specified ranges.

The second measure $M(V, \mathbf{g}_V)$ has a similar shape to that depicted in Fig. 2 and is responsible for the appropriate reservoir water content during the assumed time horizon.

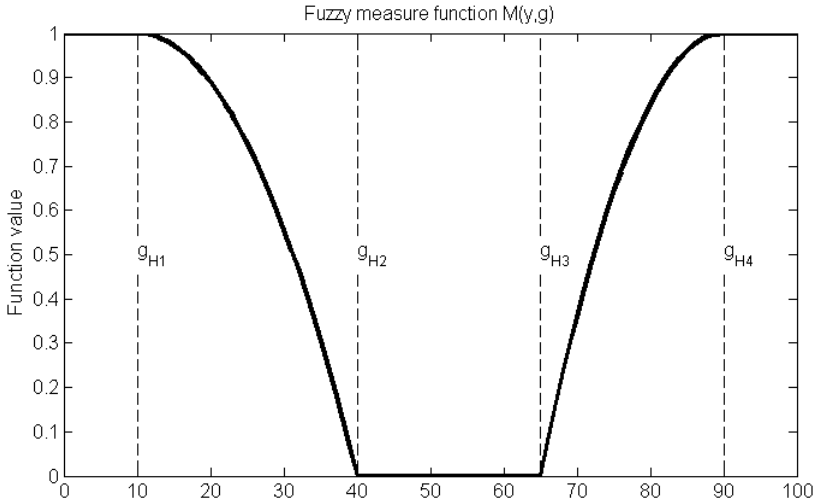

Fig. 2. Fuzzy measure function, where g_{H1} – minimum water level, g_{H2} – lower bound of acceptable water level values, g_{H3} – upper bound of acceptable values, g_{H4} – maximum water level.

At present, the reservoir management is based on "Reservoir Siemianówka management instructions" written by BIPROMEL (1999). This document focuses on the reservoir's operational requirements and the agricultural demands for water levels during a year. During flooding events, the reservoir is supposed to reduce the height and extent of a flood wave downstream. From a wetland ecosystem mitigation point of view, it is an unfortunate demand (IWOR 2002). In this work, criteria for water levels were adjusted to preserve and extend the duration of the spring freshet, according to the recommendations for improving water condition at wetland areas. However, agricultural water demands were also included. Requirements for reservoir water storage values were taken directly from the reservoir management instructions. The fuzzy objective function for water levels applied here changes in time (Fig. 3).

All considered criteria were merged into a unique objective function, discretised in time and space, in the following manner:

$$J(H,V) = \sum_{k=1}^{T} W_{H,k} \left(\frac{1}{N_c} \sum_{j=1}^{N_c} M(H_{kj}, \mathbf{g}_{H,kj}) \right) + W_V \sum_{k=1}^{T} \left(M(V_k, \mathbf{g}_{V,k}) \right) \tag{1}$$

where: T is the number of time steps, N_c is the number of controlled cross-sections, H_{kj} is the water level at time k at cross-sections j, V_k is the reservoir storage at time k,

$\mathbf{g}_{H,kj}$ is a vector of desirable water levels at time k and cross-section j, $\mathbf{g}_{V,k}$ is a vector of desirable reservoir storages at time k, $W_{H,k}$ is the weighting coefficient for water levels, W_V is the weighting coefficient for reservoir storage.

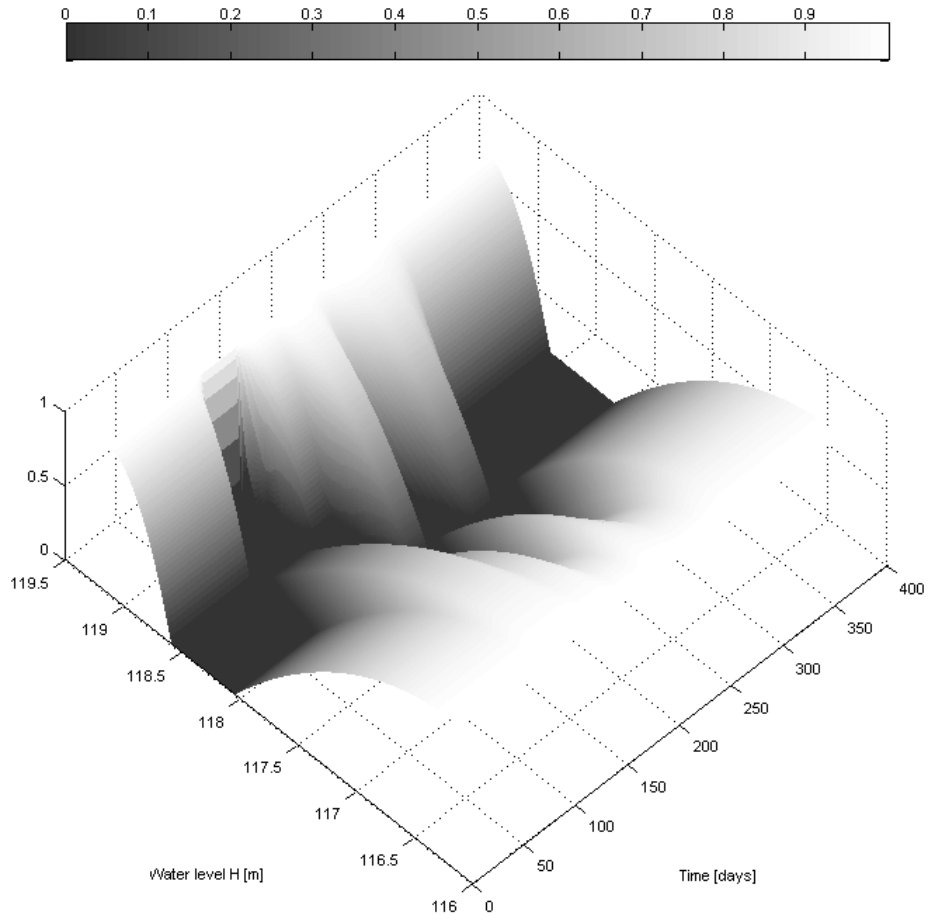

Fig. 3. Response surface of a "fuzzy-like" objective function for water levels at cross-section 51 for a one-year period.

A higher value of the weighting coefficient $W_{H,k}$ is introduced in the objective function during flood periods in order to increase the significance of spring flooding to a wetland area and to maintain the required status of riverine wetlands.

As the optimization criteria have a distributed character, a distributed flow routing model is required.

3.2 Flow routing model

The UNET (Barkau 1993) model is applied to describe flow routing in the Upper River Narew system. This code is a numerical implementation of a 1-D Saint Venant equation in the following form:

$$\frac{\partial A}{\partial t}+\frac{\partial(\Phi Q)}{\partial x_c}+\frac{\partial\left[(1-\Phi)Q\right]}{\partial x_f}=0$$

$$\frac{\partial Q}{\partial t}+\frac{\partial(\Phi^2 Q^2 A_c^{-1})}{\partial x_c}+\frac{\partial\left[(1-\Phi)^2 Q^2 A_f^{-1}\right]}{\partial x_f} + g A_C\left(\frac{\partial H}{\partial x_c}+S_{fc}\right)+g A_f\left(\frac{\partial H}{\partial x_f}+S_{ff}\right)=0 \quad (2)$$

where A_c and A_f are flow areas, respectively, for channel and floodplain; Q is the flow, H is the water level, g is the gravitational acceleration, x_c is the distance along the channel, x_f is the distance along the floodplain, S_{fc} is the floodplain friction slope, S_{ff} is the channel friction slope, Φ is the correction coefficient for momentum due to non-uniformity of velocity distribution at cross-section.

The model was calibrated by adjusting the Manning coefficients separately for the main channel and left and right floodplains. Water surface slope was used as a downstream boundary condition. Water level observations from only three river gauges were available for the whole river reach; therefore it was assumed that roughness coefficients do not change spatially between the gauges.

The model mass balance was a problematic issue because of the lack of data on lateral inflows, with the exception of the Narewka and Orlanka tributaries. It was assumed that unmeasured lateral inflows are linearly correlated with two known tributaries and can be described using a linear regression model.

Therefore, calibration was carried out for 14 parameters, 12 roughness coefficients and 2 linear correlation coefficients for unobserved inflows. The sum of squared errors between simulated and observed water levels at controlled gauging stations: Narew, Płoski and Suraż was used as an objective function for roughness coefficients calibration.

3.3 Differential Evolution Optimization Algorithm

In this paper there are two separate optimization problems to be solved. The first is the calibration of roughness coefficients in the UNET model, the second – finding the optimal discharges from Siemianówka reservoir. Please note that the notation used in this section is not linked directly to a particular optimization problem.

Both optimization problems are solved by means of the same Differential Evolution Algorithm described below. This methodology was introduced by Storn and Price (1995) and is currently considered to be one of the most promising global optimization algorithms.

The algorithm used in the present paper works as follows. In each step of the procedure, the population of N individuals $[\boldsymbol{x}_{1,G}, \boldsymbol{x}_{2,G}, ..., \boldsymbol{x}_{N,G}]$ searches for an optimum in D-dimensional space ($\dim(\mathbf{x})=D$), where G denotes the generation number, in order to find the minimum value of the objective function $f(\mathbf{x})$.

At each generation, for each individual $\boldsymbol{x}_{i,G}$ (i=1, …,N) three different population members are randomly chosen ($\boldsymbol{x}_{r1,G}$, $\boldsymbol{x}_{r2,G}$ and $\boldsymbol{x}_{r3,G}$). On this basis the ancestor ($\boldsymbol{v}_{i,G+1}$) is generated:

$$\mathbf{v}_{i,G+1} = \mathbf{x}_{r1,G} + F(\mathbf{x}_{r2,G} - \mathbf{x}_{r3,G}) \tag{3}$$

where F is a parameter, fixed here at a value of 0.8 (Storn and Price 1995). Then, each element of vectors $\boldsymbol{x}_{i,G}$ and $\boldsymbol{v}_{i,G+1}$ is recombined, yielding the final offspring $\boldsymbol{u}_{i,G+1}$:

$$u_{i,j,G+1} = \begin{cases} v_{i,j,G+1} & \text{if} \quad U_{i,j} \le CR \quad \text{or} \quad j = I \\ x_{i,j,G} & \text{if} \quad U_{i,j} > CR \quad \text{and} \quad j \ne I \end{cases} \tag{4}$$
$$j = 1, ..., D$$

where $U_{i,j}$ is a random value, I is a random integer. In this application, as is usually the case, the crossover probability CR is equal to 0.9.

The selection is performed on the basis of objective function value $f(\boldsymbol{u}_{i,G+1})$, in the following manner:

$$\mathbf{x}_{\mathrm{i,G+1}} = \begin{cases} \mathbf{u}_{i,G+1} & \text{if} \quad f(\mathbf{u}_{i,G+1}) \le f(\mathbf{x}_{i,G}) \\ \mathbf{x}_{i,G} & \text{if} \quad f(\mathbf{u}_{i,G+1}) > f(\mathbf{u}_{i,G}) \end{cases} \tag{5}$$

3.4 Global Sensitivity Analysis

Sensitivity Analysis plays a very important role in modelling practice (Romanowicz and Macdonald 2005). In the case of an over-parameterized model it provides a reasonable reduction of parameter space.

Generally, the Sensitivity Analysis consists of an evaluation of the relationship between input and output variations. In this assessment we have used the variance-based Global Sensitive Analysis approach introduced by Archer *et al*. (1997). According to this method, the whole set of model parameters acquired from Monte Carlo sampling is analysed simultaneously and there is no restriction on the monotonicity or additivity of the model. Therefore this approach is suitable for over-parameterized, nonlinear, spatially distributed models.

Following this methodology, the variance of an output Y depending on the variable input set X_i, i = 1, …, D, can be treated as a sum of the top marginal variance and the bottom marginal variance (Ratto *et al*. 2001):

$$V(Y) = V\left[E(Y \mid U)\right] + E\left[V(Y \mid U)\right] \tag{6}$$

where U is a group of one or more elements X_i. The top marginal variance from U is the expected reduction of the variance of Y in case U becomes fully known and is fixed at nominal values, whereas other inputs are normally varying. The bottom marginal variance form U is defined in the case where all parameters but U become fully known, U remaining a variable as before.

The direct sensitivity of output Y to inputs X_i, represents the first order sensitivity index S_i which takes the following form:

$$S_i = \frac{V[E(Y \mid X_i = x_i^*)]}{V(Y)}, \tag{7}$$

where x_i^* is fixed value.

The model sensitivity to the interactions among subsets of factors, the so-called higher order effects, is investigated using total sensitivity indices: S_{Ti}. They represent the whole range of interactions which involve X_i and are defined as:

$$S_{Ti} = \frac{E[V(Y \mid X_{-i} = x_{-i}^*)]}{V(Y)}, \tag{8}$$

where the term X_{-i} indicates all the factors but X_i.

The use of total sensitivity indices is advantageous, because there is no need to evaluate a single indicator for every possible parameter combination. On the basis of these two indicators, S_i and S_{Ti}, it is possible to trace the significance of each model parameter efficiently. In this study, the estimation of sensitivity indexes S_i and S_{Ti} is carried out using the Sobol method (Archer *et al*. 1997).

There are two different sensitivity problems studied, following from the two optimisation problems stated. One is related to the calibration of roughness parameters in the flow routing model and the other one to reservoir management. Therefore the model output Y is understood either as a criterion of calibration or reservoir management result, depending on the problem under consideration.

4. Results

4.1 Upper Narew flow model calibration and verification results

A sensitivity analysis of parameters was carried out before the calibration stage of the model. The results show (Table 1) that channel roughness coefficients have the major influence on the model results, while floodplain roughness has a minor effect. In this case parameters interactions play a significant role.

Table 1

Global Sensitivity Analysis for the flow routing model

		S_i	S_{Ti}
Manning roughness coefficient	Channel	0.016	0.267
	Left floodplain	0.000	0.026
	Right floodplain	0.003	0.104

In this application, the annual variations of roughness coefficients due to vegetation and variable winter events are difficult to estimate. In order to minimise the number of unknown parameters, it was assumed that roughness coefficients are constant during the hydrologic year. The model calibration was carried out for nearly 13 month

period (10.03.1980 – 14.04.1981) including winter months and spring freshet, as well as summer freshets (Fig. 4).

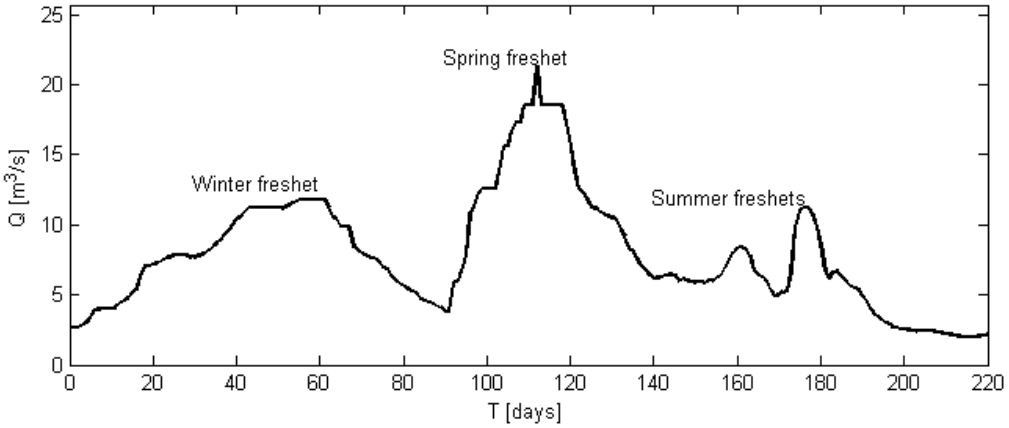

Fig. 4. Discharges at Bondary water level gauge (1980-1981): the upstream boundary condition for the model calibration.

Channel and floodplain (left and right) roughness coefficients for four separate reaches between gauging stations and downstream boundary condition were used as the model parameters. As mentioned above, optimization was carried using the DE algorithm. Verification was done for the period 27.08.1982 – 23.07.1983, giving a good fit with a mean standard deviation less than 0.14 m for each gauging station (Fig. 5).

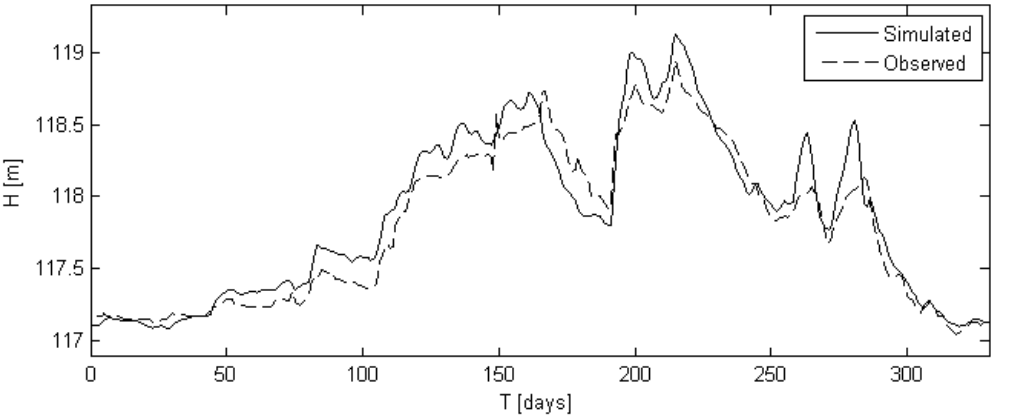

Fig. 5. Model verification at Suraż river gauge for 27.08.1982 – 23.07.1983 period; solid line denotes simulations, dashed line observations.

4.2 Optimization of discharges from Siemianówka reservoir (control stage)

The Siemianówka water reservoir was described using a simple discrete balance model:

$$V_{k+1} = V_k + Q_k^{in} - Q_k^{out}, \qquad k = 1, ..., N_t \tag{9}$$

where V_k is the reservoir capacity in time instant k, Q_k^{in} is the reservoir inflow, Q_k^{out} is the reservoir outflow. Reservoir outflows are represented as the sum of rectangular pulses represented in continuous time t as:

$$Q_{out}(t) = Q_{base} + \sum_{j=1}^{NP} P_j(t, t_j, dt_j, q_j) \tag{10}$$

where Q_{base} is the minimum flow (a minimum allowed discharge from the reservoir), t_j is the time middle point of j-th pulse, dt_j is the pulse duration time, q_j is the discharge and NP is the number of considered pulses.

The j-th rectangular is defined as a

$$P_j(t, t_j, dt_j, q_j) = \begin{cases} 0 & \text{for} \quad t \in \left\langle t_0, t_j - 0.5dt_j \right) \\ q_j & \text{for} \quad t \in \left\langle t_j - 0.5dt_j, t_j + 0.5dt_j \right\rangle \\ 0 & \text{for} \quad t \in \left(t_j - 0.5dt_j, t_k \right)\rangle \end{cases} \tag{11}$$

where t_0 is the initial time and t_k is the optimization horizon.

Historical observations of discharges at the Bondary river gauge before the time when the reservoir was built were used as an inflow to the reservoir. Currently, the reservoir outflow is located in that place. This is a relatively simple approach but it is sufficient for this application, where focus is placed on the reservoir's management abilities to improve water conditions, rather than on a classical control problem.

Initial reservoir storage was set to the recommended value for a chosen control period. Additionally it was assumed that each of the goals included in the global objective function (1) has the same significance. Therefore the weighting coefficients for the reservoir storage and water levels were set to 1, except for flood periods where the weights for water levels were doubled.

Analysis was performed for three different management scenarios:

Scenario A

20.03.1980 – 08.06.1980 – wet period of a maximum discharge in Suraż at 101 m^3/s level, 0.28 probability of exceedance during a year (Rowiński *et al*. 2005);

Scenario B

23.02.1981 – 11.10.1981 – also wet period of a maximum discharge in Suraż at 111 m^3/s level, 0.22 probability of exceedance during a year;

Scenario C

05.10.1982 – 13.07.1983 – rather dry period, of a maximum discharge in Suraż at 68 m^3/s level, 0.53 probability of exceedance during a year.

The periods were chosen from the time before the Siemianówka reservoir was built in the early 1990s. Thus the impact of the reservoir on observed water levels was excluded, which allowed the reservoir's ability to mitigate water conditions at ecologically valuable sites to be investigated. This makes it possible to answer the elemen-

tary question of whether a reservoir can improve the water conditions in a natural river system.

In each case, optimization was carried out for 30 parameters, i.e., 3 parameters of $NP = 10$ rectangular pulses. Numerical investigations showed that higher values of NP did not improve solutions significantly for the scenarios considered and they made the optimization process computationally ineffective. The optimization procedure for each scenario was evaluated many times for different starting points in order to ensure finding a value close to the global optimum.

In Table 2, the objective function values acquired for optimal management solution for each scenario are compared with the values for historical water levels not affected by the reservoir.

Table 2

Comparison of objective functions for optimal management scenarios and natural conditions; $J(H,V)$ – objective function as defined by Eq. (1), $J(H)$ – the first part of objective function related to the water levels along the river (without reservoir storage part); $J_n(H)$ – objective function for natural conditions; A, B, C – analyzed scenarios

	Management solution		Observation	Improve
	$J(H,V)$	$J(H)$	$J_n(H)$	
A	0.383	0.345	0.388	12%
B	0.679	0.494	0.533	8%
C	0.708	0.456	0.544	19%

Figure 6 presents a comparison of estimated optimal discharges from the Siemianówka reservoir and observed flows for the third scenario (05.10.1982 – 13.07.1983).

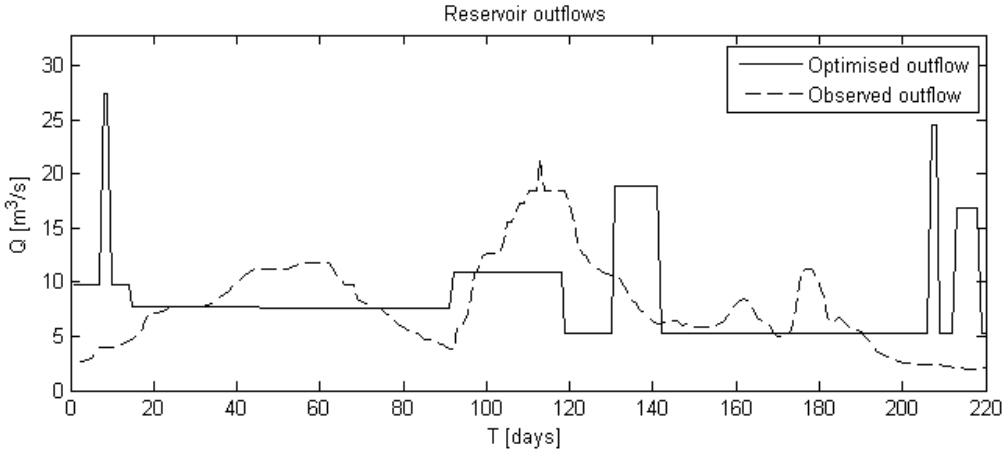

Fig. 6. Evaluated optimal discharges from the Siemianówka reservoir and observed flows (scenario: 05.10.1982 – 13.07.1983).

Figure 7 presents the variation with time of the estimated reservoir storage, with the values of objective function shown in the background as a gradually varying shaded area. At the beginning of, in this case the winter period (0-100 days), the reservoir storage is kept slightly above desired levels. However it allows the achievement of optimal storage during freshet (100-150 days) and following periods (150-220 days).

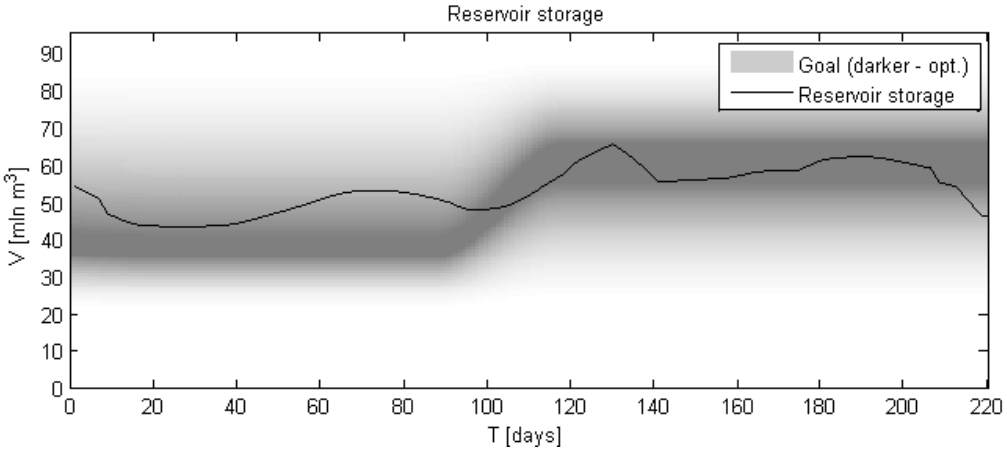

Fig. 7. Computed reservoir storage for the optimal management scenario; the values of goal function are shown as the gradually changing shaded background, demands are shown in dark grey (scenario: 05.10.1982 – 13.07.1983).

Figure 8 presents a comparison of the historical and controlled water levels at cross-section 51 for the third scenario (05.10.1982 – 13.07.1983) with the values of objective function shown as a shaded background.

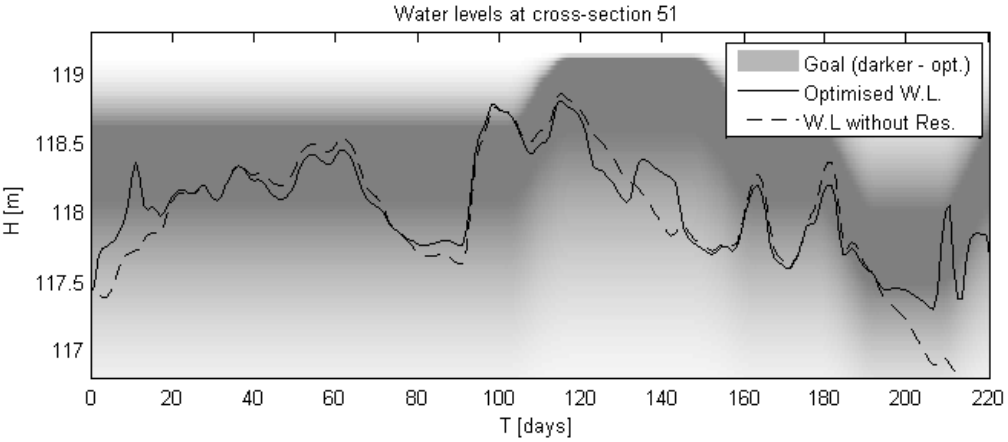

Fig. 8. Water levels at cross-section 51 and observed data; the values of goal function are shown as gradually changing shaded background, demands are shown in the darkest gray (scenario: 05.10.1982 – 13.07.1983).

4.3 Sensitivity analysis of water management scenario

The solutions for management presented in the previous section are obtained for the case of an "unlimited prediction" condition. In other words, all the management decisions presented were carried out assuming a full knowledge of present and future river inflows. Obviously, such a situation does not take place under real management conditions, where all decisions have to be carried out using short-term, uncertain predictions.

In this section we investigate the significance of a delay in reservoir management operation, by the analysis of sensitivity of the objective function to the varying delay in the reservoir discharge t_{sh}. The sensitivity was measured for three different values of pulse delay (1, 2, 3 and 4 days), that allowed to estimate an acceptable threshold for which the objective function is not seriously affected. Different sensitivity indexes of a pulse delay are compared with reference to the sensitivity index of pulse duration time t_d equal to 3 days.

The sensitivity to delays increases linearly (Table 3). A delay equal to 3 days introduces about 23% of the prediction error, whilst a 4 day delay causes a 30% error in the model response (pulse duration).

Table 3

Sensitivity profile of optimal management (scenario: 20.03.1980 – 08.06.1980)
sensitivity to pulse delay; Sensitivity to pulse duration was used as reference

Sensitivity to pulse delay			Sensitivity to pulse duration (3 days)	
Delay [day]	S_i	S_{Ti}	S_i	S_{Ti}
1	0.000	0.056	0.444	0.503
2	0.027	0.107	0.392	0.503
3	0.078	0.150	0.342	0.431
4	0.109	0.200	0.290	0.400

5. Conclusions

This paper presents the development of a sustainable water management system for a lowland river. The system consists of a storage reservoir situated upstream of the river, a river channel and wetlands which have to be maintained due to their ecological value. The proposed approach is illustrated using the Upper Narew catchment, with the Siemianówka reservoir situated upstream of the Narew National Park. The formulation of control objectives conditioned on the ecological and economical issues is one of the major issues discussed in the paper. Due to the distributed nature of the ecological objectives, the distributed 1-D model UNET is applied to describe the flow routing process through the channel and the surrounding wetland areas. Optimal discharges from the reservoir are obtained using the DE optimisation algorithm under the assumption of a perfect knowledge of the inflows to the reservoir. A comparison of op-

timal management scenarios with observed historical river levels from the time before the reservoir was built shows that properly scheduled discharges from the reservoir situated upstream are suitable for the mitigation of undesirable changes in the river flow regime. An analysis of the sensitivity of the objective function to variation in timing of the optimal discharge shows that errors in timing of up to 3 days are acceptable from the point of view of management performance. Further analysis is required to evaluate the influence of inflow and model uncertainty on the behaviour of the management system.

Acknowledgments. This work was supported by grant 2 P04D 009 29 from the Ministry of Science and Higher Education.

References

Archer, G., A. Saltelli, and I.M. Sobol (1997), *Sensitivity measures, anova-like techniques and the use of bootstrap*, Journal of Statistical Computation and Simulation **58**, 99-120.

Barkau, R.L. (1993), *UNET, one-dimensional flow through a full network of open channels*, User's Manual version 2.1. Publication CPD-66, U.S. Army Corps of Engineers, Davis, CA, Hydrologic Engineering Center.

Bipromel (1999), *Siemianówka reservoir – Water management rules*, (in Polish), Warsaw.

Dembek, W., and A. Danielewska (1996), *Habitat diversity in the Upper Narew valley from the Siemianówka reservoir to Suraż* (in Polish), *Zeszyty Problemowe Postępów Nauk Rolniczych* **428**.

IWOR (2002), *Protection plan of The Narew National Park* (in Polish), Technical report by IWOR S-ka z o.o. and IMUZ Falenty.

Junk, W.J., P.B. Bayley, and R.E. Sparks (1989), *The flood pulse concept in river floodplain systems*. **In:** D.P. Dodge (ed.), "Large River", Proc. Intern. Sym. Journal of Canadian Fisheries and Aquatic Sciences **11**, 106-107.

Kiczko, A, R.J. Romanowicz, and J.J. Napiórkowski (2007), *A study of flow conditions aimed at preserving valuable wetland areas in the Upper Narew Valley using GSA-GLUE methodology*, Proceedings 21st International Conference on Informatics for Environmental Protection, September 12-14, 2007, Warsaw, Poland, Shaker Verlag, 175-183.

Kubrak, J., T. Okruszko, D. Mirosław-Świątek, and I. Kardel (2005), *Recognition of hydraulic conditions in the Upper River Narew System and their influence on the wetland habitats in the river valley*, Publs. Inst. Geophys. Pol. Acad. Sci. **387**, 209-237.

Okruszko, T., S. Tyszewski, and D. Pusłowska (1996), *Water management in the Upper Narew valley* (in Polish), *Zeszyty Problemowe Postępów Nauk Rolniczych* **428**.

Romanowicz, R.J., and K.J. Beven (2003), *Estimation of flood inundation probabilities as conditioned on event inundation maps*, Water Resour. Res. **39**, 3, 10.1029/2001WR001056.

Romanowicz, R.J., K.J. Beven, and J. Tawn (1996), *Bayesian calibration of flood inundation models*, Floodplain Processes, 336-360.

Romanowicz, R.J., and R. Macdonald (2005), *Modeling Uncertainty and Variability in Environmental Systems*, Acta Geophys. Pol. **53**, 401-417.

Rowiński, P.M., J.J. Napiórkowski, and M. Osuch (2005), *Recognition of hydrological processes in the upper Narew multichannel river system and their influence on region sustainable development.* **In:** M.S. Altinakar, W. Czernuszenko, P.M. Rowiński, and S.S.Y. Wang (eds.), "Computational Modeling for the Development of Sustainable Water-Resources Systems in Poland", Publs. Inst. Geophys. Pol. Acad. Sc. **E-5 (387)**, 27-55.

Storn, R., and K.V. Price (1995), *Differential Evolution – a simple and efficient adaptive scheme for global optimization over continuous spaces*. Technical Report TR-95-012, International Computer Sciences Institute, Berkeley, CA, USA.

PUBLS. INST. GEOPHYS. POL. ACAD. SC., E-9 (405), 2008

An Integrated Data Based Mechanistic Lowland Catchment Model for the Upper Narew

Renata J. ROMANOWICZ and Marzena OSUCH

Institute of Geophysics, Polish Academy of Sciences
Ks. Janusza 64, 01-452 Warsaw, Poland
e-mail: romanowicz@igf.edu.pl

Abstract

The aim of this work is the development of an integrated Data Based Mechanistic (DBM) rainfall-flow/flow-routing model of the Upper River Narew catchment and the river reach between Bondary and Suraż suitable for scenario analysis. The modelling tool developed is formulated in MATLAB-SIMULINK language. It has a flexible, modular structure that can easily be extended by adding new features, such as a snow-melt module or a distributed routing module. We describe the basic system structure and rainfall-flow and flow routing modules, based on a Stochastic Transfer Function (STF) approach combined with nonlinear transformation of variables using a State Dependent Parameter (SDP) method. One possible application is the derivation of a management strategy for the Siemianówka reservoir, situated upstream of the Bondary gauging station, taking into account both economic and ecological goals. Another future application is on-line data assimilation and forecasting.

1. Introduction

Rainfall-flow modelling on a catchment scale can be approached from many different aspects, depending on the purpose of the modelling. The goal of this paper is the development of an off-line simulation model of the Upper Narew catchment and the River Narew reach from Bondary to Żółtki (Fig. 1) suitable for a scenario analysis and derivation of a management strategy for the reservoir Siemianówka, situated upstream of Bondary gauging station. It is planned to extend the model structure into an on-line forecasting form in order to update on-line maps of probability of flooding along the river. That work will be supported by snow-melt and spring flooding forecasts, developed as an independent project. We follow here the methodology presented in Romanowicz *et al*. (2006) where a system of connected STF models was applied to flood forecasting.

Models described in the literature differ in the degree of complexity, from very simplified, analytical approaches, through more complex, conceptual models to fully

distributed, physically-based approaches. Some authors introduce a classification of rainfall-runoff models based on the type of variables employed in the modelling process (e.g., hydraulic and hydrological models). However, this type of classification is not suitable for the purpose-oriented modelling approach that we follow here. Recently, researchers also started to be more concerned about the uncertainty of the identification process and therefore, the uncertainty of the predictions, resulting from the uncertainty of the observations and simplifications inherent in the modelling process (Beven and Binley 1992, Romanowicz and Macdonald 2005). We believe that the uncertainty of model predictions has to be taken into account in all environmental modelling problems, excluding strictly engineering problems (such as Hervouet and Van Haren 1996). Within models that allow for the estimation of the uncertainty of predictions, a choice has to be made between physically-based and conceptual modelling approaches. Recently, a number of physically-based models have been developed, following the belief that model complexity should correspond to the complexity of the real process and the development of computational capabilities together with advances in Digital Elevation Models (DEM). This implies that the application of distributed models becomes more and more fashionable. However, physically-based models are usually very complex and they are not designed for the most effective use of the available information about the system.

There are a number of conventional simplified approaches to flow routing. For example, there is the Muskingum model with multiple inputs (Khan, 1993), multiple regression (MR) models (Holder 1985), and autoregressive (AR) models (Box and Jenkins 1970). The Muskingum model is deterministic and does not give the required uncertainty bounds for the predictions. Moreover, all of these more conventional models have a completely linear structure and do not perform as well as nonlinear alternatives within a rainfall-flow context. A considerable amount of research has been published recently on the application of nonlinear methods in flow modelling. Among others, Porporato and Ridolfi (2001) apply a nonlinear prediction approach to multivariate flow routing and compare it successfully with ARMAX model forecasts. Another nonlinear approach is the application of neural networks (NN) for flood forecasting (e.g. Thirumalaiah and Deo 2000, Park *et al.* 2005). As discussed in these papers, NN models can yield better predictions than conventional linear models and, if designed appropriately, they also allow on-line data assimilation. However, the NN based models normally have an overly complex nonlinear structure and so can provide over-parameterized representations of the fairly simple nonlinearity that characterizes the rainfall-flow process (see later). They are also the epitome of the 'black-box' model and provide very little information on the underlying physical nature of the rainfall-flow process: information that can provide confidence in the model and allow for a better real life implementation of the algorithm.

The approach we pursue here is Data Based Mechanistic modelling (Young 2001, 2003). It is a top-down, data-based approach to the stochastic-dynamic modelling of environmental processes. It concentrates on the identification and estimation of physically interpretable states of dynamic behaviour that play the most important part in flow prediction. The methodology applied is based on statistically estimated, stochastic-dynamic models of the rainfall-flow and flow routing components of the system,

which are then integrated into a model of an entire catchment that generates both the predictions and their 95% confidence bounds. The serial input nonlinearity in the rainfall-flow model is obtained via a nonlinear transformation of rainfall, the nature of which is estimated directly from the data using a method of State Dependent Parameter (SDP) estimation for nonlinear stochastic systems (e.g., Young 2000, 2001).

One of the main differences between DBM modelling and the reductionist approach lies in the way the model structure of the process is specified. In the DBM approach, the structure is identified directly from available observations, which normally provides improved accuracy over the range of variables considered. The search for a description of process dynamics is restricted to a class of linear models, which are physically realisable (i.e., have real roots). Nonlinear transformation of rainfall measurements into an effective rainfall allows for a separation of a static nonlinearity from the linear process dynamics.

2. Methodology

The Data Based Mechanistic approach advocates the identification of a model structure and estimation of its parameters conditioned on available data using information-efficient statistical tools. Among the statistically feasible models only those that can be explained in a physically meaningful way are chosen. At the catchment (reach) scale, the discrete-time STF model can be presented as (Young 1984):

$$\begin{aligned} x_k &= \frac{B(z^{-1})}{A(z^{-1})} u_{k-\delta}, \\ y_k &= x_k + \xi_k, \end{aligned} \tag{1}$$

where $u_{k-\delta}$ denotes STF model input (effective rainfall, flow or water level), x_k is the underlying 'true' flow or water level, y_k is the noisy observation of this variable, δ is a pure, advective time delay of $\delta \Delta t$ time units, $A(z^{-1})$ and $B(z^{-1})$ are polynomials of the transfer function. These polynomials are in the form:

$$\begin{aligned} A(z^{-1}) &= 1 + a_1 z^{-1} + a_2 z^{-2} + \cdots + a_n z^{-n}; \\ \mathrm{B}(z^{-1}) &= b_0 + b_1 z^{-1} + b_2 z^{-2} + \cdots + b_m z^{-m} \end{aligned} \tag{2}$$

in which z^{-r} is the backward shift operator, i.e. $z^{-r} y_k = y_{k-r}$, and $A(z^{-1})$ is assumed to have real roots (eigenvalues) that lie within the unit circle of the complex *z* plane. The additive noise term ξ_k in (1) is usually both heteroscedastic (i.e., its variance changes over time) and autocorrelated in time. It is assumed to account for all the uncertainty at the output of the system that is associated with the inputs affecting the model, including measurement noise, unmeasured inputs, and uncertainties associated with the model structure. The orders of the polynomials, *n* and *m*, are identified from the data during the data-based identification process. The model structure identification and estimation of parameters are performed using the Simplified Refined Instru-

mental Variable (SRIV) method from Captain toolbox (Taylor *et al*. 2007). A nonlinear transformation of variables is carried out with the help of the State Dependent Parameter approach (Young *et al*. 2001). Following the DBM philosophy, all the model parameters are accepted only when a realistic physical explanation of the model structure can be found. In particular, we apply nonlinear transformation of rainfall into an effective rainfall, following the methodology described by Young and Beven (1994) and Young (2003). Namely, it was shown that the nonlinear relationship between measured and effective rainfall can be approximated using gauged flow as a surrogate for the antecedent wetness or soil water storage in the catchment. The scalar function describing the nonlinearity between the rainfall and the soil moisture surrogate is initially identified nonparametrically using SDP estimation. This nonparametric relationship may be approximated reasonably well by a power law or an exponential relationship. In the latter case, the model describing the effective rainfall takes the following form:

$$u_k = c_0\left[1-\exp(\gamma y_k)\right]\cdot r_k\,, \tag{3}$$

where c_0 denotes a scaling factor, y_k denotes discrete flow measurement at time *k*, r_k denotes the measured rainfall and γ is a parameter chosen using an optimisation routine. The optimisation of that parameter is performed using the model (1) output as a predictor.

It should be noted that the rainfall-flow model (1)-(3) is not suitable for off-line simulations as it requires flow measurement as the soil moisture surrogate. In order to make the model more general, the flow measurement in Eq. (3) may be replaced by its linear prediction obtained using the model (1)-(2), with rainfall measurements replacing effective rainfall. Application of an SMA module (two-store structure based on Penman drying scheme, Jolley and Wheater, 1996) is the other option for the derivation of effective rainfall explored in this paper. In both cases, the Stochastic Transfer Function parameters are optimised simultaneously with the parameters of the effective rainfall transformation.

3. The case study

We chose the River Narew catchment (Fig. 1) as a case study. The river reach studied starts at the Siemianówka reservoir and goes down to Żółtki over a lowland, agricultural area. The lower part of the area encloses valuable wetland ecosystems of the anastomosing Upper Narew and forms the area of the Narew National Park (NPN). Both NPN flora and fauna include many protected species and due to its unique habitats the NPN site became part of the European Ecological Natura 2000 Network (Dembek and Danielewska 1996, IWOR 2002).

In recent years both a reduction of mean flows and shorter flooding periods in the Upper River Narew have resulted in a serious threat to the rich wetland ecosystems situated along the river in NPN. These undesirable changes were caused by changes in the local climate, manifested as mild winters and a reduction in annual rainfall that have resulted in a reduction of the valley's water resources. Additionally, river regulation works performed in the river reach downstream of the NPN have lowered water

levels in the NPN upstream. Flood peaks are also reduced by a water storage reservoir constructed upstream of the NPN in Siemianówka (near Bondary).

Fig. 1. Upper Narew Valley showing the study area; stage gauging stations are shown as triangles, blue area on the right denotes Siemianówka reservoir and green area on the left denotes Narew National Park.

The available data include daily rainfall observations from 14 gauging stations, temperature measurements at Białystok and water level measurements at 7 gauging stations situated along the river reach and its tributaries (Bondary, Narewka, Narew, Płoski, Chraboły, Suraż and Żółtki). This is a very coarse time discretisation for a relatively small catchment (4303 km^2 up to Żółtki) and it limits the models' identifiability.

4. Application of the methodology to the Upper Narew catchment

The model of the entire catchment consists of independent modules, as shown in Fig. 2. Both rainfall-flow/water level catchment modules and flow/water level routing modules are derived using the STF approach with nonlinearly transformed input variables to account for the nonlinearity of the catchment hydrology, if necessary. The choice of the routing (output) variable depends on the available data and the purpose of the modelling. We present here the first stage of our research, consisting of the development of STF modules to be implemented within the SIMULINK based integrated catchment model.

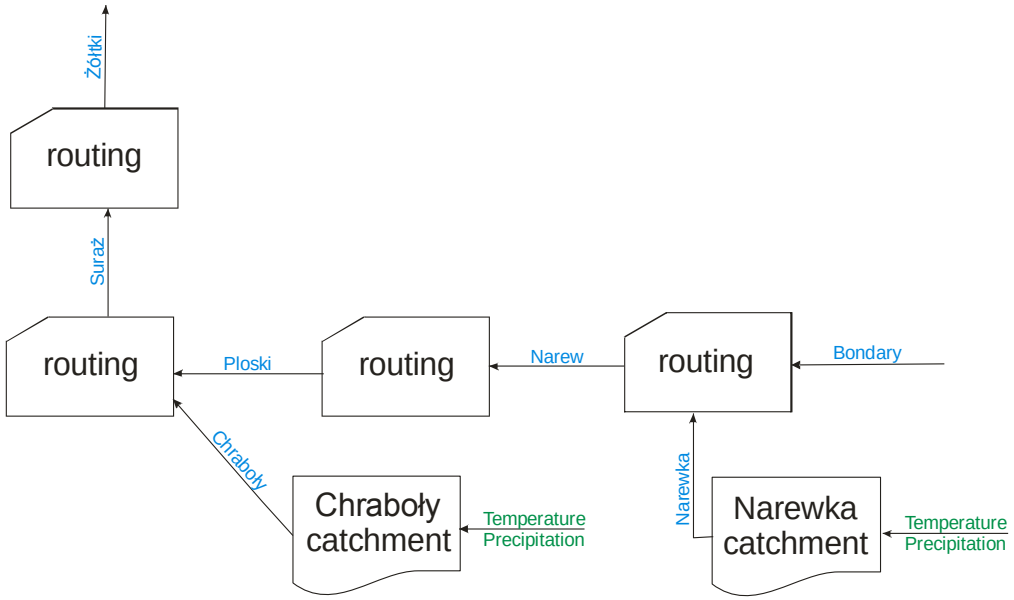

Fig. 2. Block diagram of the transfer functions model of Upper Narew catchment.

We derived a number of linear Single- and Multi-Input Single Output (SISO and MISO) STF models describing the River Narew reach from Bondary down to the Żółtki gauging station and its sub-reaches (Fig. 2), using flows and water levels as input variables. We also derived two rainfall-flow modules describing the Narewka and Chraboły catchments. Separate models were derived for flows and stages as routing model variables in order to meet possible applications of the entire system. Flow predictions are necessary for the mass balance estimation of the entire catchment, while the stage predictions are important in possible management applications, where the on-line stage predictions take the part of control variables. In the next subsection we present the results of the flow modelling followed by a stage modelling for the routing part of the model. These subsections are followed by a description of the rainfall-flow model for both catchments.

In Poland, where our case study is situated, snow melt induced floods also play an important part. Therefore the flood modelling should include temperature as one of its input variables and a mechanism relating it to the flow process. However, this problem will be addressed in the follow up to the present research.

4.1 Linear STF model structures for flow

In order to improve water balance relationship required for the application of a distributed model UNET, we derived a number of MISO and SISO STF models, using daily observations of flow. The models were calibrated on 3 years of daily observations (1978-1980) and validated on 2.5 years of daily data (1981-1983). The acquired models are listed in Table 1.

The first column shows the inputs used in each model and the second column lists the models' outputs. The third column describes the model structure (Eqs. 1-2) in the

form of a triad [n m δ], where n denotes the STF model order (i.e., the number of delayed output variables present in the model structure), m denotes the vector describing the number of delayed input variables, for each of the inputs listed in column 1, and δ

Table 1

MISO/SISO STF flow models for Bondary-Suraż reach of River Narew

Input	Output	Model	P	R	SSG	T [day]	R_T^2 c [%]	R_T^2 v [%]
Bondary Narewka	Narew	[1 1 1 0 0]	0.3546	0.6166 0.7885	0.9553 1.2217	0.96	95.43	88.69
Bondary+Narewka	Narew	[1 1 0]	0.3458	0.6844	1.0460	0.94	95.39	89.30
Narew	Ploski	[1 1 0]	0.1492	1.0851	1.2754	0.53	96.01	97.29
Bondary+Narewka	Ploski	[1 1 0]	0.3380	0.8624	1.3027	0.92	87.72	86.69
Ploski Chraboły	Suraż	[1 1 1 0 0]	0.5323	0.5016 0.4272	1.0724 0.9134	1.58	97.99	96.80
Ploski+Chraboły	Suraż	[1 1 0]	0.5533	0.4653	1.0416	1.69	97.97	96.53
Bondary Narewka Chraboły	Suraż	[1 1 1 1 4 4 1]	0.3188	0.6524 0.6731 1.6721	0.9577 0.9882 2.4548	0.87	92.30	79.44
Bondary+Narewka +Chraboły	Suraż	[1 1 1]	0.2797	0.9283	1.2887	0.78	89.59	82.25
Suraż	Żółtki	[1 1 1]	0.3689	0.8118	1.2863	1.00	90.94	95.00

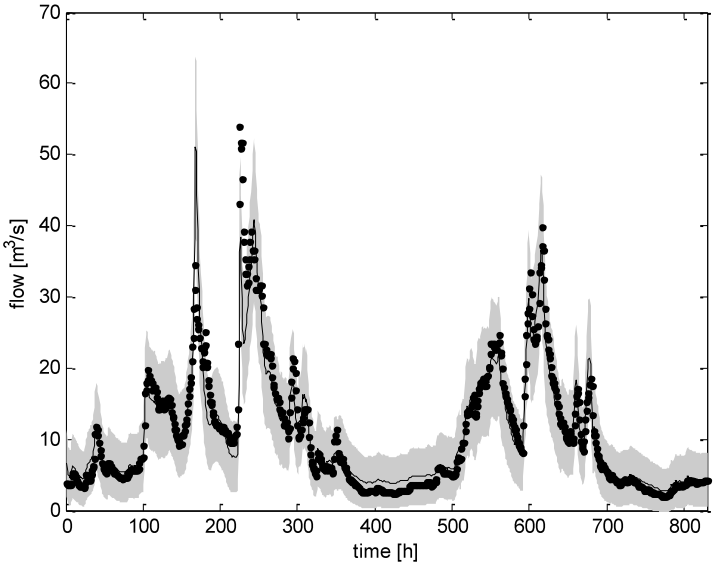

Fig. 3. Validation of daily SISO STF flow model for Narew, with Bondary and Narewka at the input (89.30% of output variation explained).

is a vector denoting the number of delays for each input variable. Column P gives the roots (always real) of the denominator of the factorized STF model structure (Eqs. 1-2) and R denotes a denominator for each factor/input variable. SSG (column 6) shows the steady state gain for each input. Column 7 presents the residence time (in days) of the obtained STF models. Columns 8 and 9 give the goodness of fit values (R_T^2) for the models obtained for the calibration and validation periods, respectively. Figures 3-6 present examples of validation results for the STF models listed in Table 1. In all the figures continuous lines denote the estimated outputs, dots denote the observed values and shaded areas denote 0.95 confidence bounds.

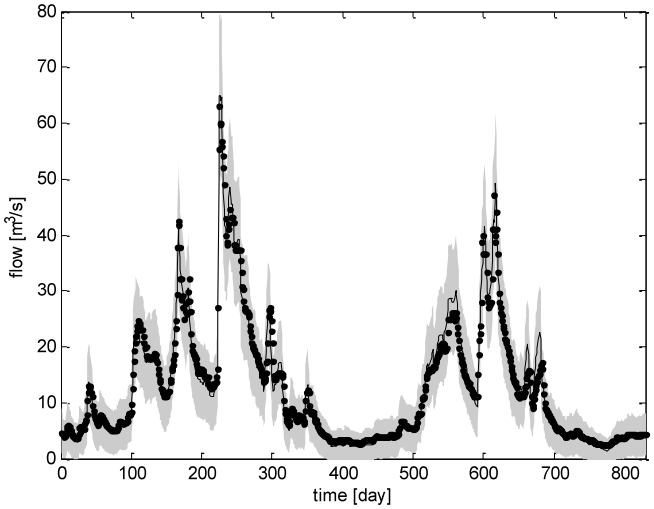

Fig. 4. Validation of SISO STF flow model for Narew/Płoski, 97.29% of output variation explained.

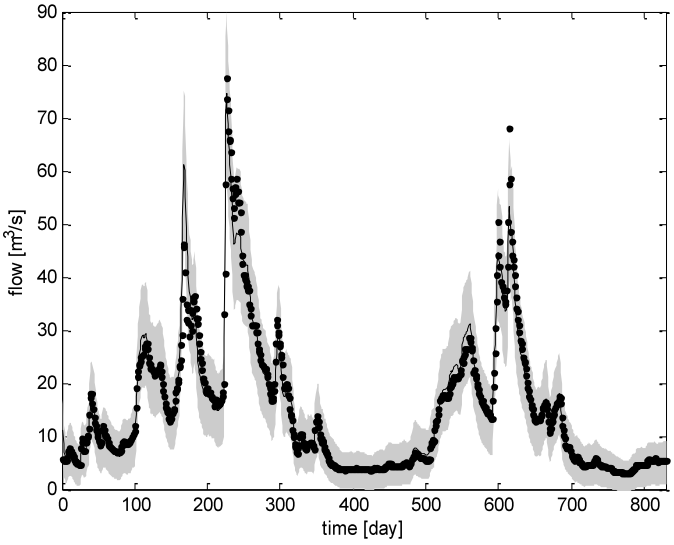

Fig. 5. Validation of MISO STF flow model for Płoski-Orlanka/Suraż, 96.79% of output variation explained.

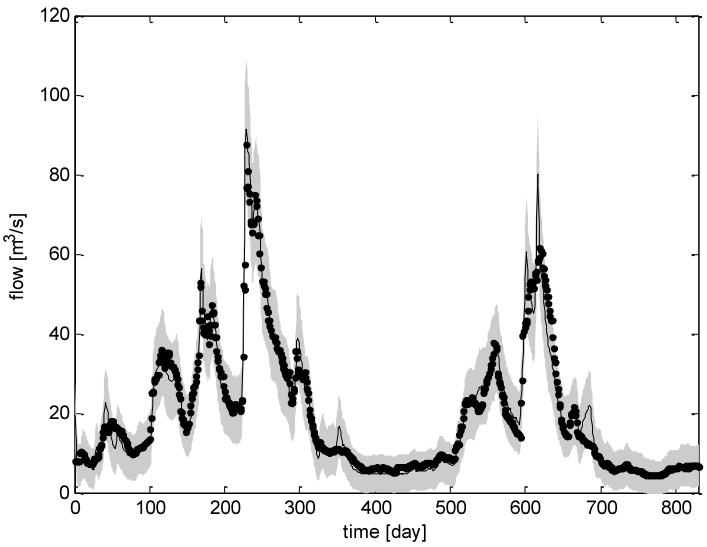

Fig. 6. SISO STF flow model for Suraż/Żółtki; validation stage: 95.00% of output variation explained.

4.1.1 Summary of modelling results

We derived a number of linear STF models describing flow process in the River Narew reach from Bondary down to the Żółtki gauging station and its sub-reaches (Fig. 1), using different sets of input variables. All the models have first order dynamics. The best results were obtained for the neighbouring sub-reaches and there was no significant improvement in model performance when separate parallel inputs were used instead of an average. This result indicates that inflows from tributaries are highly correlated. Moreover, there are many unmeasured tributaries along the river that may change the flow dynamics at the downstream reach. Therefore, even though the flood peak travels about 4-5 days from Bondary to Suraż, the maximum advective delay obtained for the Suraż model with averaged flows from Bondary, Narewka and Orlanka at the input equals only 1 day. The SSG for that model indicates that 30% of the water originates from the unmeasured tributaries. This model and the similar MISO model using parallel inputs, are the only models suitable for flood forecasting. Models obtained without advective delay may be useful during scenario analysis. The residence time obtained for the sub-reach Narew-Płoski model equal to 0.5 day indicates that one day is too large a discretisation period for that part of the river.

The fact that the Bondary/Suraż model does not reproduce low flows well suggests that a nonlinear relationship exists between flows measured at the upper (Bondary) and the lower (Suraż) river cross-sections. That indicates the need to introduce a nonlinear transformation of variables in order to model the flow routing process between these two cross-sections, as well as using stages instead of flows.

4.2 Linear STF models for the stage

Table 2 lists the linear STF models obtained for the stage measurements for the same sets of input-output combinations as flow models presented in Table 1. Some results for the validation of level-level models for the Bondary/Żółtki reach are presented in

Figs. 7-10. In all the figures continuous lines denote the estimated outputs, dots denote the observed values and shaded areas denote 0.95 confidence bounds. The level-level Bondary/Żółtki model shows the worst validation results, pointing to a worsening of the level relations resulting from the bad stage of the gauging station at Żółtki. The fact that the flow model performed well for the same river reach may be a coincidence, or it may result from the flow data post-processing. It is worth remembering here that flow data are obtained from the level measurements via an application of a rating curve specific for each gauging station.

Table 2

MISO/SISO TF models for water levels measured at Bondary-Żółtki reach of River Narew

Input	Output	Model	P	R	SSG	T [day]	R_T^2 c [%]	R_T^2 v [%]
Bondary Narewka	Narew	[1 1 1 0 0]	0.3033	0.4325 0.1337	0.6209 0.1919	0.84	89.94	92.80
Bondary+Narewka	Narew	[1 1 0]	0.5120	0.3810	0.7808	1.49	88.49	93.40
Narew	Płoski	[1 1 0]	0.6232	0.5348	1.4194	2.11	89.08	94.01
Bondary+Narewka	Płoski	[1 1 0]	0.7572	0.2919	1.2022	3.60	84.41	92.14
Ploski Chraboły	Suraż	[1 1 1 0 0]	0.6094	0.3468 0.1241	0.8880 0.3176	2.02	95.50	96.28
Ploski+Chraboły	Suraż	[1 1 0]	0.7710	0.3207	1.4003	3.84	93.51	93.77
Bondary Narewka Chraboły	Suraż	[1 1 1 1 3 3 1]	0.5677	0.4936 -0.1103 0.3604	1.1420 -0.2551 0.7088	1.77	89.38	89.13
Bondary+Narewka +Chraboły	Suraż	[1 1 1]	0.8083	0.3162	1.6497	4.70	75.50	90.47
Suraż	Żółtki	[1 1 1]	0.7682	0.2423	1.0450	3.79	85.60	62.28

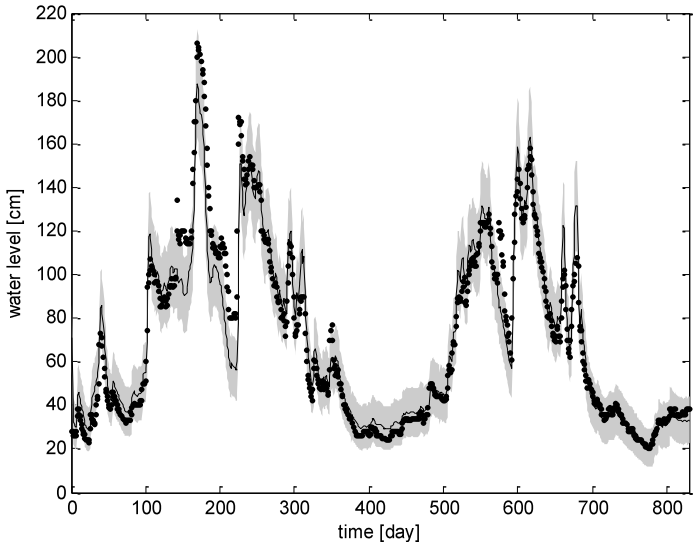

Fig. 7. SISO STF water level model at Narew based on averaged Narewka and Bondary water levels observations; validation stage, 93.40% of output variation explained.

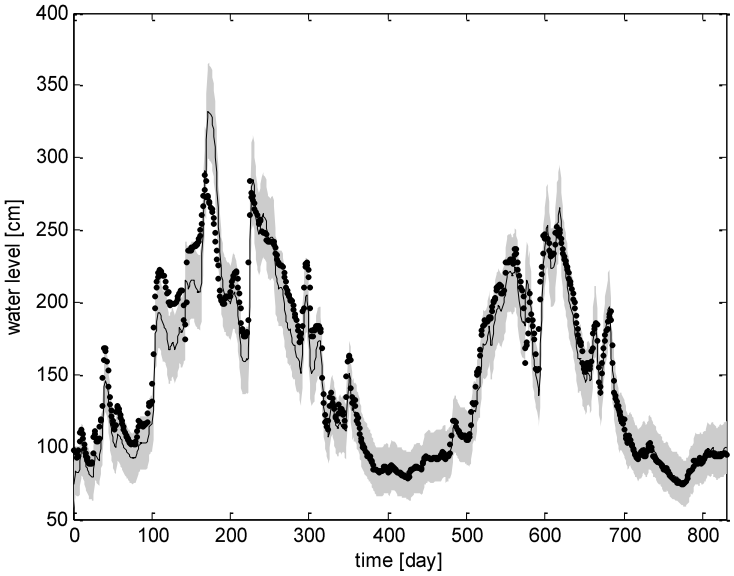

Fig. 8. Validation of Narew/Płoski SISO STF model for water levels; 94.01% of output variation explained.

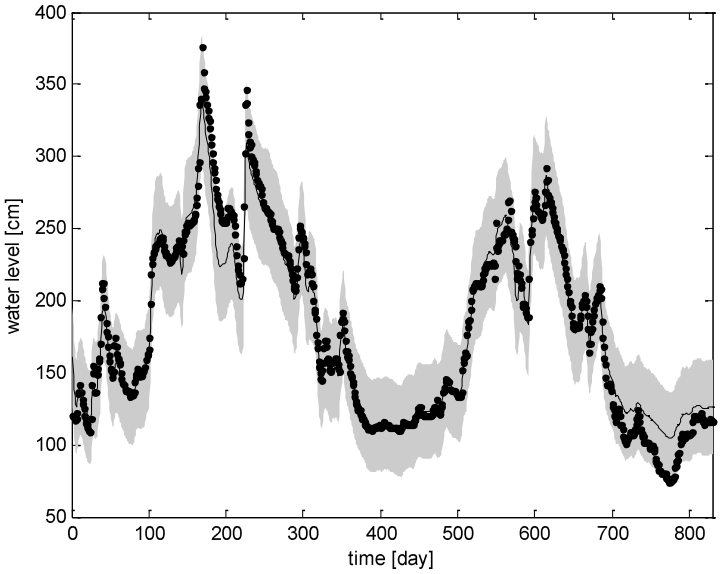

Fig. 9. Validation of MISO STF model for water levels: Płoski, Chraboły/Suraż, 96.28% of output variation explained.

4.2.1 Summary of modelling results

The modelling results for the water levels are very similar to those obtained for the flows, with the exception of Suraż/Żółtki model. That model showed a much worse performance when water levels were used as the state variable. The gauging station at

Żółtki has not operated since 1983 as it was malfunctioning; therefore the results from this station are not reliable.

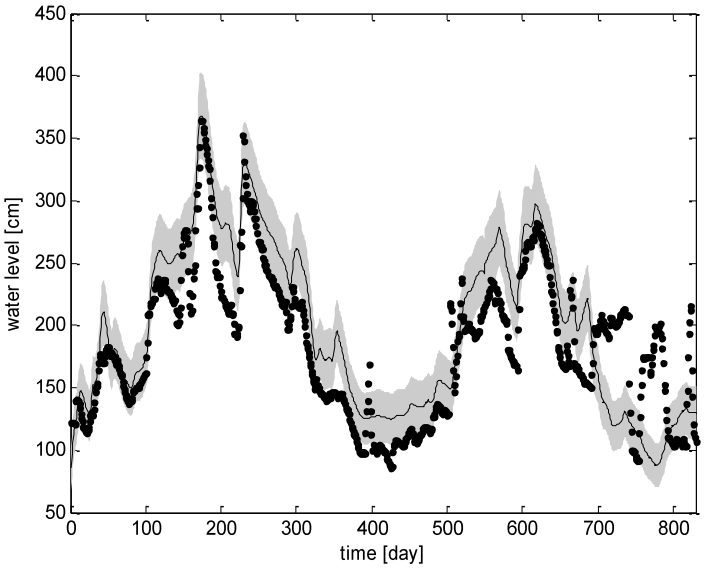

Fig. 10. Validation of SISO STF model for water levels at Żółtki based on water levels at Suraż; 62.28% of output variation explained.

The STF models obtained for each gauging station are first-order with a zero advective time delay resulting from a daily discretization period of the observations. Only the Bondary–Narewka/Suraż model and the Suraż/Żółtki model have a one day time delay. Therefore only these models can be used within the optimization routine, which requires a one step-ahead solution with regard to the input variables.

4.3 Nonlinear STF models for rainfall/flow and rainfall/water level predictions

There are daily rainfall measurements available from gauging stations situated within and around the Upper Narew catchment. In our analysis we applied an exponential relationship between flow and effective rainfall (Eqs. 1-3) using rainfall measurements and flow from the Narewka and Chraboły gauging stations. Table 3 presents the results of the DBM analysis describing rainfall-flow and rainfall-stage processes for the Narewka and Chraboły sub-catchments. The validation results for the DBM rainfall-flow models for Narewka and Orlanka are shown in Figures 11 and 12.

The linear STF models applied to these catchments explained only 10-20% of the output variation. Therefore, it was not possible to obtain reasonable flow predictions using linear STF model predictions as a surrogate of soil moisture content. We decided to use Soil Moisture Accounting (SMA) technique (Jolley 1995) to derive the effective rainfall nonlinearity for the off-line simulations. This method applies two-store structure based on Penman drying curve to derive effective rainfall with temperature and measured rainfall used as input variables. The SMA model parameters were optimized together with the dynamic (STF) model parameters to obtain the best model

performance and are given in Table 3. The validation results shown in Figs. 13 and 14 (respectively, Narewka and Chraboły catchments) have large 0.95 uncertainty bounds (shown by shaded gray areas) and explain much less of the output variance than STF models obtained for the flow/stage routing. In the figures the continuous lines denote the estimated output and dots denote the observations. Further research is undergoing towards introducing snow melt model and application of logarithmic transformation of flows to improve model predictions.

Table 3

SISO nonlinear STF models describing rainfall-flow process in the catchments of Narewka and Orlanka

Input	Output	Model	P	R	T [day]	R_T^2 c [%]	R_T^2 v [%]
Nowosady rainfall	Narewka flow	[1 1 2] +exp	0.8853	0.0826	8.21	73.05	78.02
Tykocin rainfall	Chraboły flow	[1 1 1] +exp	0.8814	0.0896	7.92	68.40	70.99
Kleszczele rainfall +Białystok temp.	Narewka low	[1 1 2] +SMA	0.9375	0.3333	15.49	61.24	60.84
Kleszczele rainfall +Białystok temp.	Chraboły flow	[2 2 1] +SMA	0.8830 0.1488	0.3955 -0.1642	8.04 0.52	73.66	69.18
Białowieża rainfall +Białystok temp.	Narewka water level	[1 1 1] +SMA	0.9372	1.6850	15.43	66.46	59.84
Białowieża rainfall +Białystok temp.	Chraboły water level	[1 1 1] +SMA	0.9721	1.8080	35.32	56.54	60.31

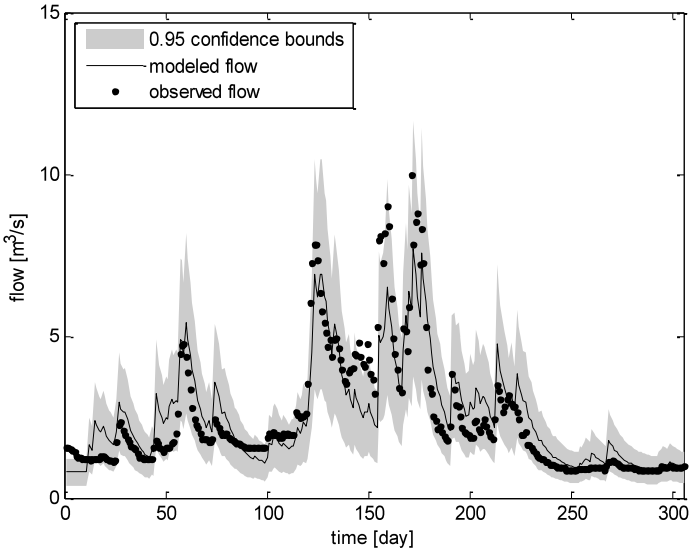

Fig. 11. Validation of STF model with effective rainfall for the Narewka subcatchment.

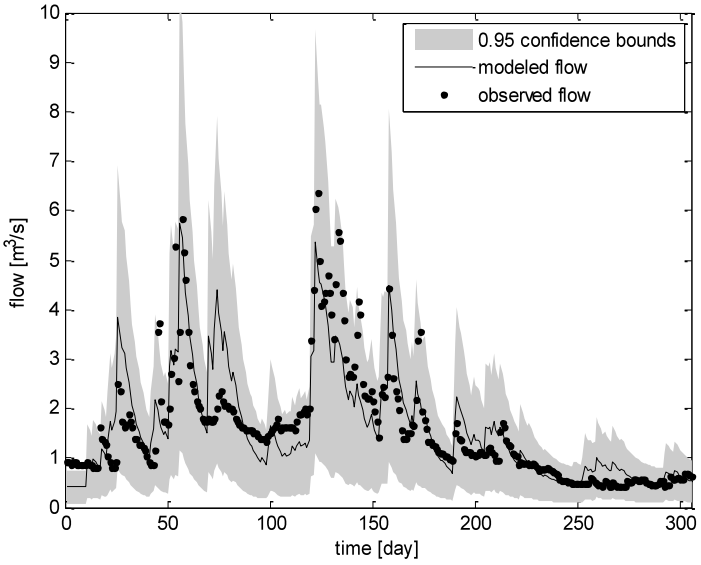

Fig. 12. Validation of STF model with effective rainfall for the Orlanka subcatchment.

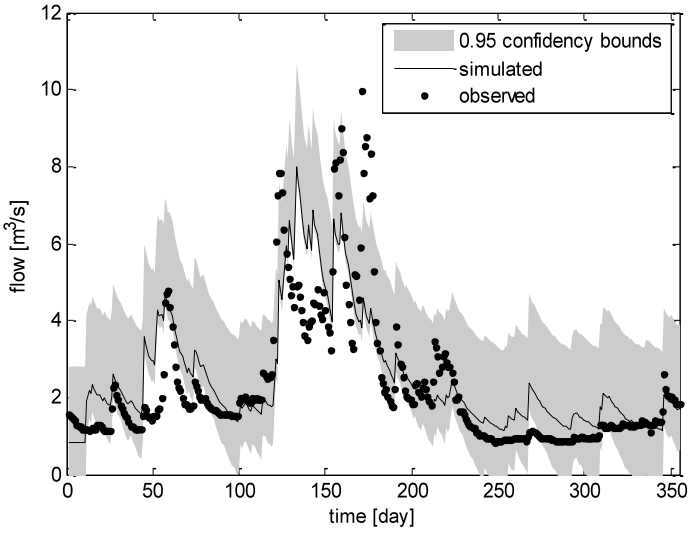

Fig. 13. Validation of SMA model on Narewka subcatchment: 60.84% of output variation explained.

4.3.1 Summary of the results of modelling

The models of rainfall-flow processes gave much worse results than the flow/stage modelling presented in previous sections. One of the reason may be the fact that daily data are not suitable for Narewka and Chraboły because of their small catchment area. Further work is required towards better catchment instrumentation and gathering hourly rainfall and stage records to improve the modelling results. The Upper Narew catchment spring floods are also affected by snow-melt processes, which were not in-

cluded in the model. Therefore, the results obtained indicate the need to extend the sub-catchment integrated model by a model of snow-melt.

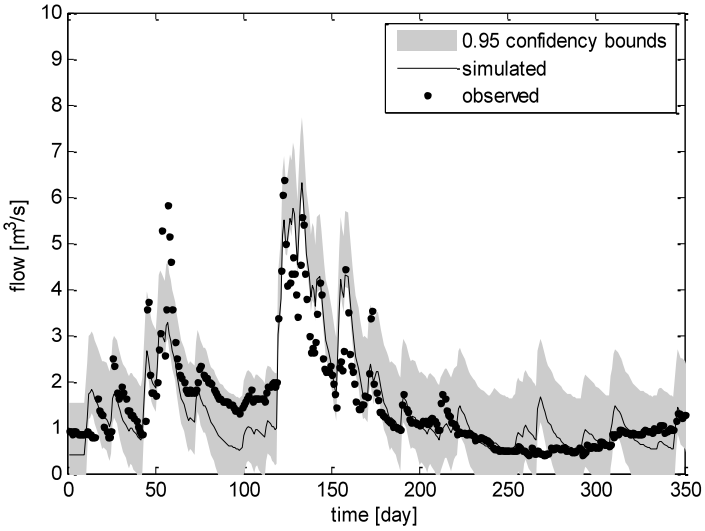

Fig. 14. Validation of SMA model on Orlanka subcatchment: 69.18% of output variation explained.

4.4 Derivation of SIMULINK model

The modules derived in the previous sections were combined together within SIMULINK-MATLAB programming language to form the simulation model for the entire catchment. The model structure is shown in Fig. 15.

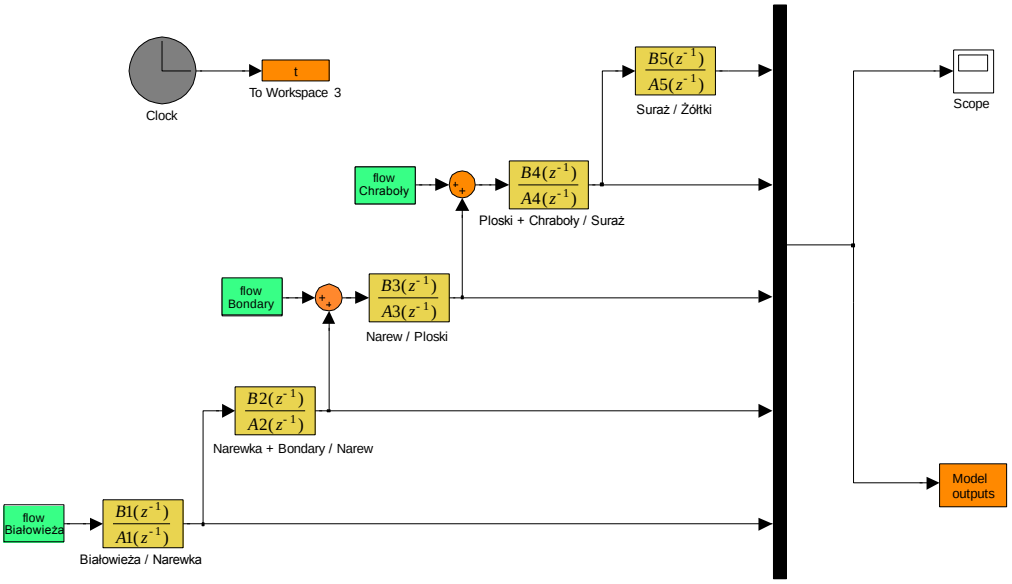

Fig. 15. SIMULINK model structure.

This model simulates flow/stage routing from Bondary gauging station down to Żółtki. The model structure includes the inflows measured at Bondary, Narewka and Chraboły. The system can be easily extended by the other modules such as rainfall-flow or snow-melt module, if available. The model simulations are stored in computer memory and/or displayed on-line thus making the program very useful during the scenario analysis of the possible management practices.

5. Conclusions

Most of the estimated routing models have first-order dynamics. The best results were obtained for the neighbouring sub-reaches and there was no significant improvement of model performance if separate parallel inputs were used instead of an average sum. This result indicates that inflows from tributaries are highly correlated. Moreover, there are many unaccounted for tributaries along the river, which change the flow dynamics at the downstream reach. Therefore, even though the flood peak travels in about 4-5 days from Bondary to Suraż, the maximum advective delay obtained for the Suraż model with averaged flows from Bondary, Narewka and Orlanka on the input equals only 1 day. This model and the similar, MISO model using parallel inputs, are the only models suitable for flood forecasting. Models obtained without advective delay may still be useful during scenario analysis. The residence time obtained for the model of the Narew-Płoski sub-reach, equal to 0.5 day, indicates that one day may be too large a discretisation period for that part of the river. Modelling results for the water levels are very similar to those obtained for the flows, with the exception of the Suraż/Żółtki model. That model showed a much worse performance when water levels were used as the output variable. As the water levels are the observed variable and flows are obtained after applying the rating curve, we investigated the transformation between levels and flows for that station which showed that flows at Żółtki were altered to adjust for the malfunctioning of the gauging station. The STF models derived to describe the rainfall-flow processes in the sub-catchments of Narewka and Chraboły apply an exponential transformation of rainfall with flow measurements used as the surrogate of soil moisture content. This approach is suitable for "what-if" scenario analysis of water management policy down the river Narew, but it is not suitable for off-line model simulations. Therefore, the SMA technique was used to obtain the effective rainfall transformation, used in the STF model as an input variable. The derived STF modules describing rainfall/flow and flow routing in the Narew catchment were combined into an integrated rainfall-flow/level routing system (Romanowicz *et al*. 2006). The system is subsequently used to build a SIMULINK model of the entire Upper Narew catchment, for the purpose of scenario analysis. That model will be also used for the testing and derivation of optimal reservoir releases for the purpose of draught and flood mitigation.

References

Beven, K.J, and A. Binley (1992), *The future of distributed models: model calibration and uncertainty prediction*, Hydrological Processes **6**, 279-98.

Box, G., and G. Jenkins (1970), *Time series analysis: Forecasting and control*, Holden Day, USA.

Dembek, W., and A. Danielewska (1996), *Habitat diversity in the Upper Narew valley from the Siemianówka reservoir to Suraż*, Zeszyty Problemowe Postępów Nauk Rolniczych **428**.

Hervouet, J.M., and L. Van Haren (1996), *Recent Advances in Numerical Methods for Fluid Flows*. **In:** M.G. Anderson, D.E. Walling, and P.D. Bates (eds.), "Floodplain processes", John Wiley and Sons, Chichester, U.K.

Holder, L. (1985), *Multiple regression in hydrology*, Institute of Hydrology, Wallingford.

IWOR (2002), *Protection plan of the Narew National Park*, technical report, IWOR S-ka z o.o. and IMUZ Falenty.

Jolley, T.J., and H.S. Wheater (1996), *A large-scale grid-based hydrological model of the Severn and Thames catchments*, Journal of the Chartered Institution of Water and Environmental Management **10**, 4, 253-262.

Khan, M.H. (1993), *Muskingum flood routing model for multiple tributaries*, Water Resour. Res. **29**, 1057-1062.

Park, J., J. Obeysekera, and R. Van Zee (2005), *Prediction boundaries and forecasting of nonlinear hydrologic stage data*, J. Hydrol. **312**, 79-94.

Porporato, A., and L. Ridolfi (2001), *Multivariate nonlinear prediction of river flows*, J. Hydrol. **248**, 109-122.

Romanowicz, R.J., and R. Macdonald (2005), *Modelling Uncertainty and Variability in Environmental Systems*, Acta Geophys. Pol. **53**, 401-417.

Romanowicz, R.J., P.C. Young, and K.J. Beven (2006), *Data assimilation and adaptive forecasting of water levels in the river Severn catchment, United Kingdom*, Water Resour. Res. **42**: W06407. doi:10.1029/2005WR004373.

Taylor, C.J., D.J. Pedregal, P.C. Young, and W. Tych (2007), *Environmental time series analysis and forecasting with the Captain toolbox*, Environmental Modelling and Software **22**, 6, 797-814.

Thirumalaiah, K., and M.C. Deo (2000), *Hydrological forecasting using neural networks*, J. Hydrol. Eng. **5**, 2, 180-189.

Young, P.C. (1984), *Recursive Estimation and Time Series Analysis*. Berlin: Springer-Verlag.

Young, P.C. (2001), *Data-based mechanistic modelling and validation of rainfall-flow processes*. **In:** M.G. Anderson, and P.D. Bates (eds.), "Model Validation: Perspectives in Hydrological Science", 117-161, Wiley.

Young, P.C. (2000), *Stochastic, dynamic modelling and signal processing: time variable and state dependent parameter estimation*. **In:** W.J. Fitzegarald, A. Walden, R. Smith, and P.C. Young (eds.), "Nonstationary and nonlinear signal processing", 74-114, Cambridge.

Young, P.C. (2003), *Top-down and data-based mechanistic modelling of rainfall-flow dynamics at the catchment scale*, Hydrol. Process. **17**, 2195-2217.

Young, P.C. (2006), *Transfer function models*. **In:** M.G. Anderson, J. Wiley (eds.), "Encyclopedia of Hydrological Sciences", Chichester.

Young, P.C., and K.J. Beven (1994), *Data-based mechanistic modelling of rainfall-flow nonlinearity*, Environmetrics **5**, 335-363.

PUBLS. INST. GEOPHYS. POL. ACAD. SC., E-9 (405), 2008

Sensitivity and Uncertainty Analysis Applied to Water Management Problem: Upper Narew Case Study

Adam KICZKO, Renata J. ROMANOWICZ, and Jarosław J. NAPIÓRKOWSKI

Institute of Geophysics, Polish Academy of Sciences
Ks. Janusza 64, 01-452 Warszawa, Poland
e-mail: akiczko@igf.edu.pl

Abstract

The aim of this paper is to investigate the methods of maintaining desired flow conditions in the reaches of the ecologically valuable upper reaches of the River Narew taking into account the uncertainty in modelling process. The study is based on Global Sensitivity Analysis (GSA) and Generalised Likelihood Uncertainty Estimation (GLUE) techniques applied to a 1-D river flow model. We compare specified water management scenarios applied to the river and a water storage reservoir upstream. A locally conditioned GSA is used to estimate the influence of each conservation action scenario. The estimated uncertainty of model predictions is presented as a map of probability of inundation of the Narew National Park wetlands.

1. Introduction

In recent years alarming changes have been observed in the hydrologic regime of the River Narew, shown in a reduction of mean flows and shorter flooding periods. This has resulted in a serious threat to the rich wetland ecosystems. Many local management activities address this problem and a number of concepts for conservation actions have evolved. In this paper we apply Global Sensitivity Analysis (GSA), described in Archer et al. (1997), and Generalised Likelihood Uncertainty Estimation (GLUE) technique, introduced by Beven and Binley (1992), to analyse the influence of activities aimed at preserving the semi-natural state of marsh ecosystem localised downstream of the Suraż water level gauge. As far as we know, it is the first joint application of the GSA and GLUE techniques to the environmental management problem that additionally takes into account the uncertainties involved in the modelling process. The management activities have the form of water management scenarios applied to the river and a water storage reservoir upstream. The paper is a continuation of the work presented in Kiczko *et al*. (2007).

The estimation of uncertainty is a fundamental issue in hydrology and hydraulic modelling (Romanowicz and Macdonald 2005, Beven 2006, Pappenberger and Beven 2006). It is performed here using multiple Monte Carlo model simulations following the GLUE approach which was applied to flood inundation modelling by Romanowicz *et al.* (1996) and Romanowicz and Beven (2003). A computationally efficient distributed flow routing model is required for the estimation of uncertainty in flood inundation predictions used in the evaluation of the impact of water management scenarios on water conditions on the wetlands. The UNET 1D model (Barkau 1993) was chosen due to its short run times. As a result, maps showing the probability of inundation in the wetland area have been obtained.

We apply the GSA technique (Ratto *et al*. 2001) together with the GLUE approach to obtain a quantitative measure of the significance of each water management scenario. The results of the analysis are important for the future formulation of a water management system in the region.

2. Study area

The Valley of the Upper Narew is located in north-east Poland. The study area includes a 70 km long reach that begins at the Siemianówka Water Reservoir and ends at the water level gauging station in Suraż (Fig. 1). Generally, with the exception of areas close to the reservoir built in the early 1980s, this part of the river has not been modified by human activity. The valley is approximately 1-2 km wide. It has been shaped by a meandering river channel and presents a natural form of a lowland river system, with relatively small water slope values, at the level of 0.24‰. The annual river discharge varies from 5.72 to 15.50 m^3/s. In this area the river generally flows in one channel. However, due to the existence of meanders and old river beds, this river system has a rather complex structure during high flows.

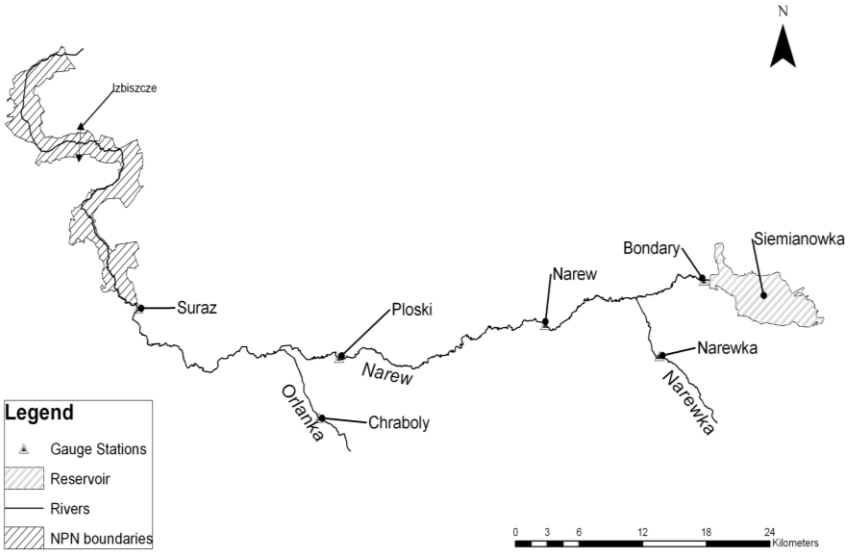

Fig. 1. Schematic map of the study area.

Almost 90% of the valley is occupied by rich wetland ecosystems, mostly marshes (55%) and peat lands (31%). Ten percents of the area is covered by postglacial mineral soils and sand dunes. Moreover, mud soils filling the old river beds play an important role in maintaining local ecosystems. Under these conditions extensive agriculture is possible only in the valley terrains. The semi-natural character and environmental conditions of the region implicate that this part of the Narew valley has great value from the ecological point of view (Dembek and Danielewska 1996).

3. Approach and methods

Wetland ecosystems depend largely on flooding (Junk *et al*. 1989). Therefore, actions aimed at preserving their quasi-natural character rely generally on the range of flooding parameters, such as flooding area, average depth and flood frequency in the wetland area (Kubrak *et al*. 2005, Okruszko *et al*. 1996). There are many different suggestions of how to improve water conditions in this region. The following approaches to this problem, aimed at affecting the chosen site through modification of river water stages, are analysed:

1. Modification of the Siemianówka reservoir releases under low flow conditions;
2. Water level control system on Narew tributaries under low flow conditions;
3. Changes in floodplain land-use under high flow conditions;
4. Changes in channel conveyance under high flow conditions.

In this paper we investigate the joint applications of GSA and GLUE techniques to assess the efficiency of the above listed management approaches when applied to the upper reaches of the River Narew. The river system is described using a One-Dimensional Unsteady Flow Through a Full Network of Open Channels model (UNET), developed by the U.S. Army Corps of Engineers, Hydrologic Engineering Center.

Irrigation of the downstream valley is one of the main purposes of the Siemianówka reservoir; therefore, it is the most suitable tool for intervention in the natural system. Following the first of approaches listed above, we investigate the impact of the generated "artificial flood pulses" (Tockner *et al*. 2000) on the chosen wetland area during summer water shortage periods. Reservoir discharges were chosen in the form of rectangular pulses, characterized by a discharge value and duration time. In the case of a low flow control system (second approach), the assumption was made for the Narew tributaries (Narewka and Orlanka) that it is possible to store water in the subcatchments during rain periods and release it during low water periods. Until now, low flow control on the River Narew has consisted of a restoration of formerly existing semi-natural river barriers, maintained by local communities for fishing purposes. The influence of such barriers on river flow was analysed through the investigation of spatial impacts caused by the modification of roughness parameters in the numerical model of the Narew reach (third approach). Changes in the floodplain land-use were considered here as a modification of terrain roughness coefficients (the fourth approach).

Because of the complexity of the problem, the study of influence of channel and floodplain conveyance (roughness coefficients) is limited to an analysis of changes of flood peak levels in the chosen wetland area. As flood area and average depth depend strongly on flood wave height, this should provide a satisfactory approximation to the influence of control variables on hydrological conditions in the area.

A sensitivity analysis was performed on locally conditioned model performance measures, which additionally allowed spatially distributed effects to be investigated. Each intervention investigation was performed in separate runs, thus it was necessary to introduce some reference factors to enable comparability of results. For this purpose, Manning roughness coefficients were used, and the other resulting sensitivity indices were normalized in relation to those indices.

The choice of parameter ranges necessary for the management scenario analysis, was achieved via a model calibration using the combined GSA and GLUE methodology. Model parameter ranges assessed in this stage of work were used in the GSA for the chosen river management scenarios. The posterior distribution of parameters obtained during the GLUE calibration stage was used to derive uncertainty of UNET model predictions in the validation stage. It has a form of varying-with-time probability distribution of water level predictions for each of the UNET model cross-sections. The quantiles of these distributions are mapped onto the digital elevation data of the studied River Narew reach to give varying-in-time maps of probability of inundation. These maps may be compared with water demands under low and high water conditions, thus helping in specifying the goals and an assessment of water management policies.

3.1 Experimental design

We performed four numerical experiments:

(i) A sensitivity analysis of model predictions at three cross-sections (Narew, Płoski and Suraż) to the following parameters: roughness coefficients, tributaries and lateral inflow correlation coefficients, lateral inflow delay, the upstream boundary condition error and the downstream water surface slope for the whole hydrologic year;

(ii) Model calibration and validation using the GLUE methodology and derivation of map of probability of maximum inundation under the natural flow conditions;

(iii) Sensitivity of model predictions at Suraż cross-section to the shape and timing of reservoir releases and controlled tributaries' outflows under low flow conditions;

(iv) Influence of modification of channel conveyance upstream and downstream of Suraż cross-section on maximum water level distribution in its vicinity.

3.2 The flow routing model

The UNET (Barkau 1993) code is a numerical implementation of the 1-D Saint Venant equation. The current version is capable of performing one-dimensional water

surface profile calculation for gradually varied flow in natural or constructed channel. Subcritical, supercritical, and mixed flow regime water surface profiles can be calculated.

The River Narew reach is represented by 49 cross-sections at about 2 km intervals, obtained from a terrain survey. The model was calibrated by adjusting the Manning coefficients separately for the channel, left and right floodplains, and a water surface slope used as a downstream boundary condition. To filter out the influence of the downstream condition, an additional cross-section, 10 km downstream of the reach was included. It was assumed that the value of roughness coefficients changes linearly between cross-sections. Therefore, the variability of this parameter was described in the form of values on nodes, between which the roughness coefficient was interpolated.

The model mass balance was difficult to maintain due to a lack of data on lateral inflows, with the exception of the Narewka and Orlanka tributaries. It was possible to estimate the unobserved lateral inflows using the assumption that they are linearly correlated with observed tributary inflow and can be described using a linear regression model with a constant delay corresponding to the tributary location.

3.3 The GSA methodology

In this study, the GSA methodology (Ratto *et al*. 2001, Kiczko *et al.* 2008) was applied to determine model sensitivity to Manning coefficients and to boundary conditions. GSA also allows the significance of a particular model input to be evaluated, making it possible to investigate the effects of a particular river management action (such as discharges from Siemianówka reservoir and floodplain land-use upstream) on flow conditions downstream.

According to this approach, the variance of an output Y depending on the input set X_i can be treated as the sum of a top marginal variance and a bottom marginal variance (Ratto *et al*. 2001):

$$V(Y) = V\left[E(Y \mid X_i = x_i^*)\right] + E[V(Y \mid X_{-i} = x_{-i}^*)\Big]. \tag{1}$$

where the term X_{-i} indicates all the inputs but X_i and V and E denote variance and expectation operators, respectively.

The main effect or the first order sensitivity index S_i, representing the sensitivity of output Y to the input X_i, is defined as a top marginal variance divided by the total variance:

$$S_i = \frac{V[E(Y \mid X_i = x_i^*)]}{V(Y)}. \tag{2}$$

The total sensitivity index S_{Ti} for the input X_i combines in one single term all the interactions involving X_i. It is defined as an average output variance that would remain as long as X_i stays unknown:

$$S_{Ti} = \frac{E[V(Y \mid X_{-i} = x_{-i}^*)]}{V(Y)} \tag{3}$$

where X_{-i} denotes all X input elements except X_i.

During the first application of the GSA (in the calibration stage) mean water levels at 3 gauging stations were taken as output *Y* and Manning coefficients, boundary water slope, correlation coefficients of tributaries with lateral inflows and error of upper boundary condition (inflow at Bondary) were used as input parameters *X*.

After the calibration stage, an investigation of the influence of different control variables on flood wave propagation was carried out for the maximum peak value as an output (*Y* variable) and Siemianówka reservoir, Narewka and Orlanka tributaries outflow characteristics and Manning coefficients as input parameters (*X* variables), following the experimental design outlined in Section 3.1.

3.4 The GLUE methodology

Model calibration and estimation of predictive uncertainty were carried out following the GLUE methodology. The basic assumption of this methodology (Beven and Binley 1992) is that in the case of over-parameterized environmental models, a unique solution of the inverse problem is not possible due to a lack of data (an interactive discussion of this topic is promoted by Pappenberger *et al*. 2007). There can be many different parameter sets which provide reasonable results. Therefore, calibration should consist of the estimation of the multidimensional distribution of model parameters. For such an analysis the Bayesian formula is used:

$$f(\mathbf{X}\,|\,\mathbf{z}) = \frac{f_0(\mathbf{X})L(\mathbf{z}\,|\,\mathbf{X})}{L(\mathbf{z})} \tag{4}$$

where $\mathbf{z}$ is the observation vector, $f(\mathbf{X}\,|\,\mathbf{z})$ is the posterior distribution (probability density) of the parameters conditioned on the observations $\mathbf{z}$, $f_0(\mathbf{X})$ is the prior probability density of the parameters, $L(\mathbf{z})$ is scaling factor, $L(\mathbf{z}\,|\,\mathbf{X})$ represents the likelihood measure based on the relationship between $\mathbf{z}$ and $\mathbf{X}$. On the basis of information on the prior distribution of model parameters, which comes from knowledge of the physical structure of the modelled process and available observations of process output, it is possible to estimate the posterior distribution of parameters. In this study water levels at 3 gauging stations (Narew, Płoski and Suraż) were used as the observation vector $\mathbf{z}$; Manning roughness coefficients, discharge estimation error and value of water slope at the end of reach were used as parameter vector $\mathbf{X}$.

It is important to note that Eq. (4) is defined over the specified parameter space; therefore, the parameter interactions will be implicitly reflected in the calculated posterior distribution. This feature is especially important in the case of spatially distributed models, where parameters are inter-dependent. The marginal distributions for single parameter groups can be calculated by an integration of the posterior distribution over the rest of the parameters as necessary.

The essential element of the GLUE technique is a practical determination of the likelihood measure $L(\mathbf{z}|\mathbf{X})$. In this paper it was assumed that it is proportional to the Gaussian distribution function (Romanowicz and Beven 2006):

$$L(\mathbf{z}\,|\,\mathbf{X}) \approx e^{(\mathbf{z}-Y(\mathbf{X}))^2/\sigma^2} \tag{5}$$

where $\mathbf{z}$ is the observed water level, *Y* is a computed water level and σ^2 denotes the mean error variance determining the width of the distribution function. It is important

to note that in the GLUE methodology a subjective choice of the distribution width is allowed. On the basis of posterior likelihood values, the distribution of simulated water levels can be evaluated and subsequently used to derive spatial probability maps of the risk of flooding or drought in the area.

The model parameter space is sampled using the Monte Carlo method. The prior distribution $f_0(\mathbf{X})$ of parameters is introduced at this stage. A number of required model realizations depend on the modality of the resulting distribution and the dimension of the parameter space.

4. Results

4.1 Calibration and validation

The UNET model calibration was performed for the observation period 23.07.1981 – 28.08.1982. At the beginning of the calibration stage, the sensitivity of model parameters was analysed using the GSA method (this constitutes the first numerical experiment from the list given in Section 3.1). The analyzed parameters are: downstream gradient, uncertainty of boundary condition in Bondary, delay periods of Orlanka and Narewka inflows, Orlanka and Narewka flow coefficients (explained at the end of Section 3.2), right and left floodplain and channel roughness coefficients. Results presented in Figs. 2 and 3 show that the channel roughness and Narewka flow coefficient for additional lateral inflow are the major sources of uncertainty. The floodplain roughness has a marginal influence, with only a minor effect on the right side of the floodplain. The downstream boundary condition does not affect flow characteristics in the study area and this parameter was fixed during the following GLUE analysis stage. According to these results, the uncertainty related to the specification of upper boundary condition can also be neglected.

As there was no *a priori* information on parameter distribution, a uniform prior distribution was assumed during the GLUE analysis stage (Beven 2001). Finally, the parameters were sampled within the following ranges: channel roughness coefficient 0.015 – 0.045, floodplain roughness coefficient 0.08 – 0.12, the error of upper boundary condition as ±7%, lateral inflow correlation coefficients 1.5 – 4.5 and delay of lateral inflow: 0 – 10 days.

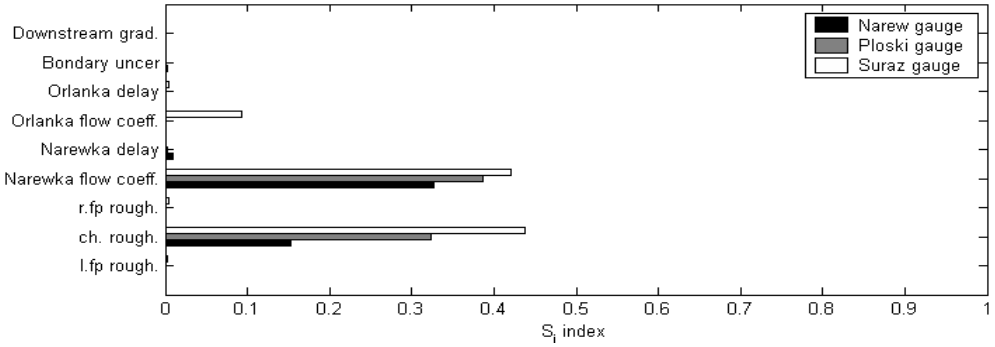

Fig. 2. First order sensitivity indices (S_i) of model input parameters listed along the *Y* axis.

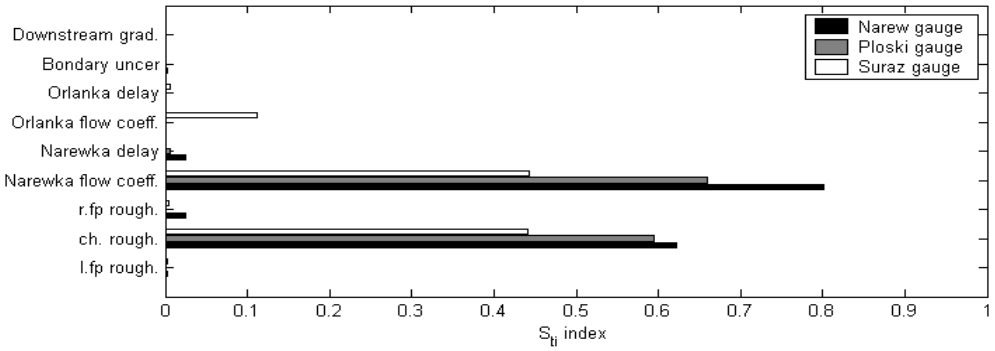

Fig. 3. Total sensitivity indices (S_{Ti}) of model input parameters listed along the *Y* axis.

The validation was performed using the observations from 3 gauging stations for the spring freshet 1981 and the period 0.5.10.1982 – 13.07.1983. Results of the model validation at Suraż are shown in Fig. 4. The observations are marked with a dotted line, thin continuous line shows the estimated water levels, and shaded area denotes 0.95 confidence bounds.

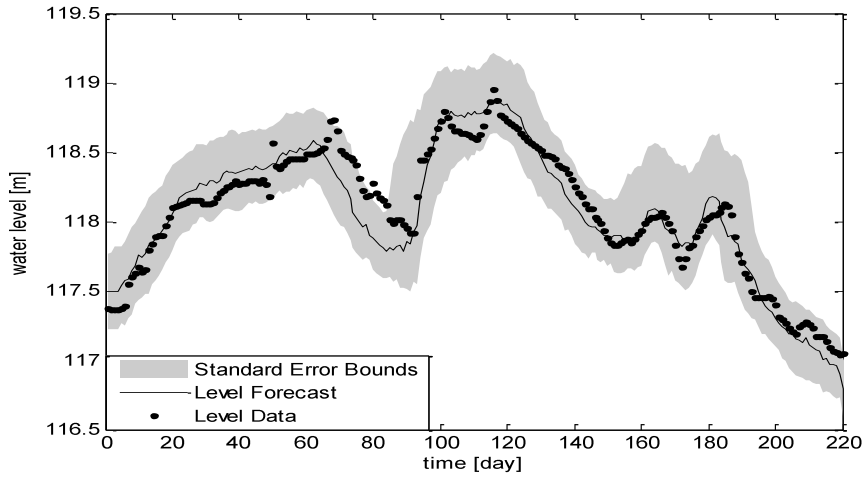

Fig. 4. Model validation for Suraż, observation period: 0.5.10.1982 – 13.07.1983, shaded areas denote 95% confidence bounds for the predictions shown by the continuous line, the observations are shown by dotted line.

The quantiles of maximum water levels along the river reach obtained during the validation stage were subsequently transformed into a map of probability of inundation shown in Fig. 5 for the spring freshet 1981.

Similar maps can be used by the water management team to assess the effects of different management scenarios on water conditions along the River Narew reach and in particular, in the Narew National Park wetland region. In this particular case, the map presents the probability of inundation under the natural conditions during the spring freshet in 1981, without the implementation of any reservoir control scheme. The detailed map of probability of inundation for the same maximum flood peak during the spring freshet in 1981 for the River Narew reach situated within the Narew National Park, downstream of Suraż (left hand corner of Fig. 5), is shown in Fig. 6.

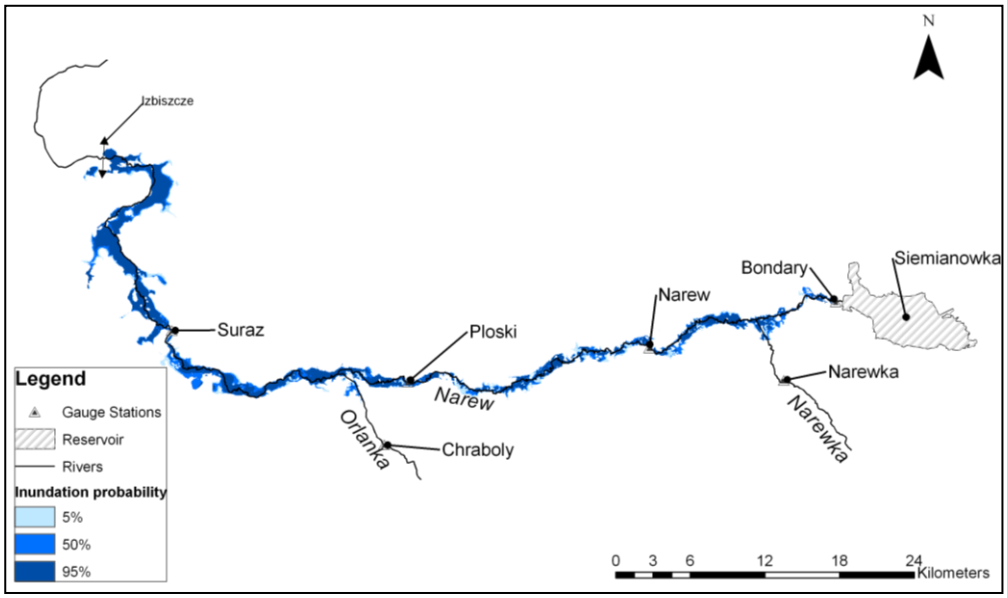

Fig. 5. Probability of inundation for maximum water levels along the Upper Narew reach during the spring freshet in 1981.

4.2 Scenario analysis

During the third numerical experiment (Section 3.1) consisting of an analysis of the impact of releases from the Siemianówka reservoir, it was assumed that 1,000,000 m^3 of water was available for control purposes during the low flow period. This value, denoting a special irrigation water reserve, was based on the present reservoir control scheme, developed by Bipromel (1999). Maximum reservoir discharges were limited by the capacity of power plant culverts to the value of 11.6 m^3/s. Storages in subcatchments Narewka and Orlanka were assumed to be equal to 86 000 m^3, with a maximum discharge increase of 1 m^3/s. The sensitivity of the river system to the modification of channel roughness was analysed within the parameter ranges of 0.02 – 0.06, with the lower and upper ranges corresponding to a change from a straight channel to a wooded and weedy reach. The influence of floodplain roughness was neglected, as the sensitivity analysis performed during the calibration stage showed that effects caused by its variations were marginal.

The impact of the reservoir and tributaries' discharge characteristics on wetland area is presented in Table 1.

The fourth numerical experiment consisted of an analysis of the influence of channel conveyance values on water levels. Results presented in Fig. 7 show the changes of the first order and total sensitivity indices for maximum water levels at three different cross-sections situated near Suraż. The sensitivity is evaluated with respect to channel roughness variations at 6 neighbouring cross-sections indicated in Fig. 7 by stars. It should be noted that these results cannot be directly compared with the results of reservoir and tributaries' outflow impact, as they were estimated under different parameter

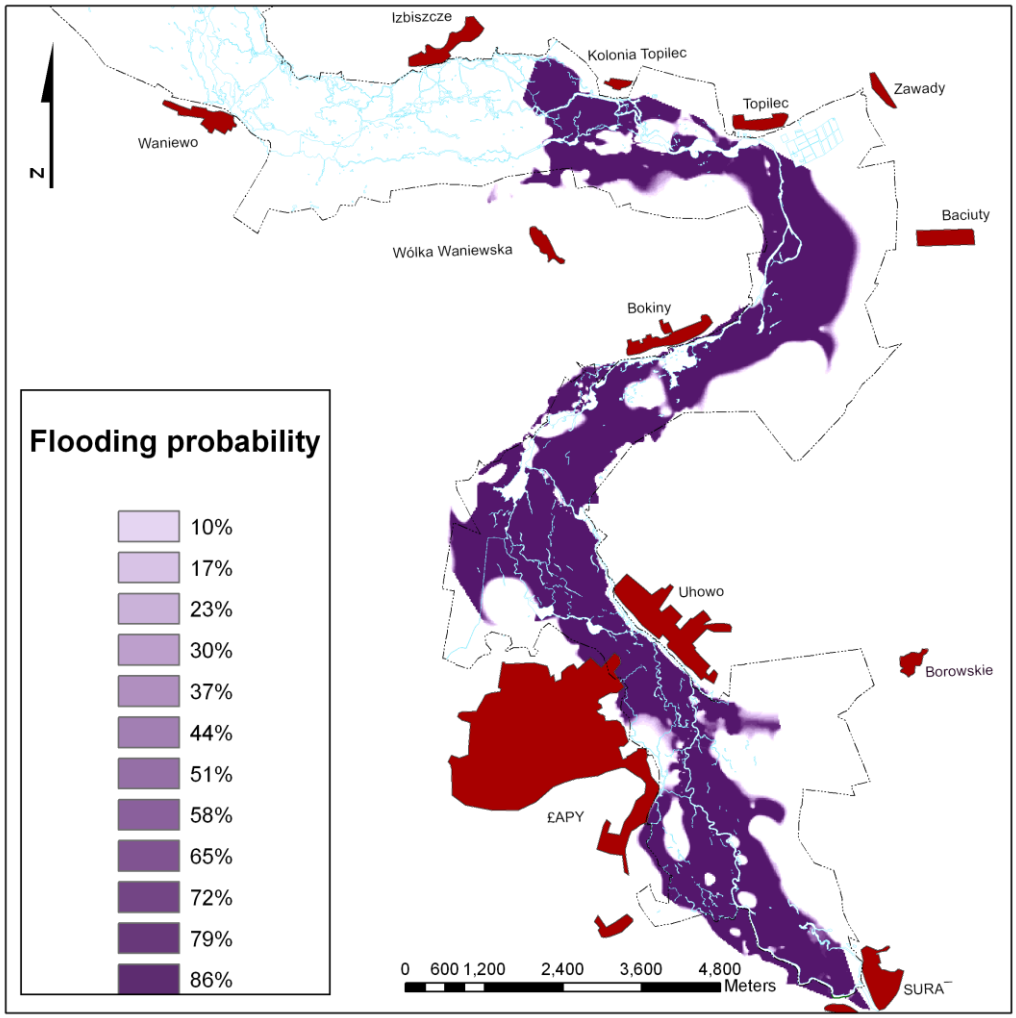

Fig. 6. Detailed map of probability of inundation for the River Narew reach situated downstream from Suraż (left hand corner of Fig. 5).

Table1

Impact of discharge characteristics on flow during the water shortage period

		Siemianówka reservoir	Narewka tributary	Orlanka tributary
Peak High	S_i	0.446	0.000	0.001
	S_{Ti}	0.510	0.011	0.009
Total discharge volume	S_i	0.446	0.000	0.002
	S_{Ti}	0.510	0.012	0.009

variations. However, as shown in Kiczko *et al.* (2007), the channel roughness has a similar impact to the modification of releases from the Siemianówka reservoir. In this experiment the range of influence varies along the river reach. In conclusion, the changes of channel roughness have an influence on the water levels within 4 km range, but the impact of these changes varies with location, probably due to some other factors, such as geometry of the channel and the floodplain.

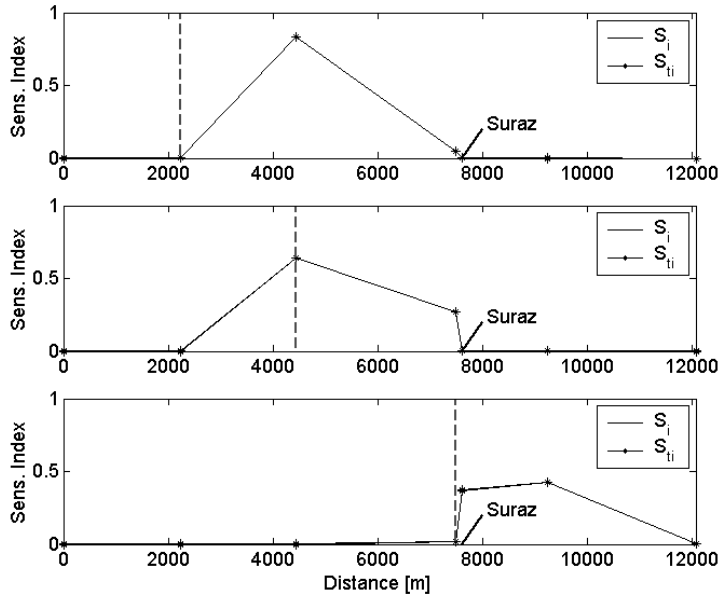

Fig. 7. Sensitivity of maximum water levels at 3 cross-sections upstream from Suraż indicated by the dashed lines (panels 1-3), to the variations in channel roughness at 6 cross-sections at the locations shown by stars.

5. Conclusions

We have reported here sensitivity and uncertainty analyses applied to water management scenarios aimed at wetland mitigation under different flow conditions. A 1D distributed flow routing model was used to derive distributed water level predictions along the Upper River Narew reach as a case study. The study included (i) a sensitivity analysis of distributed model predictions for the whole hydrologic year; (ii) model calibration and validation using GLUE and derivation of maps of probability of maximum inundations under the natural flow conditions; (iii) a sensitivity analysis of water level predictions downstream to changes of reservoir and tributary releases upstream under low flow conditions; (iv) the influence of local modifications of channel conveyance on water levels under high flow conditions. The uncertainty and sensitivity analyses were performed using GSA and GLUE techniques, which enabled a quantitative assessment of the impact.

In summary, the results show that channel roughness coefficients, Siemianówka reservoir releases and the Narewka tributary have major impacts on water conditions in the Upper Narew reach under study, whilst downstream boundary conditions and

floodplain roughness coefficients have a much smaller influence. The conclusion on small influence of floodplain roughness is consistent with the results obtained by Romanowicz *et al.* (1996). Therefore, land-use along the river reach might also have a small influence. However, modification of the channel conveyance may have a large local effect on water levels in the wetland areas. The uncertainty analysis allows the maps of probability of maximum inundation along the river to be estimated. These maps can be used in the specification and assessment of the reservoir and river management scenarios.

The results show unequivocally that the river reach can be successfully controlled at the Siemianówka reservoir and the wave height can be locally increased in specific areas through the restoration of semi-natural river barriers. The results obtained should help in formulating a suitable water management policy along the selected river reach.

Acknowledgments. This work was supported in part by grant 2 P04D 009 29 from Ministry of Science and Higher Education. We thank Marzena Osuch for her valuable comments.

References

Archer, G., A. Saltelli, and I.M. Sobol (1997), *Sensitivity measures, anova-like techniques and the use of bootstrap*, Journal of Statistical Computation and Simulation **58**, 99-120.

Barkau, R.L. (1993), *UNET, One-Dimensional Flow through a Full Network of Open Channels*, User's Manual version 2.1. Publication CPD-66, U.S. Army Corps of Engineers, Davis, CA, Hydrologic Engineering Center.

Beven, K.J. (2006), *A manifesto for the equifinality thesis*, J. Hydrol. **320**, 1-2, 18-36.

Beven, K.J., and A. Binley (1992), *The future of distributed models: model calibration and uncertainty prediction*, Hydrol. Process. **6**, 279-298.

Bipromel (1999), *Siemianówka reservoir – Water management rules*, (in Polish), Warsaw.

Dembek, W., and A. Danielewska (1996), *Habitat diversity in the Upper Narew valley from the Siemianówka reservoir to Suraż*, (in Polish), *Zesz. Probl. Post. Nauk Roln.* **428**.

Junk, W.J., P.B. Bayley, and R.E. Sparks (1989), *The flood pulse concept in river floodplain systems*. **In:** D.P. Dodge (ed.), "Large River", Proceedings of International Symposium Journal of Canadian Fisheries and Aquatic Sciences **11**, 106-107.

Kiczko, A., R.J. Romanowicz, and J.J. Napiórkowski (2007), *A study of flow conditions aimed at preserving valuable wetland areas in the Upper Narew Valley using GSA-GLUE methodology*, Proceedings 21st International Conference on Informatics for Environmental Protection, September 12-14, 2007, Warsaw, Poland, Shaker Verlag, 175-183.

Kiczko, A., R.J. Romanowicz, J.J. Napiórkowski and A. Piotrowski (2008), *Integration of reservoir management and flow routing model – Upper Narew case study*, Publ. Inst. Geophys. Pol. Acad. Sc. **E-9** (405), (this issue).

Kubrak, J., T. Okruszko, D. Mirosław-Świątek, and I. Kardel (2005), *Recognition of hydraulic conditions in the Upper Narew River System and their influence on the wetland habitats in the river valley*, Publs. Inst. Geophys. Pol. Acad. Sc. **387**, 209-237.

Okruszko, T., S. Tyszewski, and D. Pusłowska (1996), *Water management in the Upper Narew valley*, (in Polish), *Zesz. Probl. Post. Nauk Roln.* **428**.

Pappenberger, F., and K.J. Beven (2006), *Ignorance is bliss: or seven reasons not to use uncertainty analysis*, Water Resour. Res. **42**, 5, DOI: 10.1029/2005WR004820.

Pappenberger, F., K.J. Beven, K. Frodsham, R.J. Romanowicz, and P. Matgen (2007), *Grasping the unavoidable subjectivity in calibration of flood inundation models: A vulnerability weighted approach*, J. Hydrol. **333**, 2-4, 275-287.

Ratto, M., S. Tarantola, and A. Saltelli (2001), *Sensitivity analysis in model calibration: GSA-GLUE approach*, Computer Physics Communications **136**, 212-224

Romanowicz, R.J., K.J. Beven, and J. Tawn (1996), *Bayesian calibration of flood inundation models*, Floodplain Processes, 336-360.

Romanowicz, R.J., and K.J. Beven (2003), *Estimation of flood inundation probabilities as conditioned on event inundation maps*, Water Resour. Res. **39**, 3, DOI: 10.1029/2001WR001056.

Romanowicz, R.J., and K.J. Beven (2006), *Comments on Generalised Likelihood Uncertainty Estimation*, Reliability Engineering and System Safety, DOI: 10.1016/j.ress.2005.11.030.

Romanowicz, R.J., and R. Macdonald (2005), *Modeling uncertainty and variability in environmental systems*, Acta Geophys. Pol. **53**, 401-417.

Tockner, K., F. Malard, and J.V. Ward (2000), *An extension of the flood pulse concept*, Hydrol. Process. **14**, 2861-2883.

PUBLS. INST. GEOPHYS. POL. ACAD. SC., E-9 (405), 2008

Solute Transport Processes in Wetlands – Application of Data Based Mechanistic and Transient Storage Models

Marzena OSUCH, Renata J. ROMANOWICZ, and Jarosław J. NAPIÓRKOWSKI

Institute of Geophysics, Polish Academy of Sciences
Ks. Janusza 64, 01-452 Warszawa, Poland
e-mail: marz@igf.edu.pl

Abstract

The aim of this paper is the analysis of solute transport processes in Upper Narew River based on the results of tracer experiment. Data Based Mechanistic and transient storage models were applied to Rhodamine WT tracer observations. We focus on the analysis of uncertainty and the sensitivity of model predictions to varying physical parameters, such as dispersion and channel geometry. The study is based on a combined Global Sensitivity Analysis (GSA) and Generalized Likelihood Uncertainty Estimation (GLUE). The breakthrough curves for the chosen cross-sections are compared with those simulated with 95% confidence bounds. Apart from the predictions of the pollutant transport trajectories, two ecological indicators are also studied (time over the threshold concentration and maximum concentration). These indicators show an interesting multi-modal dependence on model parameters.

1. Introduction

The present study has been motivated by the need to understand the dynamics of the spread of pollutants in a unique river system situated within the Narew National Park. The River Narew reach chosen for the study has recently been identified as an anastomosing river, which is regarded as a separate group to braided, meandering and straight rivers.

A widely accepted method to understand the fate of solutes in streams is to perform a tracer study, in which a known mass of usually conservative solutes is released into the stream. The study consists of a recording at downstream stations of concentration versus time curves of the artificially released dye and of fitting appropriate models.

The first model considered was advection-dispersion with dead zones that can adequately describe the process of transport of pollutants in a single-channel river with multiple storages. As an alternative to that transient storage model, the Data Based

Mechanistic (DBM) approach introduced by Young (1974) was tested. In this approach, the model is identified and the parameters are estimated from the collected time series data using system identification techniques (Young 1984). These techniques also provide estimates of the modelling errors and the uncertainties of the model parameters.

The applied transient storage model is deterministic; it assumes that observations are without errors and the model structure perfectly describes the process of transport of conservative pollutants. In order to take into account the model and observation errors, an uncertainty analysis is required. In this study we applied a combination of the Generalized Likelihood Uncertainty Estimation technique (GLUE) of Beven and Binley (1992) and the variance based Global Sensitivity Analysis (GSA). The combination is straightforward as the same samples (Sobol samples) were generated for GLUE analysis and for sensitivity assessment. Additionally, the results of the sensitivity analysis were used to specify the best parameter ranges and their prior distributions for the evaluation of predictive model uncertainty using the GLUE methodology.

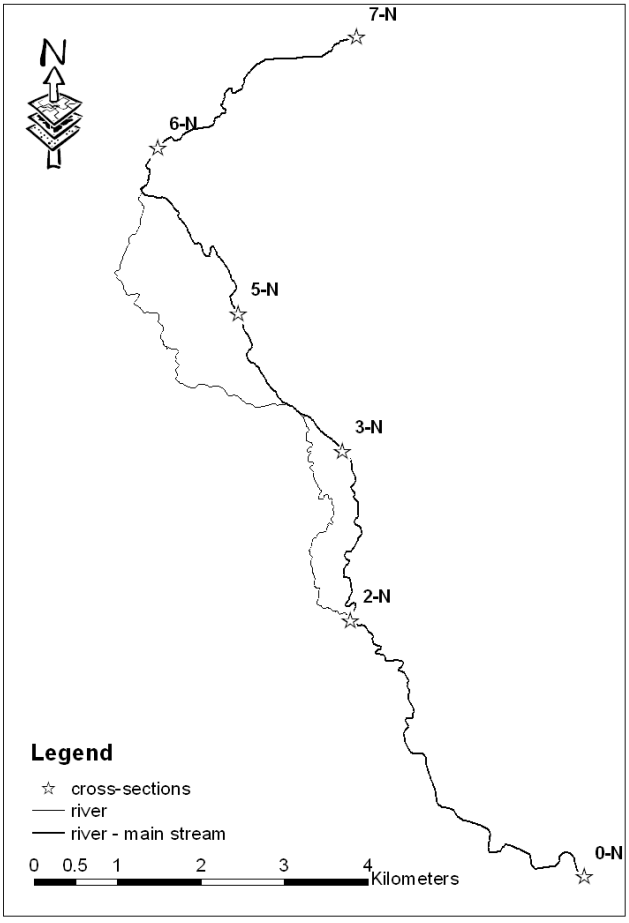

Fig. 1. Map of the experimental reach of upper River Narew.

2. Description of the experiment and case study

The present paper is based on a tracer test performed in a unique multi-channel system of the River Narew reach within the Narew National Park in northeast Poland (Fig. 1). A description of the experiment is presented in Rowiński *et al*. (2003a, b). The dye consisted of 20 liters of 20% solution Rhodamine WT injected at cross-section 0-N. Concentrations were measured in the River Narew at five transects, 2-N, 3-N, 5-N, 6N, and 7N, corresponding to flow distances of 5.75 km, 8.34 km, 10.62 km, 13.58 km, and 16.83 km, respectively. The dye was detected using the field fluorometer Turner Design with a continuous flow cuvette system. Water samples were also collected at sampling points.

3. Methodology

3.1 Applied models

Distributed transient storage model

The transport of a conservative soluble pollutant along a uniform channel is described by the well-known Advection-Dispersion Equation. To apply this equation to a practical scenario, a dispersion coefficient for the reach is required. Since a dispersion coefficient cannot be measured *in situ* directly from a simple individual measurement, it has to be estimated (optimized) on the basis of available experimental data. The One-dimensional Transport with Inflow and Storage (OTIS) model introduced by Bencala and Walters (1983) was applied in this study. The OTIS model is formed by writing mass balance equations for two conceptual areas: the stream channel and the storage zone. The stream channel is defined as that portion of the stream in which advection and dispersion are the dominant transport mechanisms. The storage zone is defined as the portion of the stream that contributes to transient storage, i.e., stagnant pockets of water and porous areas of the streambed. Water in the storage zone is considered immobile relative to water in the channel. The exchange of solute mass between the channel and the storage zone is modelled as a first-order mass transfer process. Conservation of mass for the stream channel and storage zone yields (Bencala and Walters 1983, Runkel and Broshears 1991):

$$\frac{\partial C}{\partial t} = -\frac{Q\partial C}{A\partial x} + \frac{1}{A}\frac{\partial}{\partial x}(AD\frac{\partial C}{\partial x}) + \alpha(C_S - C) + \frac{q_{LIN}}{A}(C_L - C) \tag{1}$$

$$\frac{dC_S}{dt} = \alpha\frac{A}{A_S}(C - C_S) \tag{2}$$

where: C is the solute concentration in the stream [g/m^3], t the time [s], Q is the flow discharge [m^3/s], A is the main channel cross-sectional area [m^2], x is the distance downstream [m], D is the coefficient of longitudinal dispersion [m^2/s], C_S is the concentration in the storage zone [g/m^3], α is the exchange coefficient [1/s], A_S is the storage zone cross-sectional area [m^2], q_{LIN} is the lateral volumetric inflow rate [m^2/s], and C_L is the solute concentration in lateral inflow [g/m^3].

Aggregated Dead Zone (ADZ) model

As an alternative to the transient storage model described by means of partial differential equations (Eqs. 1-2), a Data-Based Mechanistic (DBM) approach was introduced (Beer and Young 1983, Beven and Young 1998, Wallis 1989, Young and Lees 1993). In this approach, a so-called aggregated dead zone (lumped) model is formulated based on the observed time series data using system identification techniques (Young 1984). In the ADZ model the change of solute concentration in a river reach is described as:

$$Cout_k = \frac{B(z^{-1})}{A(z^{-1})} Cin_{k-\delta}$$
$$Cobs_k = Cout_k + \xi_k \tag{3}$$

where Cin_k is the concentration at the upstream end of the river reach at time *k*, the $Cout_k$ is the estimated concentration at the downstream end of the river reach, $Cobs_k$ is the measured concentration at the downstream end of the river reach, z^{-1} is the backshift operator, δ is an advection time delay, *A* and *B* are the polynomials of the backshift operator of the order *m* and *n*, respectively, and ξ_k represents the combined effect of all stochastic inputs to the system, including measurement noise.

$$B(z^{-1}) = b_0 + b_1 z^{-1} + b_2 z^{-2} + \ldots + b_m z^{-m} \tag{4}$$

$$A(z^{-1}) = 1 + a_1 z^{-1} + a_2 z^{-2} + \ldots + a_n z^{-n} \tag{5}$$

The order of the ADZ model describing the transport of solute in the river reach is described by triad [*n*, *m*, δ] and is determined in a statistical time series analysis technique using the recursive-iterative simplified, refined instrumental variable (SRIV) method (Young 1984) available in Captain Toolbox developed at the University of Lancaster. The best model structure is identified using three criteria. The first, coefficient of determination, R_T^2, shows how much of the data variation is explained by the model output. The second measure is the Young Information Criterion (YIC), which is related to the fit and error on parameter estimates and takes into account the problem of over-parameterization. A low value of YIC indicates a well defined model. The third measure is the Akaike Information Criterion. AIC has a component related to the simulation fit but is penalized by the number of parameters in the model. A low value of AIC indicates a well defined model.

3.2 Sensitivity and uncertainty assessment

In the case of over-parameterized environmental models, a unique solution of the inverse problem is not available due to a limited amount and/or poor quality of the data. That results in equifinality problem, i.e. an application of different parameter sets leads to similar results. The Generalised Likelihood Uncertainty Estimation (GLUE) technique was introduced by Beven and Binley (1992) to deal with the problem of the non-uniqueness of the solution of environmental models. This technique is based on

multiple Monte Carlo runs of a deterministic model with parameters chosen randomly from a specified *a priori* distribution. The posterior distribution of the model predictions is obtained using a likelihood measure conditioned on observations. The choice of the likelihood measure should reflect the purpose of the study. There are many different likelihood measures based on the variance of errors. One of them is the Nash-Sutcliff coefficient of determination. A second, often applied measure is inverse error measure with a shaping factor suggested by Box and Tiao (1992). This measure was applied by Beven and Binley (1992). An exponential transformation of sum of the square errors is also encountered in the literature (Romanowicz *et al.* 1994), where a formal definition GLUE was introduced.

In the case of measures based on error variance there are practical and theoretical limitations. They give unbiased and statistically efficient estimates of model parameters when errors between predictions and observations are normally distributed and they are not correlated. These assumptions are not often met in hydrological modelling but the approach is still used when violation of the assumptions is not large. In the present paper the non-formal GLUE approach presented by Romanowicz and Beven (2006) is applied. The likelihood function has the form of an exponent to the minus of the sum of square errors between simulated and observed concentrations, divided by the reduced (here multiplied by 0.1) mean error variance (Romanowicz and Beven 2006).

$$L(C|\theta) \sim \exp\left(-\sum_{t=1}^{T} \left(C_{OBS} - C_{SIM}(\theta)\right)^2 \Big/ 0.1\sigma_T^2 \right) \tag{6}$$

where C_{OBS} are the measured concentrations, C_{SIM} are computed concentrations, and σ_T^2 is the estimate of the variance of prediction error.

This likelihood measure was used to evaluate the posterior probability of model predictions and to define the 0.95 confidence bounds of these predictions.

Sensitivity analysis is "The study of how the uncertainty in the output of a model (numerical or otherwise) can be apportioned to different sources of uncertainty in the model input" (Saltelli et al., 2004). In this work we have used the variance based Global Sensitivity Analysis approach introduced by Archer *et al.* (1997), described in more detail in Kiczko et al. (this issue). That approach does not require an assumption of additivity or monotonicity of model components. The variance of an output Y depending on the variable input set X_i, is based on estimating the fractional contribution of each input factor to the total variance $V(Y)$ of the model output Y.

The direct sensitivity of output Y to the input X_i represents the Sobol first order sensitivity index S_i, which takes the following form:

$$S_i = \frac{V[E(Y|X_i = x_i^*)]}{V(Y)} \tag{7}$$

where $V[E(Y|X_i = x_i^*)]$ is the variance of estimated output Y with X_i parameter fixed, and the other parameters varying, and E denotes expectation operator. Therefore, the

first order sensitivity index represents the average output variance reduction that can be achieved when X_i becomes fully known and is fixed.

The model sensitivity to the interactions among subsets of factors, so-called higher order effects, is investigated using the Sobol total sensitivity indices: S_{Ti}. They represent the whole range of interactions which involve X_i and are defined as:

$$S_{Ti} = \frac{E[V(Y|X_{-i} = x^*_{-i})]}{V(Y)} \tag{8}$$

where $E[V(Y|X_{-i} = x^*_{-i})]$ is the estimated variance in the case where all parameters are fixed, except X_i which is varying.

The use of total sensitivity indices is advantageous because there is no need for the evaluation of a single indicator for every possible parameter combination. On the basis of the two indices, S_i and S_{Ti}, it is possible to trace the significance of each model parameter in an efficient way.

4. Discussion of the results

4.1 OTIS

Since it is not possible to estimate solute transport parameters reliably from hydraulic variables and channel characteristics, an application of the transient storage model (Eqs. 1-2) requires an estimation of model parameters for each particular river reach, 2N-3N, 3N-5N, 5N-6N and 6N-7N (Fig. 1), based on data from tracer experiment including measurements of lateral inflow and discharge. Estimation of model parameters, namely D, A, A_S and α, was performed by minimizing the residuals between the simulated and observed concentrations. A general least squares objective function and the Nealder-Mead minimization algorithm were used in this study. The results of the estimation procedure are given in Table 1. They are analogous to that obtained by Rowiński *et al*. (2004) for a similar model but a different numerical scheme.

Table 1

Estimated parameters of transient storage models

Parameters	Sections			
	2N-3N	3N-5N	5N-6N	6N-7N
D [m^2/s]	10.31	1.65	6.96	1.59
A [m^2]	9.71	34.70	11.29	25.02
A_s [m^2]	6.13	22.62	4.46	7.05
α [1/s]	4.82e-006	1.7863e-005	1.2913e-005	6.5701e-005

Note that values of the parameters differ between reaches. These big differences result from a high variability of geometric and hydraulic conditions between reaches.

A comparison of observed and simulated data together with 0.95 confidence bounds obtained from the application of GLUE technique is presented in Fig. 2.

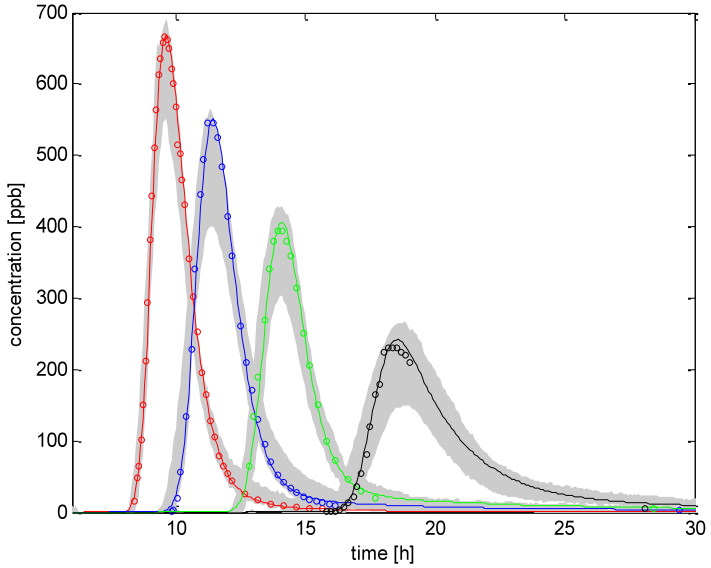

Fig. 2. Comparison of observed (dots) and simulated (solid line) concentrations of Rhodamine WT at cross-section 3N, 5N, 6N and 7N with 95% confidence bounds shown as shaded areas.

4.2 ADZ

Identification of model structure and estimations of parameters of the transfer functions models were conducted independently for every river section using the SRIV method of recursive estimation in the Captain toolbox. The values of coefficient of determination (R_T^2), Young Information Criterion (YIC) and Akaike Information Criterion (AIC) for all analyzed cross-sections are given in Table 2. Analysis shows that the second-order models are the most parametrically efficient model structures, accurately describing the observed solute transport in these reaches.

Table 2

Results of identification of Aggregated Dead Zone model

	Sections			
	2N-3N	3N-5N	5N-6N	6N-7N
Model [n, m, δ]	[2, 2, 29]	[2, 2, 19]	[2, 2, 30]	[2, 2, 50]
R_T^2	0.9996	0.9994	0.9970	0.9934
YIC	–17.454	–18.476	–17.455	–6.201
AIC	0.854	1.017	1.032	3.084

The second order models can be decomposed into a parallel connection of two first order ADZ transfer functions in the following form:

$$\text{Fast Component:} \quad y_{q,k} = \frac{\beta_q}{1+\alpha_q z^{-1}} Cin_{k-\delta}$$
$$\text{Slow Component:} \quad y_{s,k} = \frac{\beta_s}{1+\alpha_s z^{-1}} Cin_{k-\delta} \tag{9}$$

where $\alpha_s, \alpha_q, \beta_s, \beta_q$ are parameters derived from (3) and the concentration is the sum of these two components and a model error, i.e. $Cout_k = y_{s,k} + y_{q,k} + \xi_k$. The associated residence times (time constants) (T_s, T_q), steady state gains (G_s, G_q), and partition percentages (P_s, P_q) are given by the following expressions:

$$T_i = \frac{\Delta t}{\log_e(\alpha_i)};\ i = s,q \qquad G_i = \frac{\beta_i}{1+\alpha_i};\ i = s,q \qquad P_i = \frac{100 G_i}{G_s + G_q};\ i = s,q$$

In practice, the residence times of two parallel connections are of quite different magnitude and they are denoted as quick and slow processes in the above equation (subscript *q* and *s* respectively). The most plausible physical explanation is that the pure time delay allows for the flow-induced pure advection of the solute. The quick-flow parallel pathway then represents the 'main stream-flow' that is relatively unhindered by vegetation, while the slow-flow pathway represents the solute that is captured by heavy vegetation and so dispersed more widely and slowly before rejoining the main flow and eventually reaching the main channel. The resulting residence times, steady state gains and partition percentages for all analysed reaches are given in Table 3.

Table 3

Parameters of slow and fast components of ADZ models

	Sections			
	2N-3N	3N-5N	5N-6N	6N-7N
T_s [h]	0.27	13.76	13.35	1.54
T_q [h]	0.11	0.28	0.27	0.06
G_s	0.7381	0.1225	0.1003	0.6596
G_q	0.2209	0.8896	0.7698	0.2494
P_s [%]	76.97	12.11	11.534	72.56
P_q [%]	23.03	87.89	88.47	27.44

Using calibrated transfer function models, a SIMULINK system describing the transport of solutes in the Upper Narew was built. A block diagram of a full semi-

distributed system is presented in Fig. 3. Every section is modelled as a second-order transfer function model; the simulated output from a previous section becomes an input to the next section.

Figure 4 presents a comparison of measured concentrations of Rhodamine WT and those simulated using the ADZ model at four cross-sections. In the case of the cross-sections 3N, 5N and 6N, a very good fit is observed. The worst results are for cross-section 7N, caused by a gap in measurements which makes the correct identification of model parameters impossible.

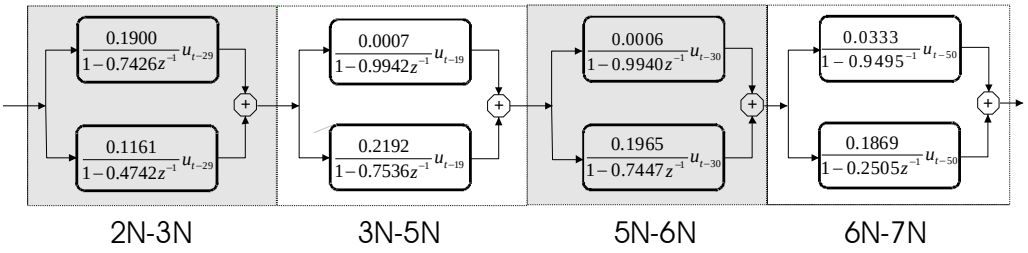

Fig. 3. Transfer function block diagram of the whole analyzed river reach model.

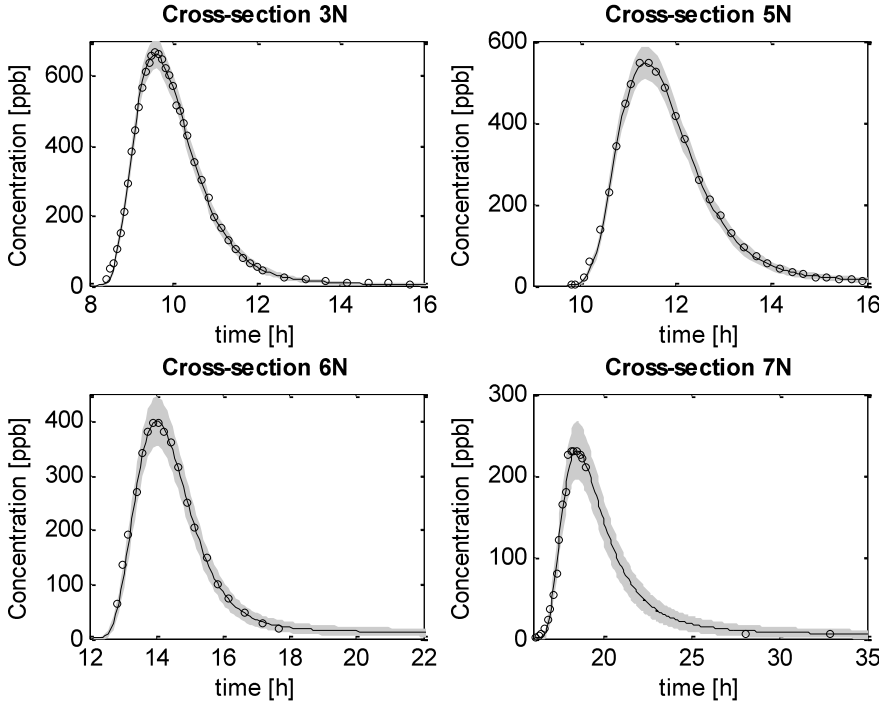

Fig. 4. ADZ model results – application to the whole river reach; open circles represent measurements and shaded areas denote 95% confidence bounds.

4.3 Comparison of ADZ and mechanistic modelling (virtual reality)

To validate the ADZ model for the whole river reach, another tracer experiment is required. Unfortunately, there was just one tracer test in this part of the river, so we used the mechanistic OTIS model to simulate *virtual reality describing solute transport* in the Upper Narew for a different input than that used in the calibration. The results were then compared with those obtained by means of the previously calibrated ADZ model. They are depicted in Fig. 5.

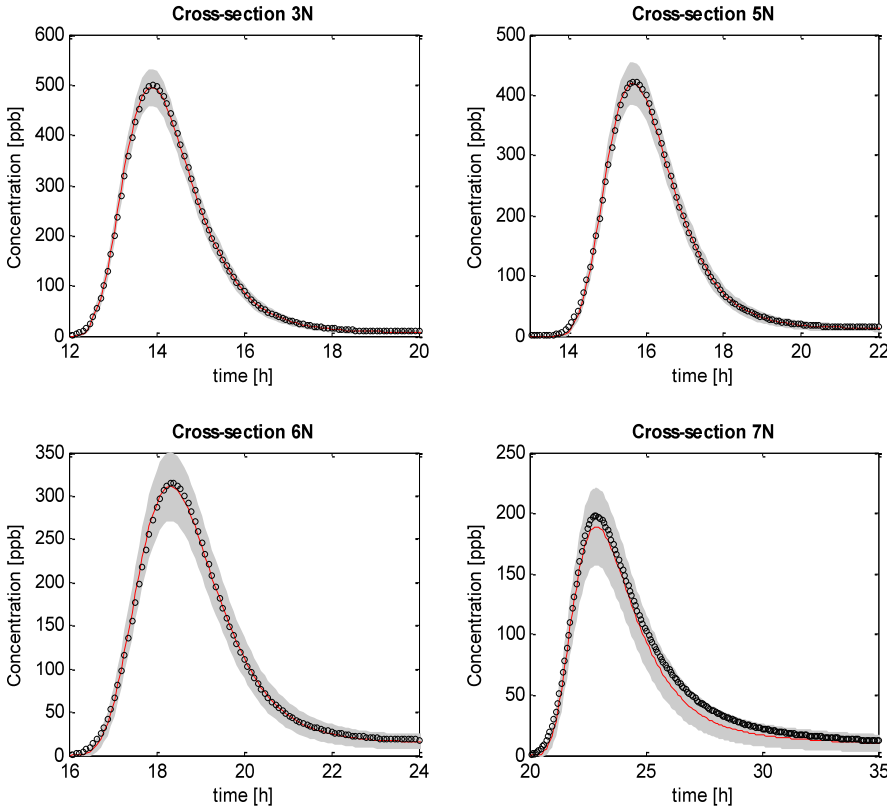

Fig. 5. Validation of active mixing volume model. Open circles represent virtual reality simulated by mechanistic model, red solid line – ADZ model; shaded areas show 95% confidence bounds obtained from the ADZ model.

The results show a good similarity, with R_T^2 equal to 0.9995, 0.9994, 0.9991 and 0.9938 for cross-sections 3, 5, 6, and 7, respectively.

4.4 Sensitivity analysis

In this paper we have analyzed the sensitivity of model output (simulated concentrations and ecologically related measures) to model parameters and model input. The parameters of the model were sampled from a uniform distribution with lower and upper bounds based on a physically justified variation of these parameters. These

bounds are: coefficient of longitudinal dispersion (D) 0.01-20 [m^2/s], the storage zone cross-sectional area (A_S) 0.01-30 [m^2], the exchange coefficient (α) 0.0000001-0.0001 [1/s], the main channel cross-sectional area (A) 5-45 [m^2], and ±10% errors of the measured model input (described as a multiplier in range from 0.9 to 1.1).

Sobol first order and Sobol total order sensitivity indices for the parameters of the OTIS model predictions and uncertainty of observations are shown in Fig. 6. The main channel cross-sectional area (A) has the largest influence on the output of all analyzed river reaches. The exchange coefficient (α), the storage zone area (A_S) and the dispersion coefficient (D) have smaller values of indices, indicating a smaller influence on the model output and a smaller identifiability of these parameters. The order of these three parameters varies in different river reaches. For the three last reaches the longitudinal dispersion coefficient has higher values of sensitivity indices than parameters describing the effect of dead zones. The lowest values of Sobol first and total sensitivity indices are obtained for ±10% variation of the model input.

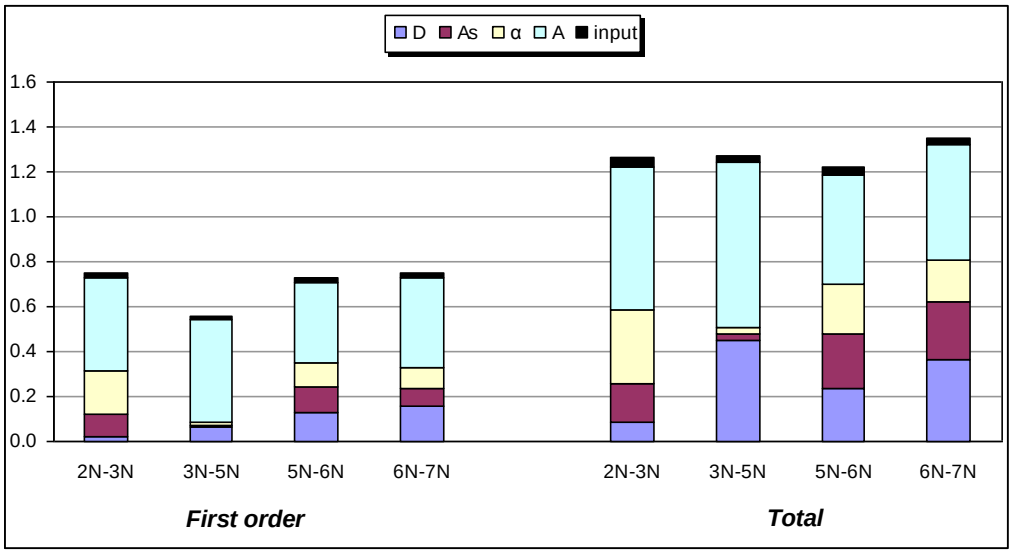

Fig. 6. Sobol first order and total sensitivity indices for OTIS model predictions for all cross-sections.

The sum of first order sensitivity indices for the analyzed river reaches is less than 1, which indicates a non-additive model.

5. Ecologically related criterion

The richness and uniqueness of the flora and fauna in the Narew National Park were the reasons for including ecologically related measures in our sensitivity analysis. The first is the maximum value of concentration, the second the length of time periods with the concentration over a specified threshold. These two variables are used in toxicological assessments.

Sensitivity indices for the maximum concentration of the tracer in relation to the model parameters are shown in Table 4 and Fig. 7. The values of the sensitivity indices are similar for all four analyzed river reaches and they resemble the results obtained for model predictions. There is a relationship between the area of the main channel and the values of maximum concentration.

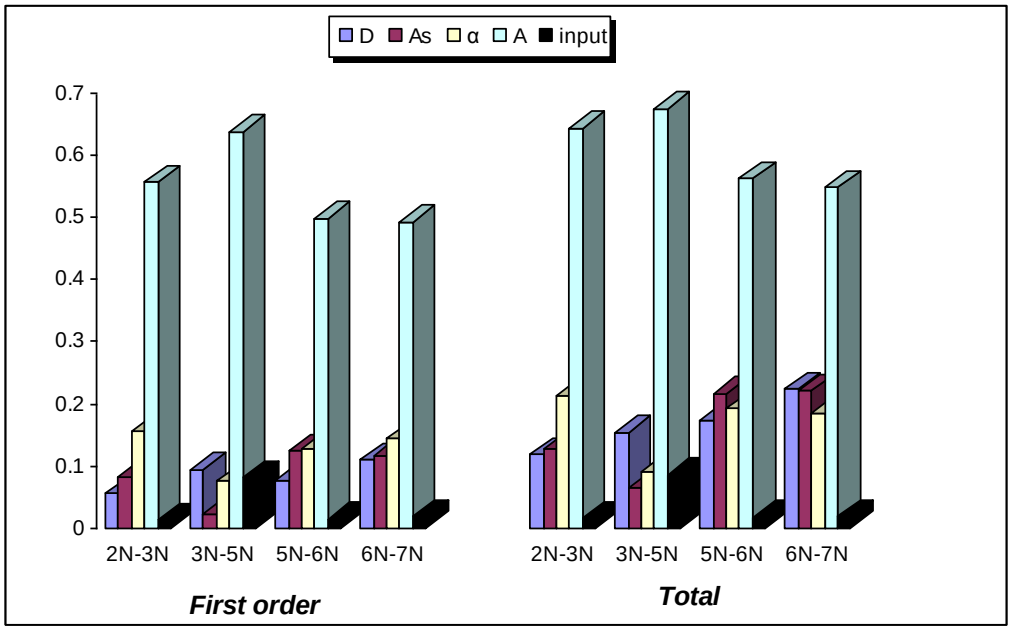

Fig. 7. Sobol first order and total sensitivity indices for OTIS model predictions on maximum concentration for all cross-sections.

Table 4

Results of the GSA sensitivity analysis on maximum concentration

River reach	S_i					S_{Ti}				
	D	A_S	α	A	input	D	A_S	α	A	input
N2-N3	0.0555	0.0827	0.1560	0.5556	0.0133	0.1187	0.1266	0.2143	0.6425	0.0166
N3-N5	0.0940	0.0227	0.0755	0.6372	0.0816	0.1542	0.0645	0.0909	0.6739	0.0857
N5-N6	0.0779	0.1236	0.1280	0.4982	0.0146	0.1744	0.2169	0.1922	0.5614	0.0183
N6-N7	0.1100	0.1178	0.1437	0.4921	0.0190	0.2238	0.2208	0.1854	0.5470	0.0194

The highest values of indices are for the second river reach (0.6372 and 0.6739 for first and total order respectively) and the lowest are for the last river reach (0.4921 and 0.5470 for the first and total order respectively). In the case of the exchange coefficient and the storage zone area this relationship is weaker (Fig. 8). The dispersion coefficient shows a small influence on maximum concentrations. Values of sensitivity indices for this parameter vary between 0.0555 and 0.1100 for first order and between

0.1187 and 0.2238 for total effect. The lowest values of sensitivity indices are obtained for a 10% input measurements error.

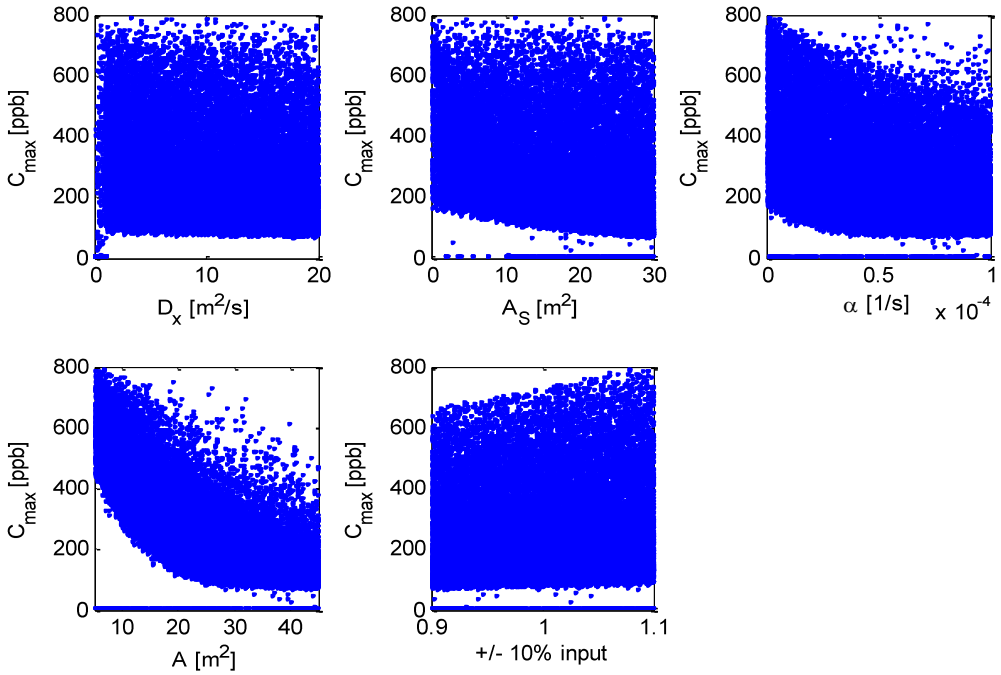

Fig. 8. Relationship between values of maximum simulated concentration and values of parameters for river reach 2N-3N.

Results of the sensitivity analysis for the "over the threshold" period depend on the threshold value. Figure 9 presents the first order and total sensitivity indices of the OTIS parameter variations as a function of the threshold value. It is interesting to note that the sensitivity of the "over the threshold" period for small and large threshold values shows different behaviour, shown in Fig. 9 as multiple minima/maxima. This behaviour is the result of two different processes. One is the direct influence of parameters on different parts of the dynamic response of the system. The other is the dependence of the maximum peak concentration at each cross-section on the parameter values, i.e. for high threshold values, the number of realisations with a non-zero "over the threshold" period decreases.

In order to explain this behaviour, we shall analyse the projections of the response surface for the parameter A_S for four different values of the threshold, 10, 60, 100 and 200 ppb, (Fig. 10 a-d). For small threshold values (Fig. 10a), the storage zone area influences the number of time periods over the threshold due to its influence on the tails of the dynamic response of the system (Wagener *et al*. 2002). This influence decreases with an increase of the threshold value, resulting in the minimum index value at a threshold of about 60 ppb (Fig. 10b). Above this threshold, due to the dependence of maximum concentration on the storage zone area A_S for higher values of this para-

meter, there is an increasing number of realizations for which the threshold concentration of 100 ppb is not reached (Fig. 10c).

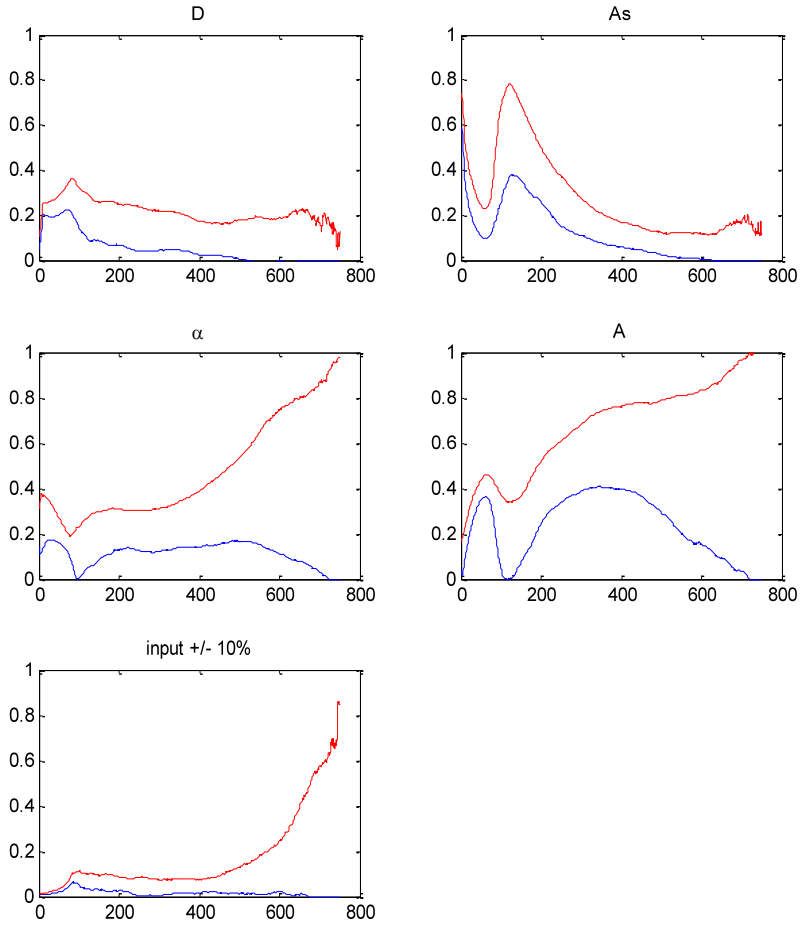

Fig. 9. Sensitivity indices for "over the threshold" period to OTIS parameters variations as a function of the threshold value for river reach 2N-3N. Blue and red lines denote Sobol first order and total sensitivity indices, respectively.

As a result, the number of realizations with decreasing or equal to zero "over the threshold" periods increases, giving a rise of the sensitivity index for this parameter. With a further increase in the threshold value, the number of realizations with "over the threshold" period stabilizes, as there are zero-length "over the threshold" periods over the whole parameter range (Fig. 10d). It is interesting to note nearly opposite relationship for parameter *A* (main channel cross-sectional area), shown in detail in Fig. 11 a-d for threshold values equal to 10, 60, 100 and 200 ppb, respectively. This parameter influences the higher parts of the dynamic response of the system, giving a rise of the sensitivity index with an increase of the threshold value (Fig. 11 a and b). With a further increase in the threshold values, zero periods appear that counteract the increase of the number of over the threshold periods, thus decreasing the sensitivity

index (Fig. 11c). This influence is limited to the higher values of that parameter, which results in a subsequent rise of the sensitivity index for values of the threshold higher than 100 ppb (Fig. 11d).

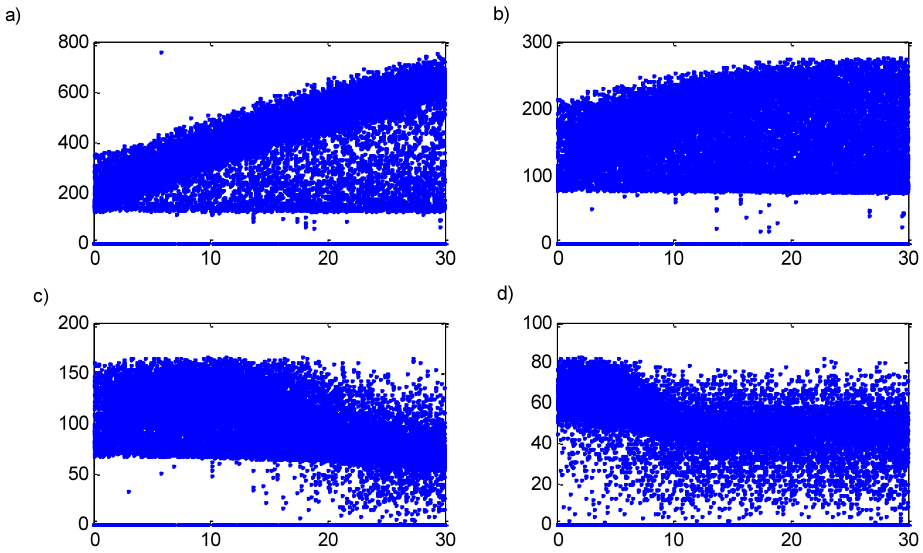

Fig. 10. Sensitivity analyses for the "over the threshold" period for the 2N-3N river reach. Dotted plots a, b, c and d show the projection of the response surface (number of time steps with concentration over the threshold) into the parameter A_S dimension for four threshold values: 10, 60, 100 and 200 ppb, respectively.

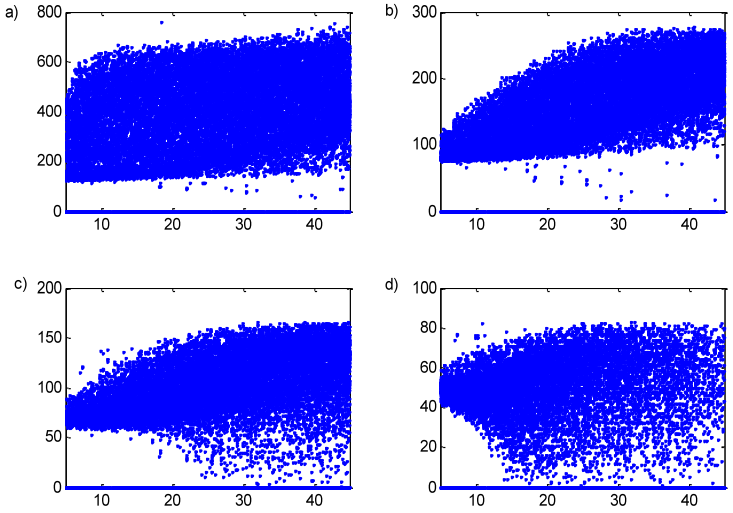

Fig. 11. Sensitivity analyses for the "over the threshold" period for the 2N-3N river reach. Dotted plots a, b, c and d show the projection of the response surface (number of time steps with concentration over the threshold) into the parameter A dimension for four threshold values: 10, 60, 100 and 200 ppb, respectively.

6. Conclusions

We have presented the application of a deterministic, mechanistic model (OTIS) and a stochastic ADZ model to describe dispersion processes in wetlands, based on tracer experiment data from the reach of the River Narew within the Narew National Park. We applied a sensitivity analysis using GSA (Saltelli *et al*. 2004) to define the most sensitive parameters and their ranges. Maximum concentrations and the length of time period with concentrations exceeding the specified threshold were used as ecologically related model outputs together with the concentration trajectories. In particular, the sensitivity analysis of the length of "over the threshold" period shows an interesting relationship for threshold values below 200 ppb. The results of this analysis were used to specify the best parameter ranges and their prior distributions for the evaluation of predictive model uncertainty, using the GLUE technique of Beven and Binley (1992). The stochastic ADZ model was used as an alternative to the mechanistic model. Due to its stochastic nature, the uncertainty of the model predictions is included in the model output. The dynamics of the dispersion process identified by the ADZ model are of second order, indicating the existence of slow and fast dispersion components in the studied River Narew reach. Due to the lack of a validation data set, we applied the mechanistic OTIS model output for a time period different from that used in the calibration stage, as a virtual reality, in order to validate the ADZ model. The results show a good fit with 99% of the variation of the OTIS model output explained.

Acknowledgments. This work was supported in part by grant 2 P04D 009 29 from the Ministry of Science and Higher Education.

References

Archer, G., A. Saltelli, and I.M. Sobol (1997), *Sensitivity measures, anova-like techniques and the use of bootstrap*, Journal of Statistical Computation and Simulation **58**, 99-120.

Beer, T., and P.C. Young (1983), *Longitudinal dispersion in natural streams*, J. Environ. Eng. **109**, 1049-1067.

Bencala, K.E., and R.A. Walters (1983), *Simulation of solute transport in a mountain pool-and-riffle stream: a transient storage model*, Water Resour. Res. **19**, 3, 718-724.

Beven, K.J., and A. Binley (1992), *The future of distributed models: model calibration and uncertainty prediction*, Hydrol. Process. **6**, 279-298.

Beven, K.J., and P.C. Young (1998), *An aggregated mixing zone model of solute transport through porous media*, J. Contaminant Hydrology **3**, 129-143.

Box, G.E.P., and G.C. Tiao (1992), *Bayesian Interface in Statistical Analysis*, Wiley Interscience, New York.

Kiczko, A., R.J. Romanowicz, J.J. Napiórkowski and A. Piotrowski (2008), *Integration of reservoir management and flow routing model¯ Upper Narew case study*, Publ. Inst. Geophys. Pol. Acad. Sc. E-9 (405), (this issue).

Romanowicz R.J., K. J. Beven and J. A. Tawn, 1994, *Evaluation of predictive uncertainty in nonlinear hydrological models using a Bayesian Approach*, **In:** "Statistics for the Environment (2), Water Related Issues", ed. V. Barnett and F. Turkman, Wiley, Chichester, pp. 297-318.

Romanowicz, R., and K.J. Beven (2006), *Comments on Generalised Likelihood Uncertainty Estimation*, Reliability Engineering and System Safety, DOI: 10.1016/j.ress.2005.11.030.

Rowiński, P.M., J. Napiórkowski, and J. Szkutnicki (2003a), *Transport of passive admixture in a multi-channel river system – the Upper Narew case study. Part 1. Hydrological survey*, Ecology and Hydrobiology **3**, 371-379.

Rowiński, P.M., J. Napiórkowski, and A. Owczarczyk (2003b), *Transport of passive admixture in a multi-channel river system – the Upper Narew case study. Part 2. Application of dye tracer method*, Ecology and Hydrobiology **3**, 381-388.

Rowiński, P.M., J. Napiórkowski, and T. Dysarz (2004), *Transport pollution in the rivers flowing through wetland areas*. **In:** "Model application for wetlands hydrology and hydraulics", Warsaw Agricultural University Press, 113-124.

Runkel, R.L., and R.E. Broshears (1991), *One dimensional transport with inflow and storage (OTIS): A solute transport model for small streams*. Tech. Rep. 91-01, Center for Adv. Decision Support for Water and Environ. Syst., Univ. of Colorado, Boulder.

Saltelli A., S. Tarantola, F. Campolongo, and M. Ratto (2004), *Sensitivity Analysis in Practice: A Guide to Assessing Scientific Models*, John Wiley and Sons.

Wagener, T., L.A. Camacho, and H.S. Wheater (2002), *Dynamic identifiability analysis of the transient storage model for solute transport in rivers*, Journal of Hydroinformatics **4**, 3, 199-211.

Wallis, S.G., P.C. Young, and K.J. Beven (1989), *Experimental investigation of the Aggregated Dead Zone (ADZ) model for longitudinal solute transport in stream channels*, Proc. Inst. of Civil Engrs **87**, 1-22.

Young, P.C.(1974), Recursive Approaches to Time-Series Analysis, Bull. of Inst. Maths and its Applications, **10**, 209-224.

Young, P.C. (1984), *Recursive Estimation and Time Series Analysis*, Springer-Verlag, Berlin.

Young, P.C., and M. Lees (1993), *The Active Mixing Volume: A new concept on Modelling Environmental Systems*. **In:** "Statistics for the Environment", John Wiley & Sons, Chichester, 3-44.

PUBLS. INST. GEOPHYS. POL. ACAD. SC., E-9 (405), 2008

Two-Dimensional Diffusion Wave Model for Numerical Simulation of Inundation – Upper Narew Case Study

Michał SZYDŁOWSKI

Faculty of Civil and Environmental Engineering
Gdańsk University of Technology
ul. Narutowicza 11/12, 80-952 Gdańsk, Poland
e-mail: mszyd@pg.gda.pl

Abstract

The purpose of this paper is to present the numerical calculations which can be useful for simulations of inundations in natural river valleys. When estimating the reach and area of the inundation related to river flow, digital elevation model and mathematical model of flood wave propagation are indispensable. For numerical simulation of flood, the mathematical model of free surface unsteady water flow can be applied. Usually, the one- or two-dimensional shallow water equations, called Saint Venant equations, are assumed. In this paper, the simplified hydrodynamics model, known as a diffusion wave model, is presented and applied for simulation of inundation along the Upper Narew reach connecting Suraż and Łapy. The model equations are solved using finite volume method.

Key words: mathematical modelling, diffusion wave model, finite volume method, floodplain inundation, flood zones, Upper Narew.

1. Introduction

Nowadays, numerical simulations of river inundations are the basic tool for flood risk mitigation and water management in the river catchments. The water flow prediction is indispensable not only for management of risk resulting from floods but can be useful for irrigation problems as well. Therefore, estimation of water flow parameters in rivers and floodplains is one of the major tasks for water engineers and hydrologists.

The Upper Narew reach, analyzed in this case study, is crossing the Narew National Park. In this region, floods are very important element of natural environment. There are even some concepts of artificial inundations in this region (controlled at Siemianówka reservoir) sustaining animal life and appropriate moisture levels in the soil (Rowiński *et al.* 2005). The hydraulic consequences of such flood waves can be simulated using mathematical models too.

When estimating the water flow parameters (depth and velocity) mathematical model to describe the free surface flow is needed. The models of water flow dynamics can range in complexity from simple one-dimensional Bernoulli equation for steady flow to full three-dimensional solutions of the Navier-Stokes equations with some turbulence models (Sawicki 1998). Unfortunately, the latter is still too complex to be applied for practical cases (Szydłowski and Zima 2006).

Recently, the most widely used models for free surface water flow modeling have been Saint Venant equations for one-dimensional open channel flow. Numerical solution of the equations provides the user with the cross-section-averaged velocity and water depth at each location. In order to estimate the inundation zone the values of water surface level can be interpolated between river (valley) cross-sections. The one-dimensional hydrodynamic models are usually efficient for modeling of water wave propagation in open channels, but they are often inconvenient for inundation prediction due to simplified representation of floodplain areas. When the flow area is defined only with some cross-sections of river channel and floodplain it can result with some errors in the inundation zone prediction. In order to overcome this problem two-dimensional models should be applied, especially for floodplain flows. They ensure the water level and averaged velocity to be computed at each computational node of numerical grid representing the flow area. Two-dimensional shallow water equations, called two-dimensional Saint Venant equations or briefly dynamic wave model) can be obtained from the Navier-Stokes equations using a depth averaging procedure (Szymkiewicz 2000). For this hydrodynamic model it is assumed that vertical component of velocity can be neglected, pressure field is hydrostatic, bottom slope is small and bottom friction can be approximated as for a steady flow.

This model can be further simplified by reducing description of some physical processes present in the water flow phenomenon. In this paper the inundation of the floodplains due to Narew flow is investigated using simplified model of two-dimensional free surface water flow, named the diffusion wave model. In order to solve the equations, numerical scheme based on finite volume method is applied.

2. Governing equations

The two-dimensional dynamic wave model can be presented as the following system of partial differential equations (Tan 1992), representing mass and momentum conservation:

$$\frac{\partial H}{\partial t} + \frac{\partial q_x}{\partial x} + \frac{\partial q_y}{\partial y} = 0, \tag{1a}$$

$$\frac{\partial q_x}{\partial t} + \frac{\partial}{\partial x}\left(\frac{q_x^2}{h}\right) + \frac{\partial}{\partial y}\left(\frac{q_x \cdot q_y}{h}\right) + gh\frac{\partial H}{\partial x} + ghS_{fx} = 0, \tag{1b}$$

$$\frac{\partial q_y}{\partial t} + \frac{\partial}{\partial x}\left(\frac{q_x \cdot q_y}{h}\right) + \frac{\partial}{\partial y}\left(\frac{q_y^2}{h}\right) + gh\frac{\partial H}{\partial y} + ghS_{fy} = 0. \tag{1c}$$

In this system of equations H and h represent the water surface level and depth, q_x and q_y are the flow rates in x and y direction, respectively. S_{fx} and S_{fy} are the bottom friction terms, g is the acceleration due to gravity and t represents time. The bottom friction can be defined using the Manning formula (Tan 1992), for example:

$$S_{fx} = \frac{n^2 \cdot q_x \cdot \sqrt{q_x^2 + q_y^2}}{h^{10/3}}, \tag{2a}$$

$$S_{fy} = \frac{n^2 \cdot q_y \cdot \sqrt{q_x^2 + q_y^2}}{h^{10/3}}, \tag{2b}$$

where n denotes the Manning friction coefficient.

To solve the shallow water equations, relatively complicated numerical methods and complex data set must be used. To reduce the mathematical complexity of the model some terms in the model can be neglected, but only when it is reasonable. Making appropriate assumption (Szymkiewicz 2000) one can find: diffusion wave model (non-inertial model), kinematic wave model, and flat pond model (if only mass conservation is considered).

The two-dimensional diffusion wave model, used here for numerical simulation of flood inundation of the Upper Narew floodplain, can be obtained following Hromadka and Yen's (1987) idea. For the sake of clarity, only one equation of motion (in the x direction, for example) can be considered. The local and convective acceleration terms can be grouped and Eq. (1b) can be rewritten as:

$$\underbrace{\frac{1}{gh}\left[\frac{\partial q_x}{\partial t} + \frac{\partial}{\partial x}\left(\frac{q_x^{\,2}}{h}\right) + \frac{\partial}{\partial y}\left(\frac{q_x q_y}{h}\right)\right]}_{m_x} = -\left(\frac{\partial H}{\partial x} + S_{fx}\right). \tag{3}$$

The same equation can be presented as a short formula:

$$S_{fx} = -\left(\frac{\partial H}{\partial x} + m_x\right). \tag{4}$$

If it is assumed that the friction slope is approximated using Manning equation for steady flow (Eq. 2a) it is possible to include this empirical formula to the equation of motion (Eq. 1b). After that, one can obtain:

$$\frac{n^2 \cdot q_x \cdot q_s}{h^{10/3}} = -\left(\frac{\partial H}{\partial x} + m_x\right), \tag{5}$$

where subscript s indicates the flow direction which makes an angle ϕ with the x direction, giving:

$$q_x = q_s \cdot \cos\phi. \tag{6}$$

Finally, after arrangement of Eqs. 5 and 6, the flow equation in the x direction can be written as:

$$q_x = -K_x \frac{\partial H}{\partial x} - K_x \cdot m_x , \tag{7}$$

where

$$K_x = \frac{\frac{1}{n} h^{5/3}}{\left| \frac{\partial H}{\partial s} + m_s \right|^{1/2}} \tag{8}$$

is the hydraulic conduction parameter in the *x* direction, which is limited in value by the dominator term being checked for a small allowable amount (Singh 1996). It should be underlined here that the assumption about the absolute value of this term seems to be limiting the hydrodynamics model and its influence on numerical simulation of water flow should be investigated in details. In a similar way, the flow in the *y* direction can be presented as:

$$q_y = -K_y \frac{\partial H}{\partial y} - K_y \cdot m_y . \tag{9}$$

Putting the flow rates formulations (Eqs. 8 and 9) into the continuity Eq. (1a) gives the following relationship:

$$\frac{\partial H}{\partial t} - \frac{\partial}{\partial x}\left(K_x \frac{\partial H}{\partial x} \right) - \frac{\partial}{\partial y}\left(K_y \frac{\partial H}{\partial y} \right) - S = 0, \tag{10}$$

where

$$S = \frac{\partial}{\partial x} \left(K_x m_x \right) + \frac{\partial}{\partial y} \left(K_y m_y \right) . \tag{11}$$

The final form of hydrodynamics model depends on the parameters m_x and m_y, which represent inertia forces in *x* and *y* directions as terms of local and convective acceleration (Eq. 3). The number of acceleration terms is related to the model simplification. Various forms of m_x can be assumed, for example:

$$m_x = \frac{1}{gh}\left[\frac{\partial q_x}{\partial t} + \frac{\partial}{\partial x}\left(\frac{\partial q_x^2}{h} \right) + \frac{\partial}{\partial x}\left(\frac{q_x q_y}{h} \right) \right], \tag{12a}$$

$$m_x = \frac{1}{gh}\left[\frac{\partial}{\partial x}\left(\frac{\partial q_x^2}{h} \right) + \frac{\partial}{\partial x}\left(\frac{q_x q_y}{h} \right) \right], \tag{12b}$$

$$m_x = \frac{1}{gh}\left[\frac{\partial q_x}{\partial t} \right], \tag{12c}$$

$$m_x = 0. \tag{12d}$$

If all acceleration terms are present in the parameter m_x (Eq. 12a) and m_y, the hydrodynamics model is full dynamic wave model written in other form than shallow water

equations (Eq. 1). Assuming $m_x = m_y = 0$, which means neglecting inertia forces terms in the flow description, one obtains a two-dimensional diffusion wave model, which can be presented in one-equation form as follows:

$$\frac{\partial H}{\partial t} - \frac{\partial}{\partial x}\left(K_x \frac{\partial H}{\partial x} \right) - \frac{\partial}{\partial y}\left(K_y \frac{\partial H}{\partial y} \right) = 0. \tag{13}$$

3. Solution method

Solution of diffusion wave model (Eq. 13) can be realized using any method of numerical integration of partial differential equation in space and time. In this paper the finite volume method (LeVeque 2002) is proposed for model space approximation. For time integration the second order Runge-Kutta (Tan 1992) scheme is used.

To integrate Eq. (13) in space using finite volume method the calculation domain can be discretized into a set of triangular cells (Fig. 1), for example. This kind of approximation ensures an unstructured numerical mesh. Each cell is defined by its centre point and variable H is averaged and constant inside the cell.

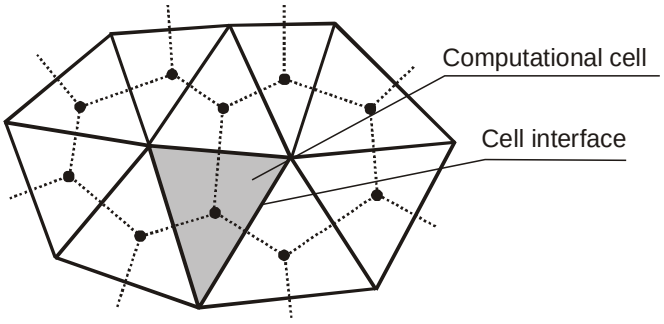

Fig. 1. FVM discretization of calculation domain.

Equation (13) can be rewritten in the following form:

$$\frac{\partial H}{\partial t} + \frac{\partial F}{\partial x} + \frac{\partial G}{\partial y} = 0, \tag{14}$$

where

$$F = -K_x \frac{\partial H}{\partial x}, \qquad G = -K_y \frac{\partial H}{\partial y}, \tag{15}$$

or shorter as:

$$\frac{\partial H}{\partial t} + \nabla \ D\mathbf{n} \ = 0, \tag{16}$$

where

$$D\mathbf{n} = F\,n_x + G\,n_y \tag{17}$$

and $\mathbf{n} = (n_x, n_y)^{\mathrm{T}}$ is an unit vector.

After integration and applying the Ostrogradski-Gauss theorem for each cell *i*, Eq. (16) can be written as:

$$\frac{\partial H_i}{\partial t}\Delta A_i + \oint_{L_i} D\mathbf{n}\; dL = 0, \tag{18}$$

where ΔA_i and L_i are the area and boundary of cell *i*. The first term of Eq. (18) represents time evolution of water surface level over cell *i*, which is related to the water volume change inside the cell. The second one is the flow rate (discharge) through the boundary of cell *i*. This flux is of diffusive type. The integral in Eq. (18) can be substituted by a sum of three components as follows:

$$\frac{\partial H_i}{\partial t}\Delta A_i + \sum_{r=1}^{3} D_r\,\mathbf{n}_r\;\;\Delta L_r = 0, \tag{19}$$

where D_r is the flux computed at the *r*th cell-interface, and ΔL_r represents the cell-interface length. In order to simulate the free surface water flow, Eq. (19) must be solved inside every finite volume *i*. Therefore, the main point of the solution technique is an approximation of fluxes between computational cells.

In order to estimate the fluxes D_r derivative of water surface level *H* at the *r*th cell-interface is required. For two cells, *i* and *ii* (Fig. 2), the derivative can be approximated by weighted average of derivatives computed inside the triangles *T*1 (vertexes *i*, *j*, *k*) and *T*2 (vertexes *j*, *ii*, *k*).

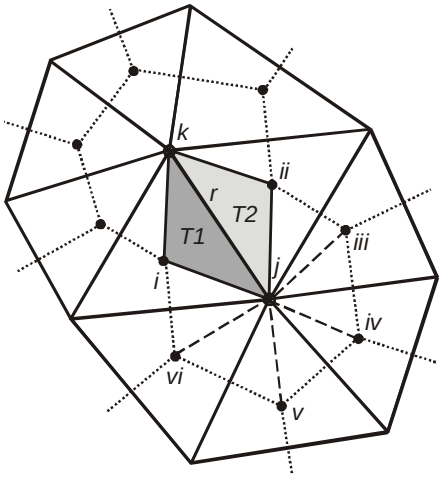

Fig. 2. Graphic scheme for *H* derivative calculation.

For the sake of clarity, only the derivative in the *x* direction, $H_x = \partial H/\partial x$, is analyzed. If the derivatives in triangles *T*1 and *T*2 (H_x^{T1}, H_x^{T2}) are known, the averaged value at the *r*th cell-interface can be expressed as:

$$H_x^r = \frac{H_x^{T1} A^{T1} + H_x^{T2} A^{T2}}{A^{T1} + A^{T2}}, \tag{20}$$

where A^{T1} and A^{T2} are the areas of triangles $T1$ and $T2$, respectively. To compute H_x^r the values of derivatives inside both triangles are needed. They can be calculated like for finite element method with linear base functions (Zienkiewicz 1972). The values of H_x and H_y in triangle $T1(i, j, k)$ can be approximated as:

$$H_x^{T1} = H_i \frac{b_i}{2A^{T1}} + H_j \frac{b_j}{2A^{T1}} + H_k \frac{b_k}{2A^{T1}}, \tag{21}$$

$$H_y^{T1} = H_i \frac{c_i}{2A^{T1}} + H_j \frac{c_j}{2A^{T1}} + H_k \frac{c_k}{2A^{T1}}, \tag{22}$$

where H_i, H_j and H_k are the values of water surface level at nodes i, j, and k, respectively. The factors b_l and c_l ($l = i, j, k$) are

$$b_i = y_j - y_k, \qquad b_j = y_k - y_i, \qquad b_k = y_i - y_j, \tag{23}$$

$$c_i = x_k - x_j, \qquad c_j = x_i - x_k, \qquad c_k = x_j - x_i, \tag{24}$$

where x_l and y_l ($l = i, j, k$) are the coordinates of the vertexes i, j, k. Unfortunately, considering the triangle $T1$, the water surface level is known only at node i (inside cell i). At vertexes j and k the H values must be approximated. They can be obtained by a distance weighted averaging of cell-centre values from cells surrounding the vertexes j and k, respectively. For instance, vertex j (Fig. 2) is included into six (i, ii, iii, iv, v, vi) neighboring cells and values of water surface levels from all these nodes must be taken into consideration. In a similar manner the derivatives in triangle $T2$ can be calculated. Finally, the flux at the rth cell-interface can be calculated from formulas (15) and (17).

4. Pilot numerical simulation of the Upper Narew inundation

In order to analyze the possibility to use the diffusion wave model to simulate and predict the floods in natural floodplains, the Upper Narew test case is presented here. The part of Upper Narew reach connecting Suraż and Łapy was considered. To make the two-dimensional numerical simulation of the flood flow on the real topography area the terrain information is necessary. It can be obtained from digital elevation model (DEM) – part of the digital terrain model (DTM). The model of relief of the Narew valley, applied in the computation, was prepared at the Institute of Geophysics of the Polish Academy of Sciences (Rowiński *et al.* 2005). The geometry of flow area and DEM of floodplain are presented in Fig. 3. The morphology of the river channel was not considered in the simulation due to coarse resolution of numerical mesh representing the flow area. To simulate the flooding the calculation domain was covered by unstructured triangular mesh composed of 14,421 computational cells of 50 m side length (Fig. 4). The mesh used in the numerical simulation was locally refined (25 m) in the vicinity of Suraż and Łapy bridges and along the valley axis. At the val-

ley side boundaries, in high lying areas, the coarse mesh was implemented (100 m). During the flow simulation the ground level is linearly interpolated inside each computational cell using DEM data. The constant value of Manning friction coefficient $n = 0.08\ \mathrm{m}^{-1/3}\mathrm{s}$ in the whole flow area was used for the calculation reported in this paper.

Initially the whole flow domain was treated as a dry area (no water condition was imposed on the valley surface). At the open inflow boundary (the Suraż bridge cross-section) the water discharge was imposed as a boundary condition. The partial water rates through each cell-interface, making the inflow section up, were calculated splitting the total water discharge. At the outflow boundary (the Łapy bridge cross-section) the critical flow condition (critical water depth) was imposed. The rest of the boundaries were treated as closed boundaries. Due to relatively large dimensions of mesh elements, some details of the Narew valley relief were lost (system of the river channels, for example). The bridges were not taken into account during simulation. The calculation

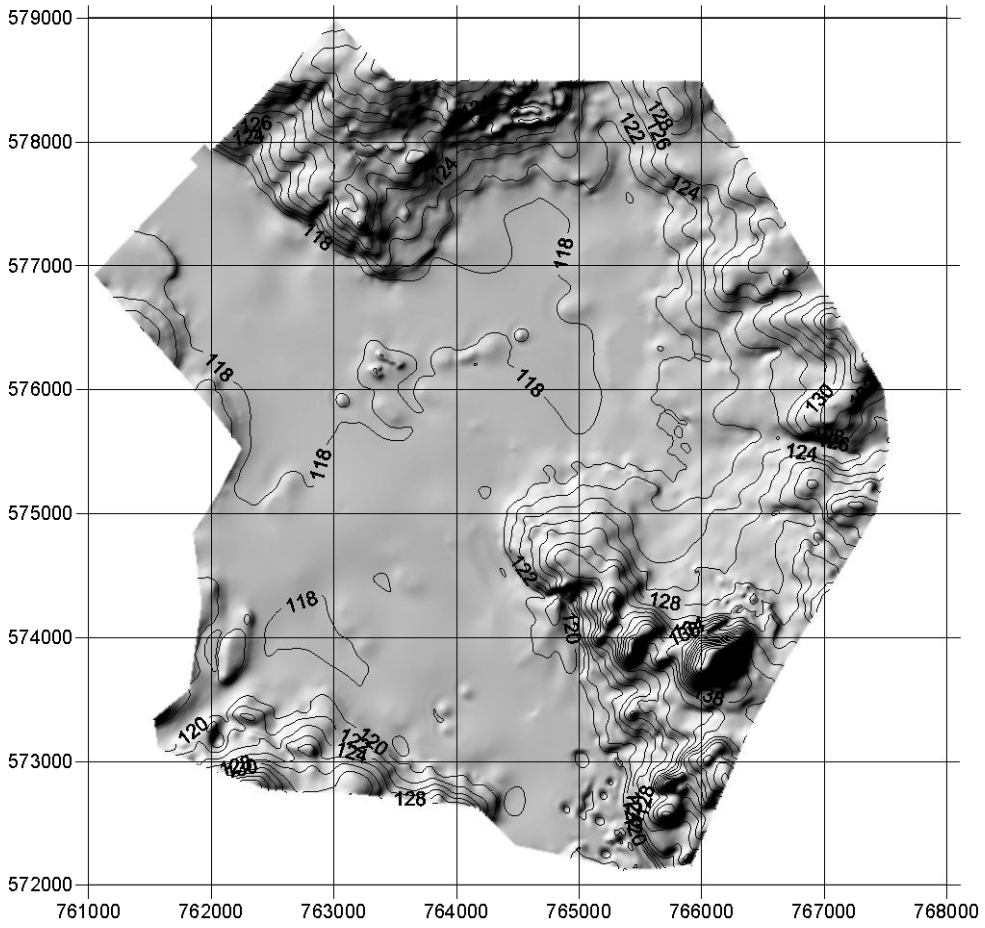

Fig. 3. DEM of the Upper Narew valley (Suraż–Łapy reach).

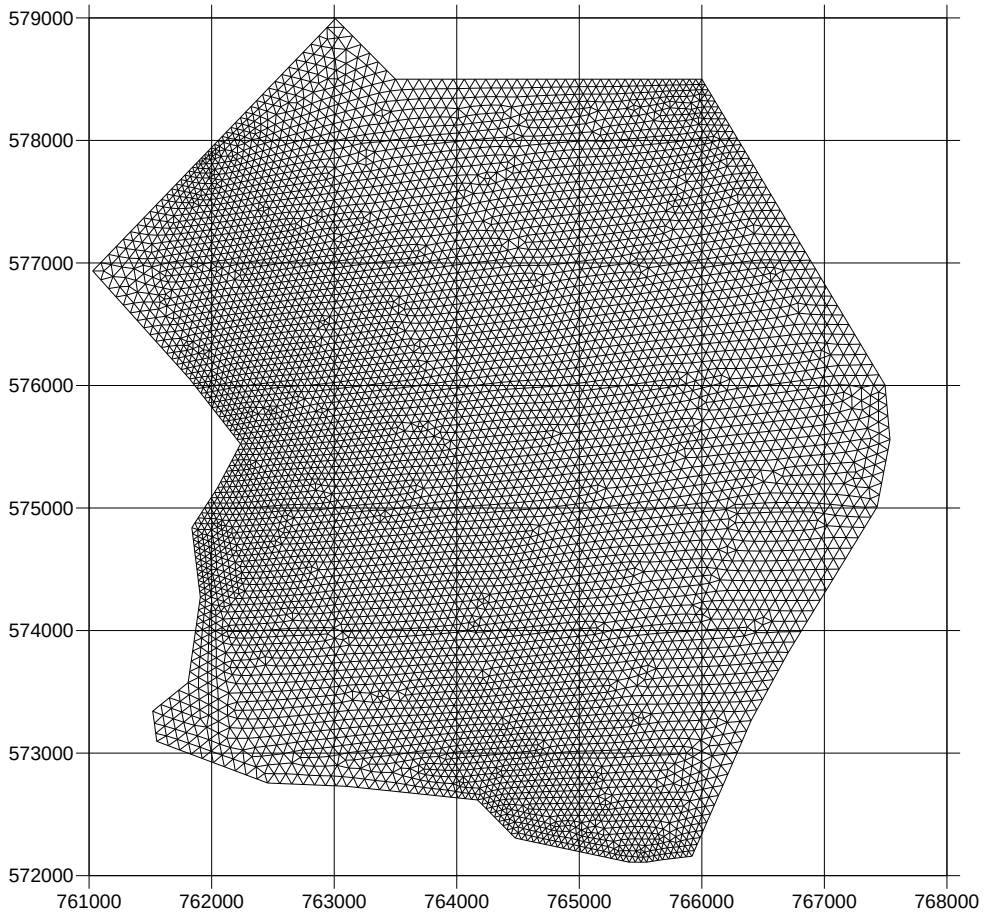

Fig. 4. Numerical mesh of the Upper Narew valley (Suraż–Łapy reach).

was carried out with the time step, $\Delta t = 0.01$ s, ensuring the calculation stability. The total simulation time was 96 hours (4 days). This time is relatively short in relation to the duration of the real floods observed at the Suraż control cross-section. The floods recorded in the Upper Narew valley are usually longer than a month. The short time of simulation was a result of computation time step, which is limited with Courant-Friedrichs-Lewy (CLF) condition (Potter 1982) holding for explicit numerical schemes. Therefore, it was decided to simulate propagation of a test case flood wave only. The hydrograph of the test flood wave is presented in Fig. 5. At the beginning of the simulation the water discharge equal to 15 m^3/s was imposed at the inflow section; then, during first twelve hours, the water rate was increased up to 250 m^3/s. The constant maximum discharge has been imposed for one day. After this time it was decreased down to the base flow (i.e. 15 m^3/s) in the next 12 hours. The base and maximum values of the water rate were assumed to represent approximately the Narew mean flow and Q_{max} of historical flood wave recorded at Suraż cross-section in 1979 (Rowiński *et al.* 2005).

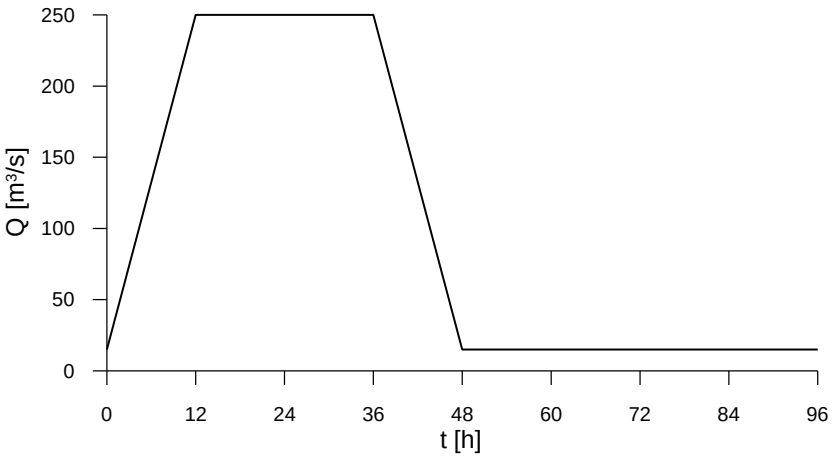

Fig. 5. Test flood wave at the Suraż cross-section.

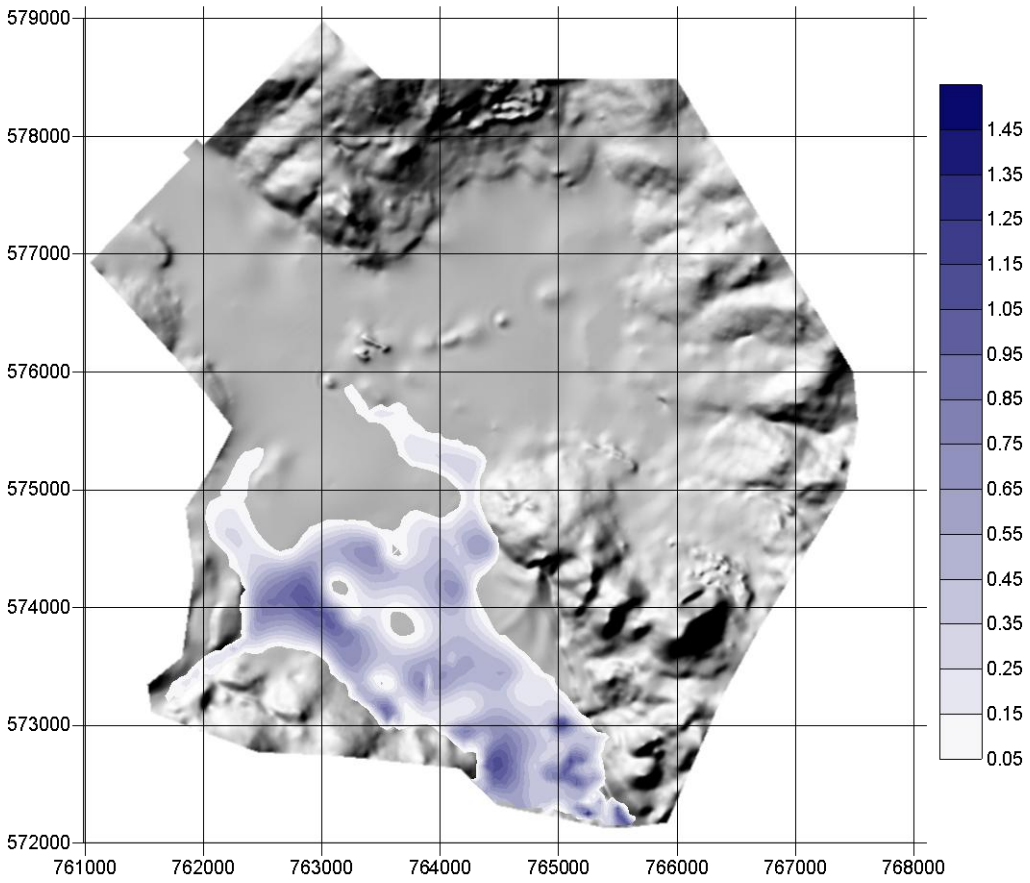

Fig. 6. Computed contours of water depth [m] after t = 12 h.

The results of Upper Narew flood test simulation are presented in Figs. 6, 7 and 8. In these figures, the evolution of flood zone in time can be investigated. The contours of water depth on the DEM background are shown there for three moments (simulation time steps) – t = 12 h, 48 h and 96 h after beginning of flood simulation. During simulation the flood wave propagates in many directions in the horizontal plane. It can be seen that the flood expands adequately to the relief of floodplain. The flow is split between the river channels along the Narew valley. The front of the flood wave, which propagates along the Narew valley, is reaching the outflow Łapy cross-section approximately after 24 hours. This time is longer than the historically observed time of the wave propagation along the Narew channel between Suraż and Łapy. This disagreement can be a result of the dry valley initial condition imposed here for two-dimensional flow modeling. Neglecting the base flow in the river channel and the channel itself due to coarse numerical mesh resolution has resulted with significant reduction of the front propagation velocity. In order to improve the calculation of the flooding time the complex – one-dimensional for the river flow and two-dimensional for floodplain inundation – simulation should be carried out.

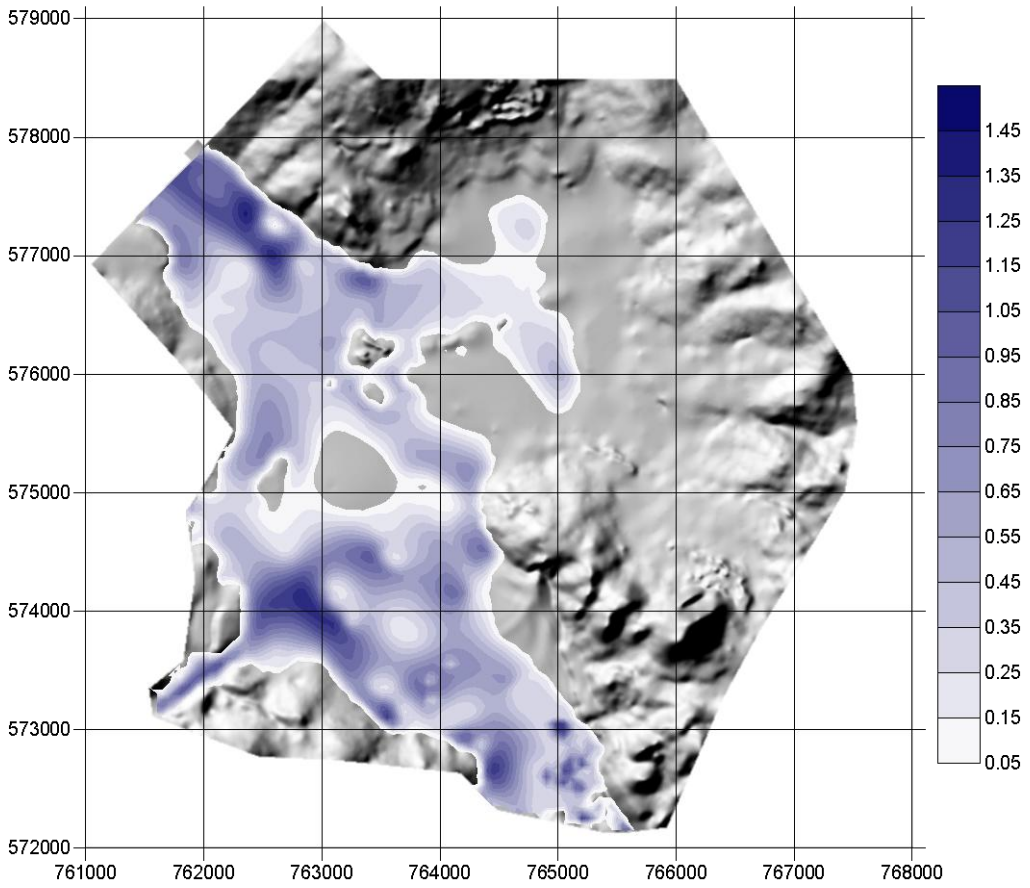

Fig. 7. Computed contours of water depth [m] after t = 48 h.

In Fig. 7 the distribution of water depth after 48 hours of simulation is shown. It is almost the moment of maximum flood range in this pilot numerical simulation. The predicted inundation can be compared with the range of historical flood (1979) computed using one-dimensional hydrodynamic model (Rowiński *et al.* 2005). The flood zone simulated with two-dimensional diffusion wave model seems to be in accordance with the mentioned one, following the floodplain relief. Further detailed investigation of this historical flood is indispensable to verify the model.

After 48 h of simulation the discharge at the inflow boundary (Suraż) is reduced to the river base flow. It has resulted with the decreasing of the flood range. In Fig. 8 the isolines of water depth after 96 hours of simulation are presented. The inundation area is significantly smaller than before. Unfortunately, the time of the Narew valley draining in this area is longer than the simulation time. It has made the total valley emptying process impossible to simulate with the explicit numerical scheme.

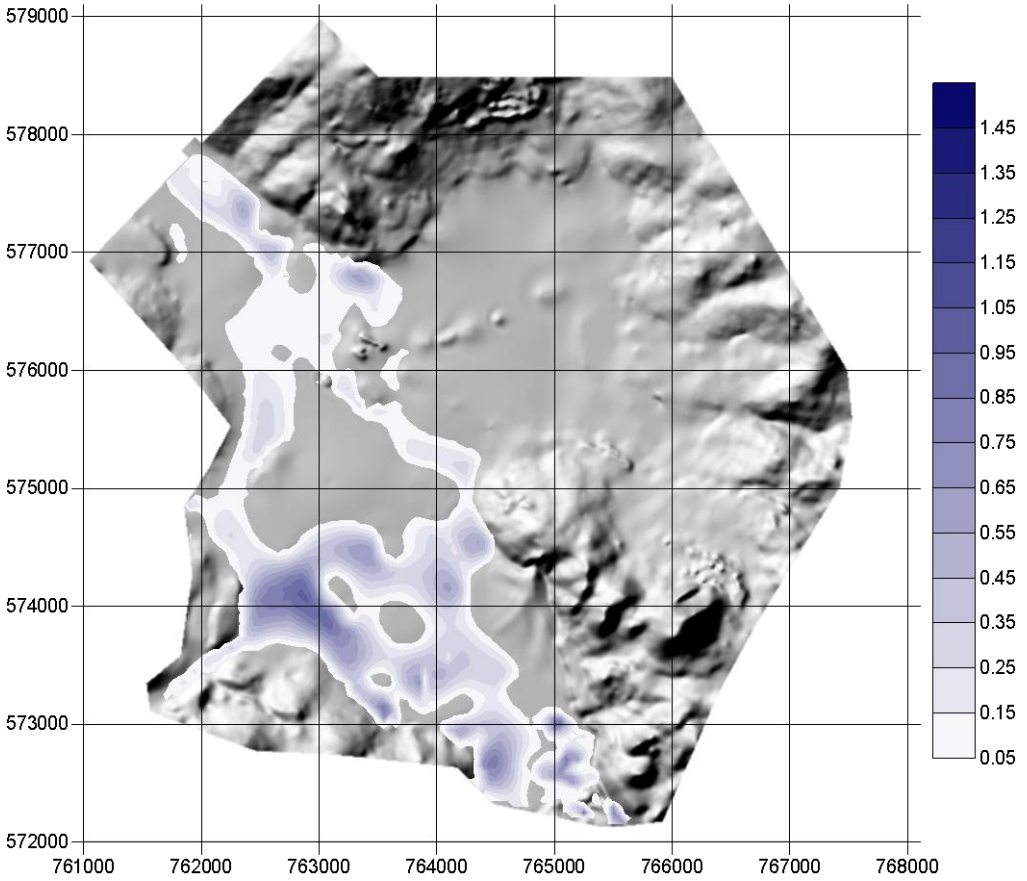

Fig. 8. Computed contours of water depth [m] after t = 96 h.

The data presented in the above-mentioned figures can be used as the background for flood mapping. The computed water depth is useful for risk identification and wa-

ter management in the river valleys. Such information can be also used for the analysis of the Upper Narew valley artificial inundations.

5. Conclusions

The pilot numerical simulation of inundation of the Upper Narew valley between Suraż and Łapy was presented in the paper. The two-dimensional diffusion wave model was proposed as a mathematical model of the free surface water flow. The equations of hydrodynamics were solved using finite volume method.

The results of numerical computation of the test inundation case have proved that the proposed mathematical model of the wave propagation in natural floodplains can be successfully applied for simulation of short time artificial flood in Upper Narew valley. It seems that diffusion wave model can be also useful for the analysis of practical (long time) inundation problems and water management in Upper Narew flow area. However, it is suggested to split mathematical modeling process into the one- and two-dimensional hydrodynamic models to separately simulate the flood wave propagation along the river and inundation of floodplain. Such a splitting technique can make the time of computations shorter ensuring longer periods of simulations.

Moreover, the detailed investigation of initial and boundary conditions is needed to properly simulate and foresee the hydraulic results of flood propagation in the Upper Narew valley. Finally, in order to confirm that the non-inertia hydrodynamics model is adequate to represent the real inundation problems in Upper Narew valley, a careful verification of the diffusion wave model, based on historical flood data is absolutely indispensable in future.

Acknowledgments. Author wishes to acknowledge the financial support offered by Ministry of Science and Higher Education for the research project 2 P04D 009 29.

References

Hromadka, T.V., and C. Yen (1987), *A Diffusion Hydrodynamic Model*, U.S. Geological Survey Report No. 874137.

LeVeque, R.J. (2002), *Finite Volume Method for Hyperbolic Problems*, Cambridge University Press, New York.

Potter, D. (1982), *Computational Physics*, PWN, Warsaw (in Polish).

Rowiński, P., J.J. Napiórkowski, and M. Osuch (2005), *Recognition of hydrological processes in the Upper Narew multichannel river system and their influence on region sustainable development*, Publs. Inst. Geophys. Pol. Acad. Sc., Monographic Volume **E-5** (378), 27-55.

Sawicki, J. (1998), *Free surface flows*, PWN, Warsaw (in Polish).

Singh, V.P. (1996), *Kinematic wave modeling in water resources: surface-water hydrology*, Wiley & Sons, New York.

Szydłowski, M., and P. Zima (2006), *Two-dimensional vertical Reynolds-Averaged Navier-Stokes equations versus one-dimensional Saint-Venant model for rapidly varied open channel water flow modelling*, Gdańsk, AHEM **53**, 4, 3-18.

Szymkiewicz, R. (2000), *Mathematical Modelling of Open Channel Flows*, PWN, Warsaw (in Polish).

Tan, W. (1992), *Shallow Water Hydrodynamics*, Elsevier, Amsterdam.

Zienkiewicz, 0. (1972), *The Finite Elements Method*, Arkady, Warsaw (in Polish).

PUBLS. INST. GEOPHYS. POL. ACAD. SC., E-9 (405), 2008

Application of the Simplified Models to Inverse Flood Routing in Upper Narew River (Poland)

Romuald SZYMKIEWICZ

Faculty of Civil and Environmental Engineering
Gdańsk University of Technology
ul. Narutowicza 11/12, 80-952 Gdańsk, Poland
e-mail: rszym@pg.gda.pl

Abstract

In the paper a problem of inverse flood routing is considered. The study deals with Upper Narew River (Poland). To solve the inverse problem two approaches are applied, based on the kinematic wave equation and the storage equation, respectively. In the first approach, the hydrograph at the upstream end is determined via the inverse solution of the governing equation with backward integration in the x direction. In the second approach, the standard initial value problem for the storage equation, completed by the steady flow equation, is solved with a negative time step, i.e., with an integration towards the diminishing time. It is shown that the proposed methods are equivalent.

Key words: open channel, flood wave, kinematic wave model, storage equation, inverse routing.

1. Introduction

Narew is a typical lowland river in the north-eastern part of Poland. The considered reach of length 100 km, between Siemianówka reservoir and gauge station Suraż, is surrounded by floodplains (Fig. 1.). This area comprises marshy meadows, famous for their exceptional biodiversity. It should be irrigated to ensure suitable conditions both for the wildlife species and for the farmers. To this order the water stored in the Siemianówka reservoir can be used. To ensure the requested flow conditions over the considered section of Upper Narew River, an appropriate reservoir operating strategy should be applied. Thus, we face a problem of flood control, typical in water management. The inverse flood routing appears to be a useful tool for decision makers responsible for water management in the valley of Narew River.

Usually the inverse routing is solved using the optimization technique. Sometimes it is solved via formulation of an inverse problem for the system of Saint Venant equations. For this reason let us recall the system of Saint Venant equations, the most

commonly used mathematical model of unsteady flow in an open channel. It can be written in the following conservation form:

$$B\frac{\partial h}{\partial t}+\frac{\partial Q}{\partial x}=q, \tag{1}$$

$$\frac{\partial Q}{\partial t}+\frac{\partial}{\partial x}\left(\frac{Q^2}{A}\right)+g\,A\frac{\partial h}{\partial x}+gAS=0, \tag{2}$$

where: t = time, x = longitudinal coordinate, h = water stage, Q = flow discharge, A = cross-sectional area of flow, B = channel width at the water surface, g = gravitational acceleration, q = lateral inflow, S = slope of energy line expressed by the Manning formula.

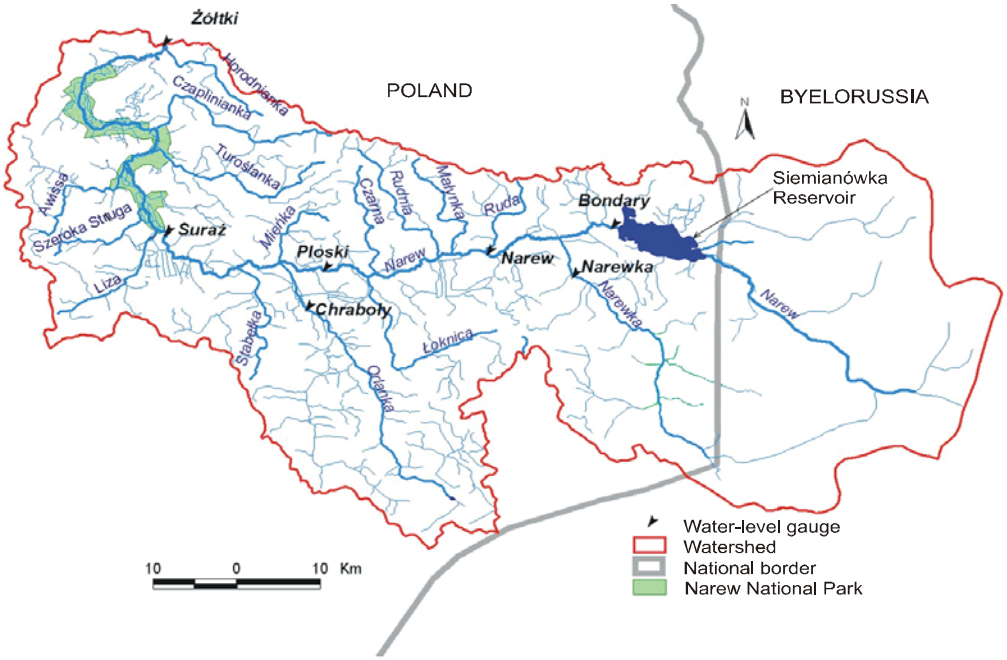

Fig. 1. Map of the considered reach of Upper Narew River.

The presented system is usually integrated in a conventional way. It means that Eqs. (1) and (2) are solved over a channel reach of length L for increasing time t, i.e., the integration is carried out in the following domain: $0 \le x \le L$ and $t \ge 0$ (Fig. 2.).

Let us consider the case of subcritical river flow, when $\sqrt{gH} > U$ (H is flow depth and U is average cross-sectional velocity). Such a kind of flow is typical for the Narew River, because of its plane character. To ensure the uniqueness of solution, the following initial and boundary conditions must be imposed (Szymkiewicz 2000):

– initial conditions

$$Q(x,t)=Q_i(x) \quad \text{or} \quad h(x,t)=h_i(x) \quad \text{for} \quad t=0 \quad \text{and} \quad 0 \le x \le L;$$

– boundary conditions

$$Q(x,t) = Q_o(t) \quad \text{or} \quad h(x,t) = h_o(t) \quad \text{for} \quad x = 0 \quad \text{and} \quad t \geq 0,$$

$$Q(t,x) = Q_L(t) \quad \text{or} \quad h(t,x) = h_L(t) \quad \text{for} \quad x = L \quad \text{and} \quad t \geq 0.$$

where $Q_i(x)$, $h_i(x)$, $Q_o(t)$, $Q_L(t)$, $h_o(t)$ and $h_L(t)$ are known functions imposed, respectively, at the channel ends. This so-called initial-boundary problem formulated for Eqs. (1) and (2) allows us to calculate the corresponding hydrographs at the downstream cross-sections for the flood wave imposed as the boundary condition at the upstream end of river reach.

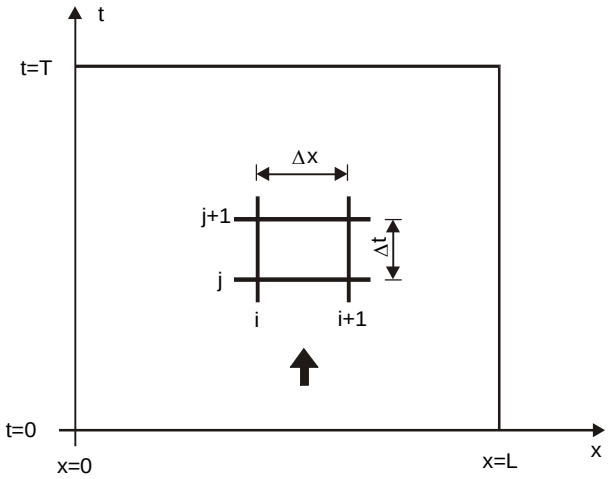

Fig. 2. Direction of integration of the Saint Venant equations in the conventional approach.

It is well known that the system of Eqs. (1) and (2) can be only solved numerically. To this order, the solution domain should be discretized and the differential equations should be approximated. The channel reach of length L is divided into M–1 intervals having length Δx, while the time domain is divided with the time step Δt. An approximation of the differential equations is carried out using the "box scheme". This scheme works on grid point presented in Fig. 3.

All derivatives are approximated at point P, which can move inside the mesh, with the following formulas (Cunge *et al*. 1980):

$$\left.\frac{\partial f}{\partial t}\right|_p \approx \psi \frac{f_i^{j+1} - f_i^j}{\Delta t} + (1-\psi)\frac{f_{i+1}^{j+1} - f_{i+1}^j}{\Delta t}, \tag{4}$$

$$\left.\frac{\partial f}{\partial x}\right|_p \approx (1-\theta)\frac{f_{i+1}^j - f_i^j}{\Delta x} + \theta\frac{f_{i+1}^{j+1} - f_i^{j+1}}{\Delta x}, \tag{5}$$

$$f_p \approx \psi\left(\theta f_i^{j+1} + (1-\theta) f_i^j\right) + (1-\psi)\left(\theta f_{i+1}^{j+1} + (1-\theta) f_{i+1}^j\right), \tag{6}$$

where ψ and θ are the weighting parameters ranging from 0 to 1.

Application of formulas (4), (5), and (6) to Eqs. (1) and (2) leads to a system of nonlinear algebraic equations, which must be completed by the imposed boundary conditions. This system is solved with an iterative method in each time step for marching time.

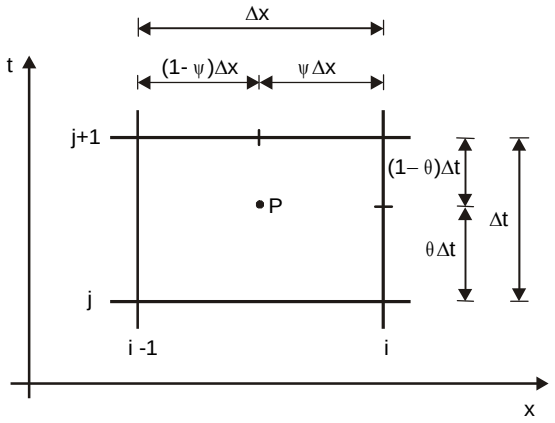

Fig. 3. Grid point applied in box scheme.

For the system of Saint Venant equations the so-called inverse problem can be formulated as well. On condition that the flow is subcritical, Eqs. (1) and (2) can be integrated over the assumed time interval [0, T], in which the flow problem is analysed, towards diminishing *x* (Fig. 4.). Such approach can be applied when we want to determine the hydrograph at the upstream end that will ensure the required flow conditions at the downstream end.

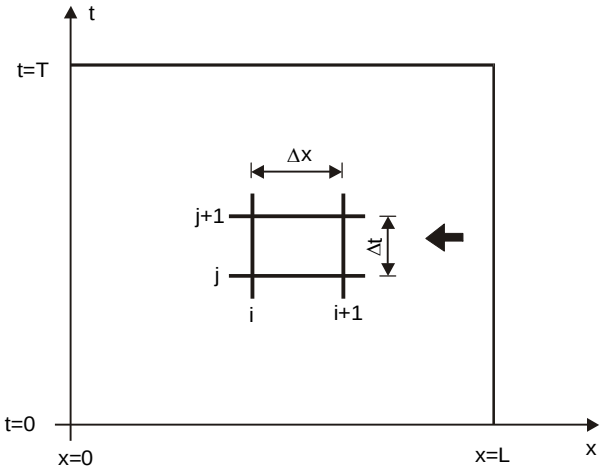

Fig. 4. Direction of integration of the system of Saint Venant equations in the inverse solution.

The inverse problem for the Saint Venant equations may be solved either with the method of characteristics or with the method of finite difference, using the well-known four-point implicit scheme (box scheme), commonly applied for conventional

solution of these equations. The first approach was proposed by Bodley and Wylie (1978), whereas the second one was applied by Szymkiewicz (1993, 1996). However, the application of these approaches to real-life problems is not easy, especially when the rivers' cross-sections have complex forms, as is the case for the river surrounded by a flood plain. In addition, the final system of algebraic equations for an inverse problem is much larger than for the direct problem. It is because in each river cross-section the governing equations are solved over the total considered time interval [0, T]. Since the acceptable time steps are relatively small, very large systems result.

It seems that the inverse flood routing can be carried out using simplified approaches. First of all, to model the unsteady flow, one can apply the simplified system of the Saint Venant equations in the form of the kinematic wave model, which is integrated backwards with respect to x, as shown in Fig. 3. The advantage of such an approach is that the final system of non-linear algebraic equations can be split into separate non-linear equations which are solved subsequently using one of the standard methods.

The second approach is based on the storage equation and the steady-state flow equation. In such a way, instead of solving the inverse problem, the initial-value problem for the system of ordinary differential non-linear equations, representing the cascade of N reservoirs must be solved. This system is solved via the numerical integration over time with negative time step. It means that to determine the hydrograph at the upstream end, instead of solving the complex inverse problem for hyperbolic equations, one can solve a relatively simple initial-value problem.

In the paper both approaches to solve the inverse routing were applied. They are shown to be equivalent for certain conditions, related to the applied numerical methods.

2. Inverse flood routing using the kinematic wave model

The kinematic wave model is derived from the system of Saint Venant equations by neglecting the inertia and pressure forces in the momentum Eq. (2) (Cunge *et al*. 1980). It takes the following form:

$$\frac{\partial h}{\partial t}+\frac{1}{B}\frac{\partial Q}{\partial x}=\frac{q}{B}, \tag{7}$$

$$Q=\frac{1}{n}R^{2/3}s^{1/2}A, \tag{8}$$

where s is the channel bottom slope, considered as an average for whole river reach of length L. Let us approximate the continuity equation (7) using formulas (4), (5) and (6), previously presented for box scheme. One obtains:

$$(1-\psi)\frac{h_i^{j+1}-h_i^j}{\Delta t}+\psi\frac{h_{i+1}^{j+1}-h_{i+1}^j}{\Delta t}+\frac{1}{B_p}\left((1-\theta)\frac{Q_{i+1}^j-Q_i^j}{\Delta x}+\theta\frac{Q_{i+1}^{j+1}-Q_i^{j+1}}{\Delta x}\right)=\frac{q_p}{B_p}, \tag{9}$$

where i is the index of cross-section and j the index of time level

$$q_p = \psi\left(\theta\, q_i^{j+1} + (1-\theta)\; q_i^{j}\right) + (1-\psi)\left(\theta\, q_{i+1}^{j+1} + (1-\theta)\, q_{i+1}^{j}\right), \tag{10}$$

$$B_p = \psi\left(\theta B_i^{j+1} + (1-\theta)\, B_i^{j}\right) + (1-\psi)\left(\theta B_{i+1}^{j+1} + (1-\theta)\, B_{i+1}^{j}\right), \tag{11}$$

$$Q_i^j = \frac{1}{n} \mathrm{s}^{1/2} (R_i^j)^{2/3} A_i^j . \tag{12}$$

In the case of conventional solution for the kinematic wave equations, the nodal values h_i^j and Q_i^j are known either from the initial condition or from the previous time step, whereas $h_1^j\,(j = 1,2,3,\ldots)$ are known from the boundary condition imposed at $x = 0$. Consequently, in Eq. (8) only one unknown h_{i+1}^{j+1} exists. It can be calculated for the subsequent nodes along the x axis, proceeding from left to right, i.e., for $i = 2,3,4,\ldots,N$.

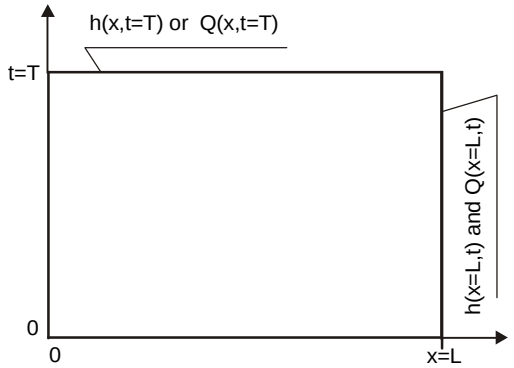

Fig. 5. Solution domain and additional condition required by the kinematic wave model applied to inverse flood routing.

Equations (8) and (9) can be used for inverse flood routing as well. For this problem, the following initial and boundary conditions should be imposed at the boundaries of the solution domain (Fig. 5):

– initial conditions:

$$Q(x,t) = Q_i(t) \quad \text{and} \quad h(x,t) = h_i(t) \quad \text{for} \quad x = L \quad \text{and} \quad 0 \le t \le T;$$

– boundary conditions:

$$Q(t,x) = Q_T(x) \quad \text{and} \quad h(t,x) = h_T(x) \quad \text{for} \quad t = T \quad \text{and} \quad 0 \le x \le L.$$

In this case the nodal values h_i^j and Q_i^j are known from the required hydrograph at $x = L (i = N)$ or as a result of calculations carried out for the previous cross-section. In addition, $h_M^j\,(j = 1, 2, 3, \ldots)$ is known as the boundary condition expected at the moment $t = T$. Therefore, similarly to the case of the direct solution, in Eq. (8) only one unknown h_i^j exists. It can be calculated for the subsequent nodes along the t axis following from the last time level $t = T$ towards $t = 0$, i.e., for $j = M–1, M–2, M–3, \ldots, 1$

(M is the total number of time steps). Since Eq. (8) is a function of h_i^j and contains a single root, it can be solved with the bisection method.

In the Manning formula (12) s is considered as the average longitudinal slope of the river bed and is assumed to be constant, whereas the cross-sectional area $A(h)$ for compound channels with flood plain is replaced by the area of the active part of cross-section, i.e., by part of total cross-sectional area in which the main stream of flowing water takes part (Fig. 6).

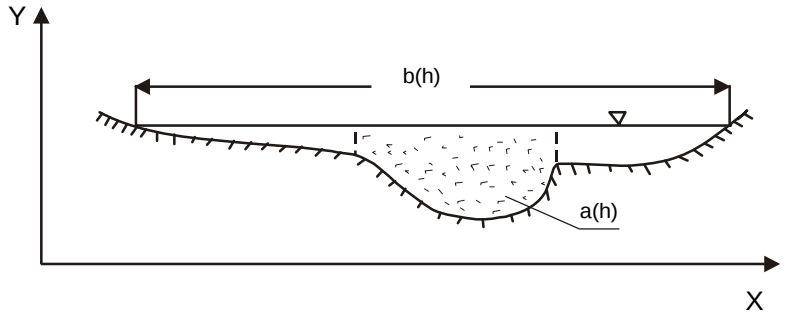

Fig. 6. Separation of active part of total cross-sectional area.

Finally, the calculations carried out in the presented way allow us to determine the required hydrograph at the upstream end of considered channel reach.

3. Inverse flood routing using the storage equation

Let us consider a channel reach of length L. Using n known cross-sections it can be divided into N–1 intervals of length $\Delta x = x_{i+1} - x_i$ (i = 1, 2, …, N–1). In such a way, one obtains a cascade of N–1 reservoirs so that the outflow from the preceding reservoir is the inflow for the next one (Fig. 7).

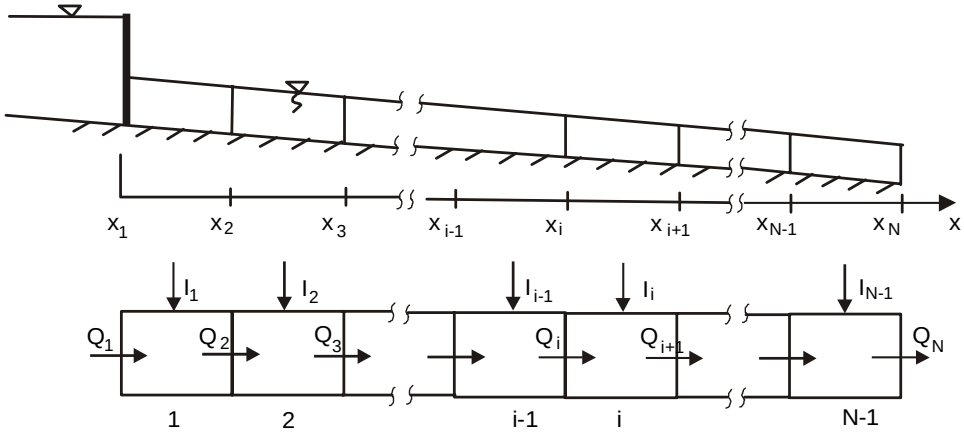

Fig. 7. Channel reach represented as a cascade of reservoirs.

The storage equation can be derived from the differential continuity equation (1). To this order, it is integrated with regard to x over a channel's increment of length Δx. Consequently, one obtains:

$$\frac{dV_i}{dt} = Q_i - Q_{i+1} + I_i, \tag{13}$$

where: i = index of reservoir and cross-section, V_i = total volume of water stored by channel reach, Q_i = flow discharge through cross-section i, I_i = total lateral inflow into reservoir (= $\Delta x \cdot q$).

To calculate the flow discharge between the neighbouring reservoirs, the Manning formula (8) is used. As previously, in this equation s, considered as average longitudinal slope of bed river, is assumed to be constant, whereas the cross-sectional area $A(h)$ for compound channels with food plain is replaced by the area of the active part of cross-section.

After eliminating V, Eq. (13) takes the following form:

$$\frac{d\overline{h}}{dt} = \frac{1}{f_i}\left(Q_i - Q_{i+1} + I_i\right), \tag{14}$$

where f_i is the area of reservoir's surface (a function of the water stage).

The mean level of the water surface above the datum $\overline{h}$ can be expressed using nodal values of h as follows:

$$\overline{h} = \psi h_i + \left(1-\psi\right)h_{i+1}, \tag{15}$$

where ψ is the weighting parameter ranging from 0 to 1. Finally, Eq. (13) takes the following form:

$$\psi \frac{dh_i}{dt} + \left(1-\psi\right)\frac{dh_{i+1}}{dt} = \frac{1}{f_i}\left(Q_i - Q_{i+1} + I_i\right). \tag{16}$$

Similar equations can be written for every reservoir (for i = 1, 2, …, N–1). Consequently, a system of N–1 ordinary differential equations is obtained. Its solution is formulated as an initial-value problem. Knowing the initial condition $h_i(t=0) = h_{i,in}$, where $h_{i,in}$(i =1, 2, …, N–1) is given, the functions $h_i(t)$ have to be calculated for $0 \le t \le T$. In this order, the equation should be numerically integrated using for example the following general two-level scheme:

$$y_{j+1} = y_j + \Delta t\left(\theta y'_j + (1-\theta)y'_{j+1}\right), \tag{17}$$

where: j = index of time level, θ = weighting parameter ranging from 0 to 1.

The value of the weighting parameter θ defines the method of integration. For θ = 0 one obtains the explicit Euler method, for θ = 1/2 – the implicit trapezoidal rule and for θ = 1 – the implicit Euler method (Press *et al*. 1992).

Application of Eq. (17) to Eq. (16) leads to the following formula:

$$\psi \frac{h_i^{j+1} - h_i^j}{\Delta t} + (1-\psi) \frac{h_{i+1}^{j+1} - h_{i+1}^j}{\Delta t}$$

$$= \frac{1-\theta}{f_i^j} \left(Q_i^j - Q_{i+1}^j + I_i^j \right) + \frac{\theta}{f_i^{j+1}} \left(Q_i^{j+1} - Q_{i+1}^{j+1} + I_i^{j+1} \right) \tag{18}$$

for $i = 1, 2, ..., N\text{-}1$.

While solving conventional flood routing, the function $h_0(t)$ is known as the flood wave imposed at the upstream end of channel. Therefore, Eq. (18) applied for the first reservoir ($i = 1$) contains one unknown only. Similar situation arises for the next reservoirs, since the outflow from the preceding one is the inflow to the next one. It means that system of equations (18) can be split and each equation can be solved separately with regard to the unknown h_{i+1}^{j+1}:

$$h_{i+1}^{j+1} = h_{i+1}^j - \frac{\psi}{1-\psi} \left(h_i^{j+1} - h_i^j \right) + \frac{1-\theta}{1-\psi} \frac{\Delta t}{f_i} \left(Q_i^j - Q_{i+1}^j + I_i^j \right)$$

$$+ \frac{\theta}{1-\psi} \frac{\Delta t}{f_i} \left(Q_i^{j+1} - Q_{i+1}^{j+1} + I_i^{j+1} \right) \tag{19}$$

for $i = 1, 2, ..., N\text{-}1$.

This equation is non-linear, since according to the Manning formula (12), Q_{i+1}^{j+1} depends on h_{i+1}^{j+1}. To solve Eq. (19), an iterative method should be applied. Finally the calculations are going for increasing time, similarly to the situation presented in Fig. 2.

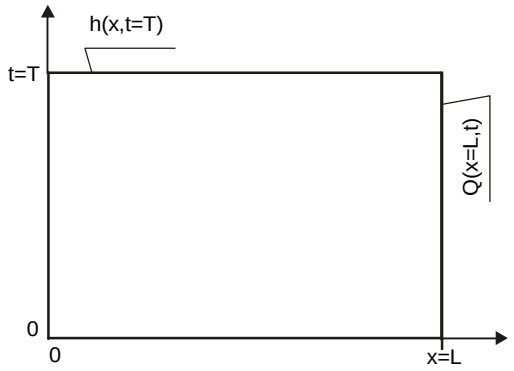

Fig. 8. Domain of integration of the storage equation and the required additional information for inverse routing.

Equation (18) can be used for the inverse flood routing. To this order a proper initial value problem should be formulated. One can assume that at the end of the considered time period T the steady flow was reached. It means that the condition $h_i(t = T) = h_{i,fin}$ for $i = 1, 2, \ldots, N$ is given. Moreover at the downstream end (cross-section N), the required hydrograph $h_N(t)$ is imposed (Fig. 8). Now, integrating

Eq. (18) with a negative time step Δt (see Fig. 9) one can arrive at the hydrograph at $x = 0$, i.e., to $h_0(t)$.

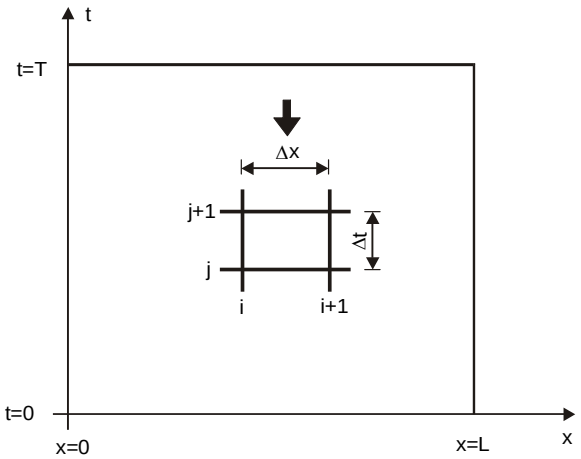

Fig. 9. Integration of the storage equation in backward direction with regard to time.

In such a case in the solved equation only the water stage h_i^j is unknown. Its value resulting from Eq. (18) is given by the formula:

$$h_i^j = h_i^{j+1} - \frac{1-\psi}{\psi}\left(h_{i+1}^{j+1} - h_{i+1}^j\right) + \frac{1-\theta}{\psi}\frac{\Delta t}{f_i^j}\left(Q_i^j - Q_{i+1}^j + I_i^j\right) + \frac{\theta}{\psi}\frac{\Delta t}{f_i^{j+1}}\left(Q_i^{j+1} - Q_{i+1}^{j+1} + I_i^{j+1}\right) \tag{20}$$

for $i = N–1, N–2, ...,1$.

This equation is a non-linear one. Its solution in the backward direction allows us to obtain at the upstream end ($x = 0$) the hydrograph corresponding to the one imposed at the downstream end ($x = L$).

4. Discussion of the numerical results

The two presented approaches were used to compute the flow in the Upper Narew River. Each one was applied for both direct and inverse problems. All the data required for the calculations had been provided by the Institute of Geophysics of the Polish Academy of Sciences.

The considered river reach between Siemianówka Reservoir and the gauge station Suraż has the length L = 101.300 km. Along the river course, N = 54 cross-sections were measured. The distances between the neighbouring sections vary from 0.360 km to 3.530 km. In Fig. 10 the shape of the cross-section at 27.920 km from Siemianówka Reservoir is shown as an example. For the considered reach of Narew River the presence of flood plains is typical. The river bed has the width of about 75 m whereas the width of the flood plains exceeds 1000 m.

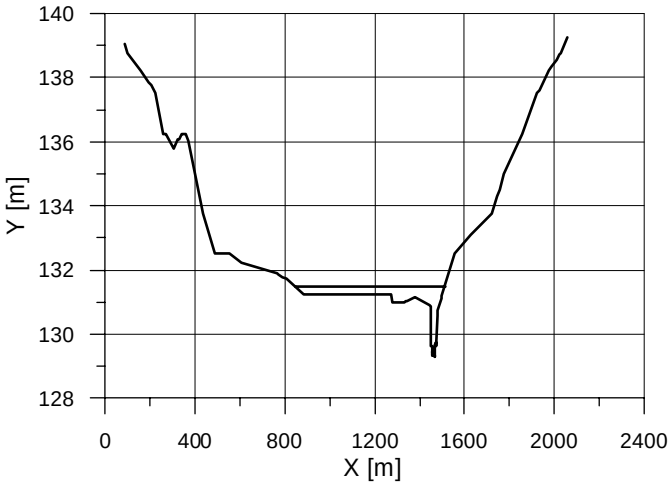

Fig. 10. Cross-section measured at x = 27.920 km.

For testing, the following general assumptions were adopted:

- In all cross-sections the active part is not separated;
- The lateral inflow is neglected;
- The initial condition is calculated via the solution of the equation for steady non-uniform flow with the discharge and water stage imposed at the down-stream end;
- The condition imposed at the upstream and for the direct solution has the form of hydrograph prescribed by the following formulas:

  for $t \le t_0$

$$Q_0(t) = Q_{in},$$

  for $t > t_0$

$$Q_0(t) = Q_{in} + (Q_{\max} - Q_{in}) \left(\frac{t}{t_{\max}} \right)^{\alpha} \exp\left(1 - \left(\frac{t}{t_{\max}} \right)^{\alpha} \right), \tag{21}$$

  where Q_{in} is the initial discharge, $Q_{\max}$ is the peak discharge, $t_{\max}$ is time to peak, t_0 is lag time and α is parameter;
- The condition imposed at the downstream end for the inverse routing has the form of hydrograph $Q_L(t)$ which is given numerically;
- All non-linear algebraic equations are solved using the bisection method. For a function having a single root this method is always convergent (Press *et al*. 1992).

The results for the direct problem are shown in Fig. 11. For the same flood wave imposed at x = 0 (Eq. (21) with t_0 = 24 h, Q_{in} = 13.55 m^3/s, $Q_{\max}$ = 80 m^3/s, $t_{\max}$ = 36 h and α = 1.25), the hydrographs calculated at the downstream end (in Suraż) appeared

practically identical. They were provided by the same set of weighting parameters, namely by $\theta = 1$ and $\psi = 0$. For the values of time step Δt taken from 0.02 h to 0.2 h the results of calculations varied slightly. The stable solution was ensured on condition that $0.5 \leq \theta \leq 1$ and $0.5 \geq \psi \geq 0$.

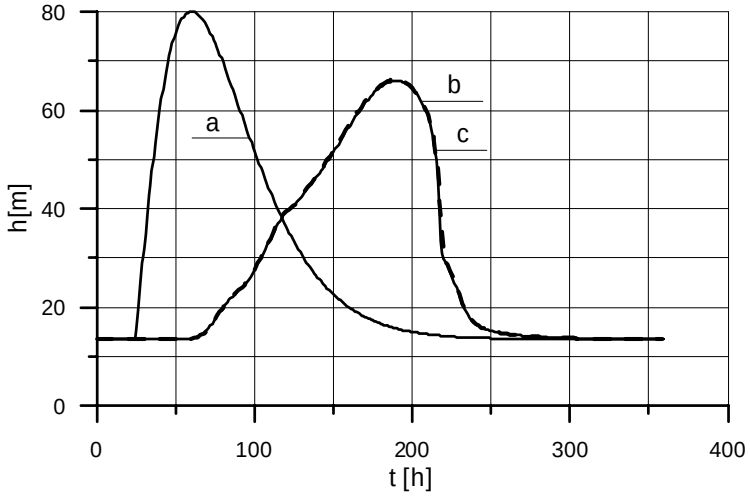

Fig. 11. Results of flood wave routing (a – imposed at upstream end, b – calculated with the kinematic wave equation, c – calculated with the storage equation).

The seemingly surprising agreement of the results can be interpreted easily. Let us compare Eq. (9), being an approximation of the kinematic wave equation using the box scheme, and Eq. (18), which was obtained by solution of the storage Eq. (16) with formula (17). In fact, the two equations are identical, although derived in different manners. To confirm this identity let us multiply and divide the right side of Eq. (9) by Δx:

$$\frac{q_P}{B_P} = \frac{q_P \cdot \Delta x}{B_P \cdot \Delta x} = \frac{I}{B_P \cdot \Delta x}. \tag{22}$$

On the other hand, the area of the reservoir at the level of its surface in Eq. (18) can be expressed by the following approximating formula:

$$f \approx B_P \cdot \Delta x. \tag{23}$$

After introduction of the above relations into Eq. (9) and Eq. (18), respectively, they become identical formulas. This result is reasonable since both approaches have the same roots: the continuity equation and the Manning formula.

The only difference between both equations is that Eq. (9) represents an integration of the kinematic wave towards diminishing x (see Fig. 4), whereas Eq. (18) expresses the numerical solution of the storage equation by the method (17) with negative time step towards diminishing time. As shown in Fig. 11, both approaches provide identical results.

The next example concerns inverse routing. At the downstream end (in Suraż) the hydrograph $Q_L(t)$, which has been previously computed via the direct solution, was imposed as the boundary condition. In this case, both approaches also gave very simi-

lar results. It appeared that stable solution is ensured for $0 \leq \theta \leq 0.5$ and $1 \geq \psi \geq 0.5$. These conditions are inverse to the ones for the conventional solution. This property of the box scheme applied to the inverse solution of the system of Saint Venant equations was shown by Szymkiewicz (1996). It holds for the kinematic wave as well, which is of hyperbolic type as the Saint Venant equations.

In Fig. 12 one can observe some oscillations of the hydrograph calculated at the upstream end (Siemianówka). They depend on the values of the weighting parameters and are caused by numerical dispersion. The displayed results were obtained for $\theta = 0.5$ and $\psi = 0.62$ (smooth curve) and for $\theta = 0.4$ and $\psi = 0.525$ (oscillating curve). The oscillations disappear with increasing numerical diffusion generated by the box scheme. It is controlled by θ and ψ. For $\theta = 0$ and $\psi = 1$ the numerical solution becomes smooth, whereas for $\theta = 0.5$ and $\psi = 0.5$ the oscillations are the most pronounced, since for these values the box scheme is dissipation-free. However, in such a situation it is practically impossible to obtain the effect of smoothing and at the same time to ensure an increase of steepness of the hydrograph at upstream end. In this case both approaches produce very similar solutions. In addition, they fulfil perfectly the law of mass conservation.

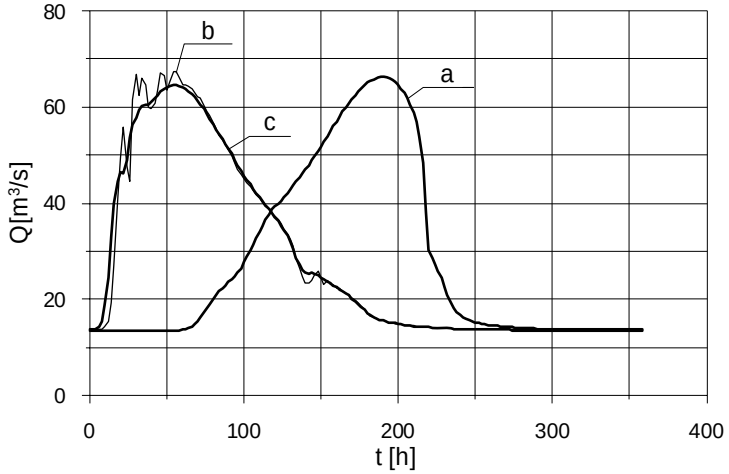

Fig. 12. Results of inverse flood wave routing carried out with kinematic wave equation (a – imposed at downstream end; calculated at upstream end: b – for $\theta = 0.4$ and $\psi = 0.525$, c – for $\theta = 0.5$ and $\psi = 0.62$).

Presented routing of the hypothetical flood wave allowed us to recognize general properties of the proposed methods of solution. In the next example, the observations of the discharges $Q(t)$, carried out at the gauges stations Bondary and Suraż between 07.03.1994 and 04.07 1994 were used. Comparison of both curves presented in Fig. 13 suggests that at the considered river reach the lateral inflow coming from subcatchments plays an essential role. Its estimation was based on the aforementioned observations as well as the observations made at the intermediate gauge stations (Narew and Ploski – see Fig. 1). Imposing as the boundary condition the hydrograph $Q(t)$ observed at the upstream end and the lateral hydrographs previously evaluated, the direct routing was

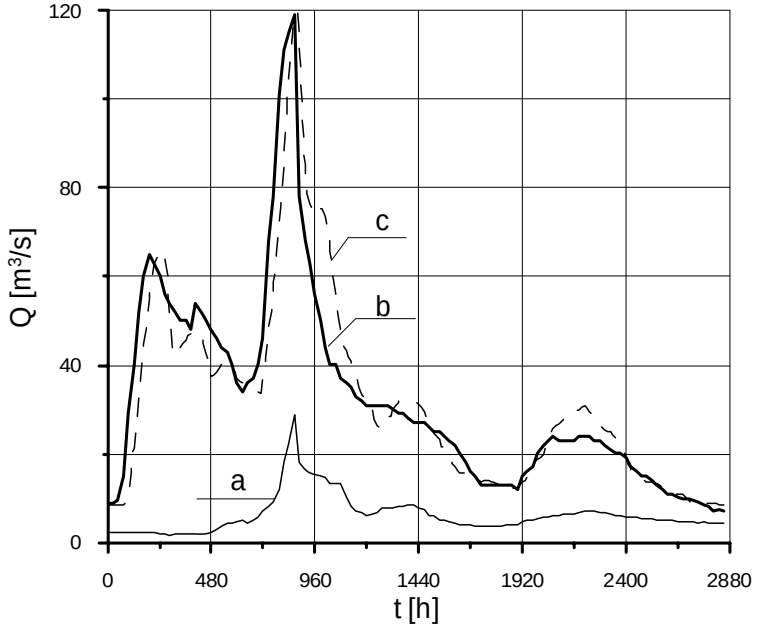

Fig. 13. Results of flood wave routing between Bondary and Siemianówka gauge station for the period 07.03 – 04.07.1994 (a – imposed at upstream end, b – observed at downstream end, c – calculated with storage equation).

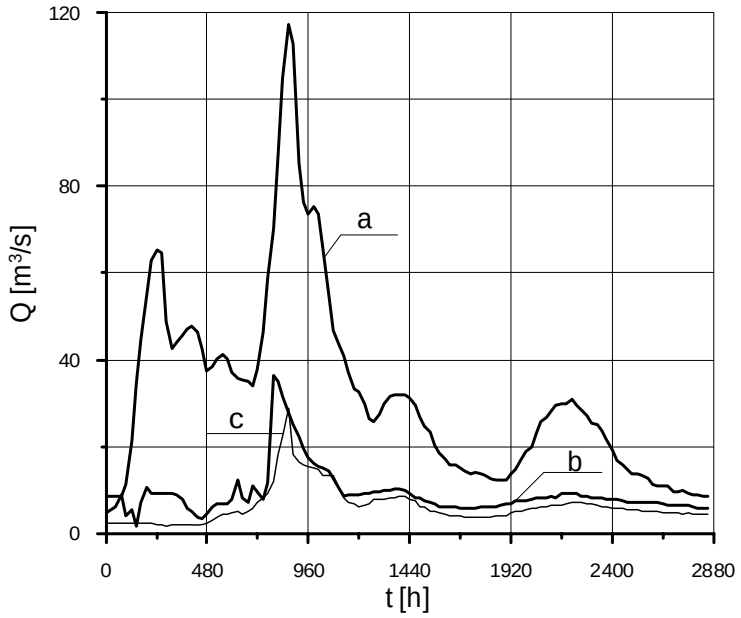

Fig. 14. Results of the inverse flood wave routing between Bondary and Siemianówka gauge station for the period 07.03 – 04.07.1994 (a – imposed at the downstream end, b – calculated with the storage equation, c – observed).

performed using the storage equation. The results of calculations seem to be quite reasonable and similar to the results of the data provided by the experiment. They were obtained for Δt = 0.25 h, θ = 1.0, and ψ = 0. In the next numerical experiment, the routing process has been inverted. Using the same model and imposing the hydrograph at the downstream end as well as the lateral ones, the hydrograph at the upstream end was calculated. The results presented in Fig. 14 were given by Δt = 0.50 h, θ = 0, and ψ = 1.0. Also in this case they can be considered as reasonably accurate.

However, to better evaluate the applied model more data are needed. Unfortunately, at the moment they are not available.

5. Conclusions

Two alternative approaches were proposed to solve the problem of inverse flood routing for Upper Narew River, between the cross-sections Bondary and Suraż. Both are based on the simplified forms of the Saint-Venant system, i.e., the kinematic wave equation and the storage equation. Consequently, one avoids the solution of a relatively complicated problem leading to large systems of algebraic equations. Instead, in the case of the kinematic wave equation one has to solve a non-linear algebraic equation for each node separately. In the case of the storage equation an ordinary differential equation is integrated backwards in time, i.e. with the negative time step. It was shown that both approaches are equivalent and they ensure very similar results. The preliminary results presented in this work seem encouraging. However, in order to better evaluate the proposed approaches more hydrological data should be acquired from field experiments, especially concerning the lateral inflow from the subcatchments of Upper Narew River.

Acknowledgments. The research was supported by the Polish Committee for Scientific Research in the framework of the Project no 2 p04d 009 29.

References

Bodley, W.E., and E.B. Wylie (1978), *Control of transient in series channel with gates*, J. Hydraul. Div. ASCE, HY10, 1395-1407.

Cunge, J., F.M. Holly Jr., and A. Verwey (1980), *Practical Aspects of Computational River Hydraulics*, London, Pitman.

Press, W.H., S.A. Teukolsky, W.T. Veterling, and B.P. Flannery (1992), *Numerical Recipes in C*, Cambridge University Press, Cambridge.

Szymkiewicz, R. (1993), *Solution of the inverse problem for the Saint Venant equations*, J. Hydrol. **147**, 105-120.

Szymkiewicz, R. (1996), *Numerical stability of implicit four-point scheme to inverse linear flood routing*, J. Hydrol. **176**, 13-23.

PUBLICATIONS OF THE INSTITUTE OF GEOPHYSICS
POLISH ACADEMY OF SCIENCES

E. HYDROLOGY

E-1 (295)	Impact of climate change on water resources in Poland.
E-2 (325)	Water quality issues in the Upper Narew Valley.
E-3 (365)	Modelling and control of floods.
E-4 (377)	Potential climate changes and sustainable water management.
E-5 (387)	Computational modeling for the development of sustainable water-resources systems in Poland. US-Poland Technology Transfer Program.
E-6 (390)	Environmental Hydraulics.
E-7 (401)	Monographic Volume, Transport Phenomena in Hydraulics.

ISBN-978-83-88765-76-6

Visit our homepage:

http://www.igf.edu.pl/pl/publikacje/publs_inst_geophys_pas